UCRL-18629

cy. 2

LIBRARY AND DOCUMENTS SECTION

OSCILLATING-JET MEASUREMENT OF DYNAMIC LIQUID-LIQUID INTERFACIAL TENSION

Sugihiko Tada, Alfred E. Vandegrift,
and Theodore Vermeulen

December 1968

TWO-WEEK LOAN COPY

This is a Library Circulating Copy which may be borrowed for two weeks. For a personal retention copy, call Tech. Info. Division, Ext. 5545

UCRL-18629

cy. 2

LAWRENCE RADIATION LABORATORY
UNIVERSITY of CALIFORNIA BERKELEY

DISCLAIMER

This document was prepared as an account of work sponsored by the United States Government. While this document is believed to contain correct information, neither the United States Government nor any agency thereof, nor the Regents of the University of California, nor any of their employees, makes any warranty, express or implied, or assumes any legal responsibility for the accuracy, completeness, or usefulness of any information, apparatus, product, or process disclosed, or represents that its use would not infringe privately owned rights. Reference herein to any specific commercial product, process, or service by its trade name, trademark, manufacturer, or otherwise, does not necessarily constitute or imply its endorsement, recommendation, or favoring by the United States Government or any agency thereof, or the Regents of the University of California. The views and opinions of authors expressed herein do not necessarily state or reflect those of the United States Government or any agency thereof or the Regents of the University of California.

UCRL-18629

UNIVERSITY OF CALIFORNIA

Lawrence Radiation Laboratory
Berkeley, California

AEC Contract No. W-7405-eng-48

OSCILLATING-JET MEASUREMENT OF DYNAMIC LIQUID-LIQUID INTERFACIAL TENSION

Sugihiko Tada*, Alfred E. Vandegrift, and Theodore Vermeulen

December 1968

* Ph. D. Thesis

OSCILLATING-JET MEASUREMENT OF DYNAMIC LIQUID-LIQUID INTERFACIAL TENSION

Contents

ABSTRACT v

I. STATEMENT OF THE PROBLEM 1

II. OSCILLATING-JET MEASUREMENT OF DYNAMIC LIQUID-LIQUID INTERFACIAL TENSION 2

A. Introduction 2

B. Theory 8

1. Summary and Extension of Bohr's Treatment 8

2. Boundary Conditions for Liquid-Liquid System 12

3. Exact Expression for σ 15

4. Empirical Expression for σ 21

C. Experimental Study 29

1. Experimental 29

2. Physical Properties 31

3. Results 31

4. Discussion 37

REFERENCES 43

III. VELOCITY PROFILE OF CYLINDRICAL LAMINAR LIQUID JETS ENTERING A STATIONARY SURROUNDING LIQUID 45

A. Introduction 45

B. Theory 47

1. Empirical Velocity Equation 51

2. Computation Procedure 53

C. Results 58

1. Comparison with Published Experimental Data 58

2. Generalized Behavior 60

3. Comparison with Schlichting-Type Solution 65

4. Effect of Density Difference 73

D. Summary 75

REFERENCES 76

IV. VELOCITY PROFILE OF CYLINDRICAL LAMINAR LIQUID JETS ENTERING A MOVING SURROUNDING LIQUID 77

A. Introduction 77

B. Theory 79

1. Empirical Velocity Equations 82

2. Computation Procedure 86

3. Generalized Behavior 89

a. Effect of viscosities and densities 90

b. Effect of average-velocity ratio 90

c. Effect of orifice-to-tube radius ratio..... 93

d. Behavior of parameters 93

REFERENCES 97

V. CONCLUSIONS 98

ACKNOWLEDGMENTS 99

APPENDIXES: COMPUTER PROGRAMS 100

I. Wavelength--Interfacial-Tension Relation 100

II. Velocity Profile in a Stationary Surrounding Liquid 122

III. Velocity Profile in a Moving Surrounding Liquid 142

OSCILLATING-JET MEASUREMENT OF DYNAMIC LIQUID-LIQUID INTERFACIAL TENSION

Sugihiko Tada, Alfred E. Vandegrift, and Theodore Vermeulen

Lawrence Radiation Laboratory and Department of Chemical Engineering
University of California, Berkeley, California 94720

December 1968

ABSTRACT

The oscillating-jet technique has been used previously for measuring the surface tension between a gas and a liquid. Here it is extended to the measurement of the interfacial tension between two immiscible liquids. This work was undertaken to establish a hydrodynamical theory for the oscillating jet, so as to allow this technique to be used to indicate interfacial concentrations in liquid-liquid systems undergoing mass transfer. The mathematical theory by Bohr for the gas-liquid case is extended to the liquid-liquid case to give an exact but implicit analytical solution, and a simple correction multiplier to the Rayleigh formula has been developed to give an explicit representation of the exact solution.

Experimental data were taken on immiscible liquid pairs whose interfacial tension ranges from 6 to 42 dynes/cm, and were analyzed by the theory developed.

As an essential step in this study, a calculational method has been developed to predict the velocity profile of a circular liquid jet in a stationary surrounding liquid. The resulting values of jet radius and interfacial velocity have been used to correlate the effective plug-flow velocity which is required as an input for the oscillating-jet theory.

In order to improve the stability of the oscillating jet, and also to approach closer to theoretical flow conditions, the use of a flowing external phase at a velocity near the average velocity of the oscillating jet is proposed. A calculational method to predict the velocity profile for such a case is given as an extension of the method used for a stationary surrounding liquid.

I. STATEMENT OF THE PROBLEM

The oscillating jet provides a well explored means of measuring surface tension of liquid jets into a gas, but has rarely been applied to determine the interfacial tension between two immiscible liquids. The measurable parameter in this method is the wavelength produced by the oscillation. Our ultimate objective, not yet reached, is to use the oscillating jet to measure dynamic interfacial concentrations during liquid-liquid mass transfer.

The present study is aimed at providing both theory and technique that will contribute toward approaching this objective.

The theoretical background needed to achieve the foregoing objectives has two parts; first, a suitable relation between wavelength, other system properties, and interfacial tension; and second, knowledge of velocity profiles of a circular jet in another liquid which is either stationary or moving.

The experimental problem is one of obtaining suitable elliptical nozzles, and of finding operating conditions that produce a maximum number of nodes in the jet and also a maximum total jet length. Because of the non-zero exterior density and viscosity, and very similar refractive indices in a liquid-liquid system, both producing the jet and measuring it appear to be considerably more difficult than working with a liquid jet in a gas.

Thus the present study deals both with development of the needed mathematical background and with analysis of representative experimental data taken on pre-equilibrated liquids.

II. OSCILLATING-JET MEASUREMENT OF DYNAMIC LIQUID-LIQUID INTERFACIAL TENSION

A. Introduction

When a jet of liquid is forced through an elliptical orifice under a constant pressure, a standing wave is formed by the oscillations of the issuing stream about its equilibrium cylindrical form. The standing-wave pattern formed by the stream is the basis for an experimental method of obtaining the surface tension between a liquid and a gas, or the interfacial tension between two immiscible liquids. While mass transfer is occurring to or from a liquid jet, that is while a solute is transferred to the interface and through it, local solute concentration and interfacial tension will change with distance from the orifice; the changes can be followed by the change in wavelength of the jet.

A jet is particularly suitable for mass-transfer studies because it allows the study of residence-time effects in the range of 0.001 sec to 0.1 sec. Also, it can be caught at a variable distance from the nozzle, and analyzed chemically to give the mass-transfer rate as a function of length or time. Knowledge of how the interfacial concentration varies during mass transfer between two liquids should give a clearer understanding of the fundamental processes involved.

Two fluid-mechanical problems must be solved in order to interpret wavelength measurements on an oscillating jet: first, the elliptical oscillation of a plug-flow jet; and second, estimation of the effective plug-flow velocity from the calculated properties of laminar-flow cylindrical jets. The present study is the first phase in adapting the oscillating-jet method to liquid-liquid systems, namely to solve the

wavelength problem mathematically and to explore the experimental techniques.

Physical analysis of the oscillating liquid jet in air dates back more than a century, when Bidone[7] and Magnus[18] independently reported on the phenomenon. Later, Lord Rayleigh[20] derived a mathematical relation [Eq. (41), below] between the stream velocity and density, the surface tension, and the oscillation frequency. Rayleigh also showed experimentally that the surface tension of a freshly formed soap solution is considerably higher than the equilibrium value. Pederson[19] improved the experimental techniques and measured surface tensions of a number of liquids, including aqueous solutions of ethyl alcohol, using Rayleigh's theory.

In a definitive analysis, Bohr[11] introduced viscous terms; and he also provided a theoretical correction for the finite amplitude of the oscillation, which introduces the maximum and the minimum diameters of the jet.

Bohr's theory has been applied by several investigators to the measurements of the surface tension of liquids. Stocker[21] measured the surface tension of inorganic salt solutions. Bond and Puls[12] used it in confirming their results on a commercial soap solution, obtained with the liquid-sheet method. Sutherland[22,23] studied the surface tensions of several systems and found the results obtained by Bohr's theory to depend upon the particular orifice used. Defay and Hommelen studied the rate of surface tension lowering of aqueous solutions of long-chain alcohols and dicarboxylic acids by the oscillating jet method, and

interpreted their results by the Bohr formula. Hansen and co-workers[16,17] also studied the rate of surface-tension depression of organic acids, in which the surface velocity calculated from a nonuniform-velocity model represents the linear velocity in the Bohr model: the depression rate could be represented by a second-order kinetic mechanism in the surface film.

Very recently Vandegrift[25] proved experimentally, by use of the oscillating jet, that water does not have a dynamic surface tension attributable to hydrogen bonding.

Addison[1,2,3,4,5,6] has also published extensive work on adsorption of alcohols at the surfaces of alcohol-water solutions, using the oscillating jet. He developed his own empirical relations from Rayleigh's solution. In those cases where Addison, Sutherland, and Defay measured the same systems, Addison's results do not agree with those of the other two workers. Burcik, who found the rate of change of surface tension to be a major factor in determining the stability of foams, used the oscillating jet with Addison's empirical formula to measure this rate experimentally.[8]

Only Addison has attempted to study liquid-liquid jets,[6] using his empirical formula, but with little success.

Thus very little use of the oscillating jet has been made in liquid-liquid systems. It is very difficult to prevent the jet's breaking up within a path length too short for measurements to be made. Breakup occurs more easily due to the outside liquid's having higher viscosity and density than a gas. A second problem is the rapid damping of the oscillations, which requires a larger eccentricity in the orifice and consequently greater instability.

Notation

A	constant, Eq. (44)
$\underset{\approx}{A}$	coefficient matrix for simultaneous homogeneous equations
a	jet radius
b, b_R	complex wave number, and $2\pi/\lambda$, real wave number
$\underset{\sim}{C}^T$	arbitrary constant column vector
c	constant axial velocity
$\underset{\approx}{D}$	matrix, Eq. (37)
D/Dt	substantial derivative
d	relative wave number defined in Eq. (14)
f	empirical multiplier defined in Eq. (43)
f_a	finite-amplitude correction by Bohr, Eq. (45)
$f(r)$, $f(x,y)$	general function to represent velocity or pressure perturbation
g	x-direction velocity
g_1	relative x-direction velocity defined by Eq. (5)
h	y-direction velocity
h_1	relative y-direction velocity
I_2, I_2', I_2''	modified Bessel function of first kind (order = 2), and its first, and second-order derivatives
i	$\sqrt{-1}$
K_2, K_2', K_2''	modified Bessel function of second kind (order = 2), and its first, and second-order derivatives
L	combined variable defined in Eq. (35)
m_1, m_2, m_3, m_4	constants in Eq. (44)

P	pressure
p	pressure perturbation
Q	constant, Eq. (30)
R_1, R_2	principal radii of curvature of surface
R_i	interior Reynolds number, Eq. (33)
R_e	exterior Reynolds number, Eq. (34)
r	radial component of cylindrical coordinate
r_{max}, r_{min}	maximum and minimum jet radius
u, v, w	components of velocity in cylindrical coordinates
u_1, v_1	relative velocity components, defined in Eq. (6) and Eq. (7)
$\underset{\sim}{W}$	velocity vector
x, y, z	rectangular coordinates
$\underset{\approx}{\Delta}$	matrix, Eq. (37)
ϵ_n	damping factor
ζ	elevation of jet surface, Eq. (30)
θ	component of cylindrical coordinates
λ	wave length
μ	viscosity
ρ	density
σ	interfacial tension
Φ	function defined in Eq. (41)
$\underset{\sim}{\Omega}$	perturbation-velocity vector
$\underset{\sim}{\Omega}_1$	relative perturbation-velocity vector, Eq. (5)
ω	component of axial perturbation velocity in rectangular or cylindrical coordinates.
ω_1	relative axial perturbation velocity component

Subscripts

a	interfacial
e	exterior
i	interior
o	at the orifice plane

B. Theory

1. Summary and Extension of Bohr's Treatment

For exterior medium without viscosity, Niels Bohr linearized the Navier-Stokes equations with respect to axial, radial, and tangential velocities, treating the axial velocity as a constant term plus a small perturbation, and the radial and tangential velocities only as small perturbations. Although the axial velocity really is radially non-uniform, especially near the orifice, it appears impractical to account for such variation.

The extension of Bohr's mathematical treatment to liquid-liquid systems, although straightforward, results only in an implicit relationship between interfacial tension and the other variables. It is therefore necessary to solve it numerically for a number of cases, and to find a suitable graphical or empirical means to describe the explicit relationships.

The equations of motion for incompressible viscous flow and the equation of continuity, in vector form, are

$$\rho \frac{D\underset{\sim}{W}}{Dt} + \text{grad } P = \mu \nabla^2 \underset{\sim}{W} \tag{1}$$

$$\text{div } \underset{\sim}{W} = 0. \tag{2}$$

Taking the divergence of Eq. (1) with Eq. (2), we obtain

$$\text{div grad } P = \nabla^2 P = 0. \tag{3}$$

Following Bohr, then linearize the Navier-Stokes equations in rectangular coordinates, x,y, and z, with respective velocities g, h, and w. We set $w = c + \omega$, where c is a constant. We also assume that the velocities are of the form $f(x,y)\cdot e^{ibz}$ where b is the wave number $2\pi/\lambda$, with λ the wavelength. Then the linearized form of Eq. (1) becomes

$$\left(\nabla^2 - \frac{ibc}{\mu}\right)\underset{\sim}{\Omega} = \frac{1}{\mu}\,\text{grad } p \tag{4}$$

where $\underset{\sim}{\Omega} = \underset{\sim}{\Omega}(g,h,\omega)$; and p is the pressure perturbation. By using the following transformation, Eq. (4) can be made homogeneous:

$$\underset{\sim}{\Omega} = \underset{\sim}{\Omega}_1 + \frac{i}{cb\rho}\,\text{grad } p \tag{5}$$

where $\underset{\sim}{\Omega}_1(g_1,h_1,\omega_1)$ is a function of the transformed perturbations. We also transform to cylindrical polar coordinates r, θ, and z, with respective velocity perturbations, ω, v, u. The following transformations are used to make the equations of motion in the latter coordinates homogeneous:

$$v = \frac{i}{cb\rho}\,\frac{\partial p}{\partial r} + v_1 \tag{6}$$

$$u = \frac{i}{cb\rho}\,\frac{1}{r}\frac{\partial p}{\partial \theta} + u_1 \tag{7}$$

Thus the component equations of motion and the equation of continuity, in cylindrical polar coordinates, as obtained by Bohr, become:

$$\left(\nabla^2 - \frac{ibc\rho}{\mu}\right) v_1 - \frac{v_1}{r^2} - \frac{2}{r^2}\frac{\partial u_1}{\partial\theta} = 0 \tag{8}$$

$$\left(\nabla^2 - \frac{ibc\rho}{\mu}\right) u_1 - \frac{u_1}{r^2} + \frac{2}{r^2}\frac{\partial v_1}{\partial\theta} = 0 \tag{9}$$

$$\left(\nabla^2 - \frac{ibc\rho}{\mu}\right) \omega_1 = 0 \tag{10}$$

$$\frac{\partial v_1}{\partial r} + \frac{v_1}{r} + \frac{1}{r}\frac{\partial u_1}{\partial\theta} + \frac{\partial\omega_1}{\partial z} = 0. \tag{11}$$

Now we specify the mode of oscillation as 2, which corresponds to the type of perturbation we impose on the stream by use of an elliptical orifice. Accordingly, we suppose that p, ω_1, v_1, and u_1 have the form $f(r)\cdot e^{2i\theta+ibz}$. The substitution yields the solution to Eq. (3)

$$p = [C_1 I_2(br) + C_2 K_2(br)] \cdot e^{2i\theta+ibz} \tag{12}$$

Similarly, Eq. (12) gives the solution:

$$\omega_1 = [C_3 I_2(rd) + C_4 K_2(rd)] \cdot e^{2i\theta+ibz} \tag{13}$$

where d is defined by the relation

$$d^2 = b^2 + \frac{ibc\rho}{\mu} \tag{14}$$

Eliminating $\frac{\partial \mu_1}{\partial \theta}$ from Eqs. (10) and (13), we find for v_1

$$\left(\nabla^2 - \frac{ibc\rho}{\mu}\right)(rv_1) = -2ib\,[C_3 I_2(rd) + C_4 K_2(rd)] \cdot e^{2i\theta+ibz} \tag{15}$$

Combining a homogeneous and a nonhomogeneous part, the general solution of Eq. (20) is

$$v_1 = \left[\frac{1}{r}\{C_5 I_2(rd) + C_6 K_2(rd)\} - \frac{1b}{d}\{C_2 I_2'(rd) + C_3 K_2'(rd)\}\right] \cdot e^{2i\theta+ibz} \tag{16}$$

The continuity relation (13) between u_1, v_1, and ω_1 now yields:

$$u_1 = -r\int\left(\frac{\partial \omega_1}{\partial z} + \frac{v_1}{r} + \frac{\partial v_1}{\partial r}\right) d\theta$$

$$= \left[\frac{2b}{rd^2}\{C_3 I_2(rd) + C_4 K_2(rd)\} + \frac{id}{2}\{C_5 I_2'(rd) + C_6 K_2'(rd)\}\right] \cdot e^{2i\theta+ibz} \tag{17}$$

2. Boundary Conditions for Liquid-Liquid System

The foregoing derivation retraces the steps taken by Bohr for solving the free-jet problem. Now, the introduction of new boundary conditions orients the derivation toward a new result. Here we note that the velocities are finite at $r = 0$ and $r \to \infty$. Therefore, for the interior fluid, the constants multiplying the modified Bessel function of the second kind K_2 and its derivative K_2' must be zero; and for the exterior fluid, the constant multipliers of the modified Bessel functions of the first kind I_2 and its derivative I_2' must be zero.

Therefore the axial, radial, and tangential velocities are, for the interior fluid:

$$w_i = c + \omega_i = c - \left\{\frac{C_1}{c\rho_i} I_2(br) - C_3 I_2(d_i r)\right\} e^{2i\theta+ibz} \tag{18}$$

$$v_i = \left\{\frac{i}{c\rho_i} C_1 I_2'(br) - \frac{ib}{d_i} C_3 I_2'(d_i r) + \frac{C_5}{r} I_2(d_i r)\right\} e^{2i\theta+ibz} \tag{19}$$

$$u_i = \left\{- \frac{2}{cb\rho_i} \frac{1}{r} C_1 I_2(br) + \frac{2bC_3}{rd_i^2} I_2(d_i r) + \frac{id_i C_5}{2} I_2'(d_i r)\right\} e^{2i\theta+ibz} \tag{20}$$

and, for the exterior fluid:

$$w_e = c + \omega_e = c - \left\{\frac{C_2}{c\rho_e} K_2(br) - C_4 K_2(d_e r)\right\} e^{2i\theta+ibz} \tag{21}$$

$$v_e = \left\{\frac{i}{c\rho_e} C_2 K_2'(br) - \frac{ib}{d_e} C_4 K_2'(d_e r) + \frac{C_6}{r} K_2(d_e r)\right\} e^{2i\theta+ibz} \tag{22}$$

$$u_e = \left\{ - \frac{2}{cb\rho_e} \frac{1}{r} C_2 K_2(br) + \frac{2bC_4}{rd_e^2} K_2(d_e r) + \frac{id_e C_6}{2} K_2'(d_e r) \right\} \cdot e^{2i\theta + ibz} \tag{23}$$

These six velocity equations contain six unknown constants, C_1, C_2, C_3, C_4, C_5, and C_6, which are to be determined by the following six boundary conditions, namely the continuity of velocities at the interface ($r = a$), and the continuity of stresses at the interface.

Continuity of velocities corresponds to

$$w_{ia} = w_{ea}, \quad v_{ia} = v_{ea}, \quad u_{ia} = u_{ea} \tag{24,25,26}$$

Continuity of normal stresses gives, to first approximation,

$$-P_e + 2\mu_e \left(\frac{\partial v_e}{\partial r}\right)_a = -P_i + 2\mu_i \left(\frac{\partial v_i}{\partial r}\right)_a + \left(\frac{1}{R_1} + \frac{1}{R_2}\right)\sigma \tag{27}$$

Continuity of tangential stresses gives, similarly,

$$\mu_e \left(\frac{\partial w_e}{\partial r} + \frac{\partial v_e}{\partial z}\right)_a = \mu_i \left(\frac{\partial w_i}{\partial r} + \frac{\partial v_i}{\partial z}\right)_a \tag{28}$$

Continuity of axial stresses gives, similarly,

$$\mu_e \left(\frac{\partial u_e}{\partial r} - \frac{u_e}{r} + \frac{1}{r}\frac{\partial v_e}{\partial \theta}\right)_a = \mu_i \left(\frac{\partial u_i}{\partial r} - \frac{u_i}{r} + \frac{1}{r}\frac{\partial v_i}{\partial \theta}\right)_a \tag{29}$$

In Eq. (27), σ is the interfacial tension, and R_1 and R_2 are the principal radii of curvature of the interface.

The equation of the surface is postulated to be:

$$r - a = \zeta = Qe^{2i\theta + ibz} \tag{30}$$

The boundary-surface continuity condition is:

$$\frac{D}{Dt}(r-a-\zeta) = 0. \tag{31}$$

These combine to give (to first-order approximation):

$$\frac{1}{R_1} + \frac{1}{R_2} = \frac{1}{a} - \frac{\zeta}{a^2} - \frac{1}{a^2}\frac{\partial^2\zeta}{\partial\theta^2} - \frac{\partial^2\zeta}{\partial z^2} = \frac{1}{a} - v_i\,\frac{i(3 + b^2a^2)}{a^2bc} \tag{32}$$

Here, the equilibrium normal pressure difference, $(P_i - p_i) - (P_e - p_e)$, is balanced by the equilibrium interfacial tension, σ/a.

3. Exact Expression for σ

If we now substitute the proper quantities, obtained from the velocity relations, into the boundary conditions, we obtain six homogeneous linear equations with six unknown constants. If we express the equations as $\underset{\approx}{A}\underset{\sim}{C} = 0$, where $\underset{\sim}{C}^T = [C_1, C_2, C_3, C_4, C_5, C_6]$, then $A_{jk}(j,k = 1,6)$ are given as follows (zero-valued elements are omitted):

$$A_{11} = I_2(ba)$$

$$A_{12} = -K_2(ba)$$

$$A_{13} = -I_2(d_i a)$$

$$A_{14} = K_2(d_e a)$$

$$A_{21} = iI_2'(ba)$$

$$A_{22} = -iK_2'(ba)$$

$$A_{23} = -\frac{iba}{d_i a} I_2'(d_i a)$$

$$A_{24} = \frac{iba}{d_e a} K_2'(d_e a)$$

$$A_{25} = I_2(d_i a)$$

$$A_{26} = -K_2(d_e a)$$

$$A_{31} = \frac{2I_2(ba)}{ba}$$

$$A_{32} = -\frac{2K_2(ba)}{ba}$$

$$A_{33} = -\frac{2baI_2(d_i a)}{(d_i a)^2}$$

$$A_{34} = \frac{2baK_2(d_e a)}{(d_e a)^2}$$

$$A_{35} = -i\,\frac{d_i aI_2'(d_i a)}{2}$$

$$A_{36} = i\,\frac{d_e aK_2'(d_e a)}{2}$$

$$A_{41} = \mu_i \left\{ 2iba I_2''(ba) - \frac{R_i I_2(ba)}{2} \right\} - i\sigma L I_2'(ba)$$

$$A_{42} = -\mu_e \left\{ 2iba K_2''(ba) + \frac{R_e K_2(ba)}{2} \right\}$$

$$A_{43} = -2i\mu_i ba I_2''(d_i a) - i \frac{ba\sigma L}{d_i a} I_2'(d_i a)$$

$$A_{44} = 2i\mu_e ba K_2''(d_e a)$$

$$A_{45} = 2\mu_i \{ d_i a I_2'(d_i a) - I_2(d_i a) \} - \sigma L I_2(d_i a)$$

$$A_{46} = -2\mu_e \{ d_e a K_2'(d_e a) - K_2(d_e a) \}$$

$$A_{51} = 2\mu_i ba I_2'(ba)$$

$$A_{52} = -2\mu_e ba K_2'(ba)$$

$$A_{53} = -\mu_i \left\{ d_i a + \frac{(ba)^2}{d_i a} \right\} I_2'(d_i a)$$

$$A_{54} = \mu_e \left\{ d_e a + \frac{(ba)^2}{d_e a} \right\} K_2'(d_e a)$$

$$A_{55} = -i\mu_i ba I_2(d_i a)$$

$$A_{56} = i\mu_e ba K_2(d_e a)$$

$$A_{61} = 4\mu_i \left\{ I_2'(ba) - \frac{I_2(ba)}{ba} \right\}$$

$$A_{62} = -4\mu_e \left\{ K_2'(ba) - \frac{K_2(ba)}{ba} \right\}$$

$$A_{63} = -\frac{4\mu_i ba}{d_i a} \left\{ I_2'(d_i a) - \frac{I_2(d_i a)}{d_i a} \right\}$$

$$A_{64} = \frac{4\mu_e ba}{d_e a} \left\{ K_2'(d_e a) - \frac{K_2(d_e a)}{d_e a} \right\}$$

$$A_{65} = -i\mu_i \left\{ \frac{(d_i a)^2 I''_2(d_i a)}{2} - \frac{(d_i a) I_2'(d_i a)}{2} + 2I_2(d_i a) \right\}$$

$$A_{66} = i\mu_e \left\{ \frac{(d_e a)^2 K_2''(d_e a)}{2} - \frac{(d_e a) K_2'(d_e a)}{2} + 2K_2(d_e a) \right\}$$

where

$$R_i = \frac{2ac\rho_i}{\mu_i} \text{ (interior Reynolds number)} \tag{33}$$

$$R_e = \frac{2ac\rho_e}{\mu_e} \text{ (exterior Reynolds number)} \tag{34}$$

$$L = i \left\{ \frac{3 + (ba)^2}{(ba)c} \right\} \tag{35}$$

We do not need to evaluate explicitly the C values, since we are interested only in a relation between interfacial tension and the wavelength of oscillation. The six linear homogeneous equations for the constants $\underset{\sim}{C}$ can have a nontrivial solution only if the determinant of

the coefficients vanishes. This furnishes the following eigenvalue equation relating interfacial tension to the wavelength of oscillation;

$$\det \underset{\approx}{A} = 0. \tag{36}$$

Equation (36) can be solved for the interfacial tension in the following manner:

$$\det \underset{\approx}{A} = \det \underset{\approx}{D} + \sigma \det \underset{\approx}{\Delta} \tag{37}$$

Hence

$$\sigma = - \frac{\det \underset{\approx}{D}}{\det \underset{\approx}{\Delta}} \tag{38}$$

Here $\underset{\approx}{D}$ is a matrix obtained by replacing the fourth-row elements of the matrix $\underset{\approx}{A}$ by the following terms:

$$A_{41} = \mu_i \left\{ 2iba I_2''(ba) - \frac{R_i I_2(ba)}{2} \right\}$$

$$A_{43} = -2i\mu_i ba I_2''(d_i a)$$

$$A_{45} = 2\mu_i \{ d_i a I_2'(d_i a) - I_2(d_i a) \}$$

Also, $\underset{\approx}{\Delta}$ is a matrix generated by replacing the fourth row of the matrix $\underset{\approx}{A}$ by the following terms:

$$A_{41} = -iLI_2'(ba) \qquad A_{45} = -LI_2(d_i a)$$

$$A_{43} = -i\,\frac{baL}{d_i a}\,I_2'(d_i a) \qquad A_{42} = A_{44} = A_{46} = 0\ .$$

From Eq. (38), σ can be evaluated numerically for given values of c, ba, R_i, R_e, μ_i and μ_e. Furthermore, by re-expressing the terms in the determinants as functions of dimensionless groups, the Weber number becomes a function of Reynolds number, dimensionless wave number, density ratio, and viscosity ratio:

$$\frac{c^2 a\rho_i}{\sigma} = \text{fn.}\left(R_i,\quad ba,\quad \frac{\rho_e}{\rho_i},\ \frac{\mu_e}{\mu_i}\right) \tag{39}$$

Equations (38) and (39) both conform to the eventual objective of this analysis, namely to observe an internodal distance and from it to determine the local value of σ. Numerical evaluation of det $\underset{\approx}{D}$ and det $\underset{\approx}{\Delta}$, so as to interrelate the dimensionless groups, has been accomplished on a digital computer (Control Data Corporation 6600) by use of a standard Gaussian reduction method.

Actually, because of the complex-number arithmetic introduced by the algebraic form of the velocity function $[f(r)\cdot e^{in\theta}\cdot e^{ibz}]$, a purely real-number b will give a complex-number σ without physical significance, and some complex-number b is needed to obtain a purely real-number σ. Thus,

$$b_n = b_R + i\epsilon_n \qquad (n = 1, 2, \ldots.) \tag{40}$$

In fact there are an infinite number of ϵ's and σ's for a given b_R. However, the oscillation will be dominated by the b with the smallest positive imaginary part, i.e., the smallest damping factor ϵ_1; the oscillations of wavelength given by all b's with larger ϵ's should rapidly be damped out.

For a given b_R, an iterative scheme (reguli-falsi method) has been explored to obtain the lowest positive value of ϵ that makes the imaginary part of σ vanish. The lowest damping factor ϵ_1 seems to be a complicated function of Reynolds number and other variables; related behavior of damping factors for capillary jets was found by Goren and Wronski.[15] As a matter of fact, one or more ϵ's usually lie within the range of 0 to 0.15; within this range, adjustments of b in the foregoing manner do not appreciably change the value of the real part of the interfacial tension. Consequently most of the calculations have been carried out without solving for a damping factor.

4. Empirical Expression for σ

With the analytical solution now solved numerically, it has seemed desirable to obtain an explicit formula to describe the Weber number as a function of the other four dimensionless variables given in Eq. (39). As a point of departure, the Rayleigh solution (20) for a perfect-fluid jet in a gas can be rearranged into the same dimensionless grouping:

$$\left(\frac{c^2 a\rho_i}{\sigma}\right) = \frac{I_2'(b_R a)}{I_2(b_R a)} \left\{\frac{3 + (b_R a)^2}{(b_R a)}\right\} \equiv \Phi(b_R a) \tag{41}$$

For convenience in evaluating $\Phi(b_R a)$, its relation to $(b_R a)$ is plotted in Fig. 1. By expanding $I_2(b_R a)$ in a Taylor series, $\Phi(b_R a)$ can be approximated as

$$\Phi(b_R a) \sim \frac{6}{(b_R a)^2} \left\{1 + \frac{5}{12}(b_R a)^2 + \frac{5}{192}(b_R a)^4\right\} \tag{42}$$

The Bohr formula[11] for a viscous-fluid jet in an inviscid fluid, with the finite-amplitude correction factor omitted for the time being, becomes

$$\left(\frac{c^2 a\rho_i}{\sigma}\right) = \Phi(b_R a) \cdot \frac{1}{\left\{1 + 2\left(\frac{4}{R_i b_R a}\right)^{3/2} + 3\left(\frac{4}{R_i b_R a}\right)^2\right\}\left(1 + \frac{\rho_e}{\rho_i}\right)} \tag{43}$$

In this way, Bohr's terms pertaining to interior-fluid viscosity and exterior-fluid density appear as simple multipliers modifying the Rayleigh solution.

Thus it appeared reasonable that a satisfactory empirical treatment of the liquid-liquid jet solution also would be found by developing a multiplier for the Rayleigh formula, one that describes the effect of exterior viscosity and density. If we designate the multiplier as f, such an equation can be expressed as,

$$\frac{c^2 a \rho_i}{\sigma} = \Phi(b_R a) \cdot f \tag{44}$$

Because $f \to 1$ as (μ_e/μ_i) or $(\rho_e/\rho_i) \to 0$, the following empirical form for f has been assumed:

$$f = \frac{1}{\left\{1 + A(R_i)^{m_1}(b_R a)^{m_2}(\mu_e/\mu_i)^{m_3}(\rho_e/\rho_i)^{m_4}\right\}} \tag{45}$$

Constants A, m_1, m_2, m_3, and m_4 have been determined from a set of exact results, by linear regression of values of f given by ratios of the exact Weber number to $\Phi(b_R a)$.

Before applying the linear regression, the separate effect of each dimensionless group was checked by changing it parametrically at fixed values of the other groups. As shown in Figs. 2 and 3, a plot of $\log[(1/f) - 1]$ against each dimensionless variable falls on a group of parallel lines, thus supporting the assumed form of correction. At low R_i, whether because of error in the computed result or in f, the

behavior given by Eq. (45) breaks down when the product of $R_i b_R a$ falls below 200. However, in successful experiments of liquid-liquid oscillating jet, all the data fall above $R_i b_R a = 200$. Therefore in applying the least-square method, the numerical result for cases where $R_i b_R a < 200$ has been omitted. Ninety-nine sets of data have been used to determine the constants; the ranges selected for the respective variables were as follows:

$$400 < R_i < 2000, \qquad 0.25 < b_R a < 1.0$$

$$0.25 < \mu_e/\mu_i < 10.0 \qquad 0.2 < \rho_e/\rho_i < 2.0$$

The linear-regression method has given the constants as follows;

$$A = 1.437$$

$$m_1 = -0.0502, \quad m_2 = -0.141, \quad m_3 = 0.0285, \quad m_4 = 0.897$$

with a standard deviation of 0.004 and a maximum deviation of ± 0.012; this corresponds to a maximum percentage error of ± 3%. The empirical function thus obtained and the data used for the calculations, plus 45 additional data, are plotted in Fig. 4. The exponents found from the regression indicate that the most significant dimensionless group is the density ratio, and that the other variables have only a secondary effect.

Also, the simpler Bohr formula as given in Eq. (43) can predict an interfacial-tension value within ± 10%, but such accuracy is probably

not sufficient in comparison with the expected accuracy for λ, a, and the physical properties.

Bohr also found it necessary to correct the foregoing theory to account for the finite amplitude of oscillation. Using the equation of continuity and the boundary-surface condition, and expanding the latter to a third-order approximation, he obtained a correction factor that is also applicable to the present problem:

$$f_a = \frac{1}{1 + \frac{37}{24}\left\{\frac{r_{max} - r_{min}}{r_{max} + r_{min}}\right\}^2} \tag{46}$$

where r_{max} and r_{min} respectively are the semimajor and semiminor elliptical axes at the nodes or antinodes. Collecting all the correction factors gives the complete solution:

$$\left(\frac{c^2 a \rho_i}{\sigma}\right) = \Phi(b_R a) \cdot f \cdot f_a \tag{47}$$

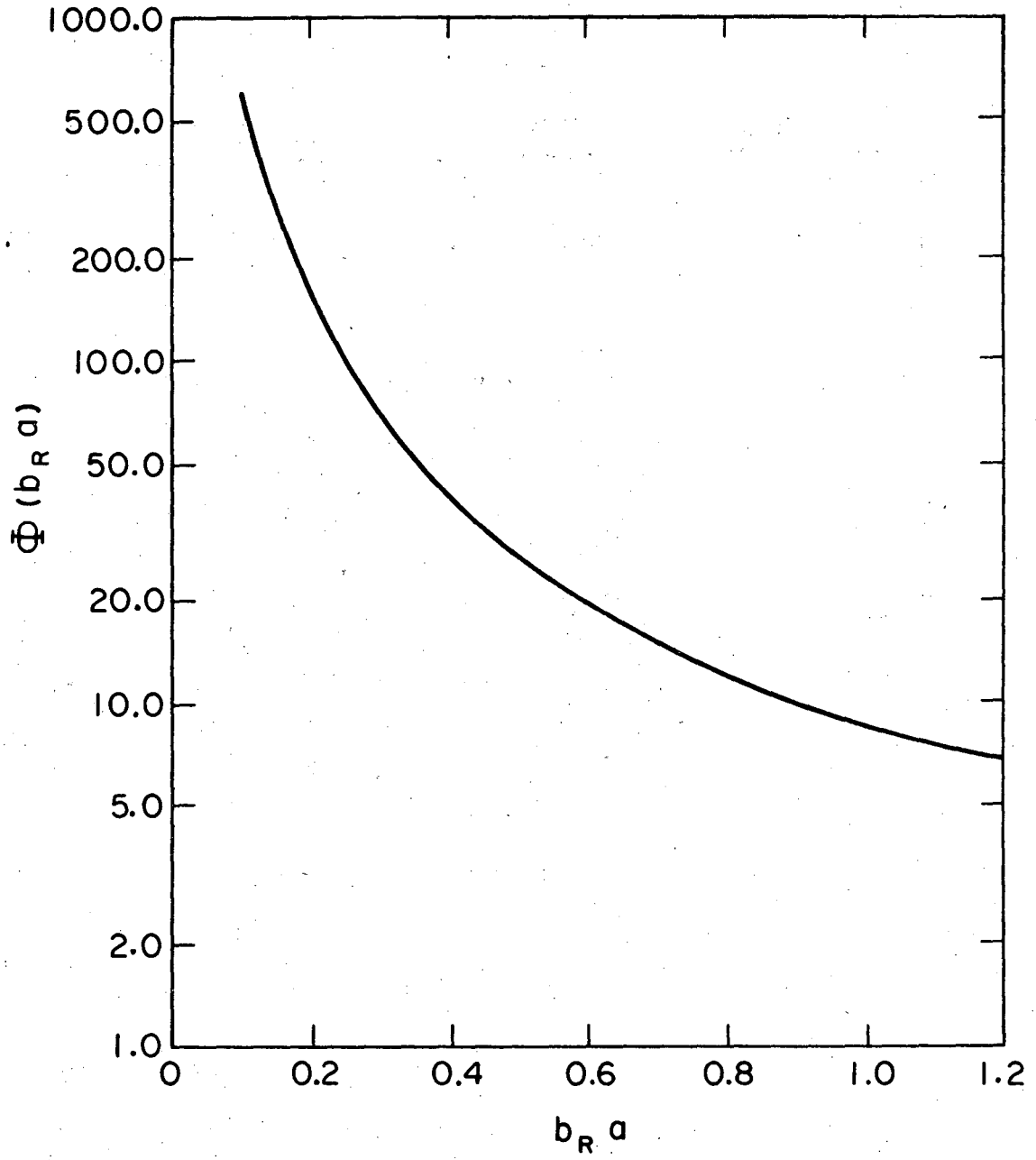

XBL 6811-7200

Fig. 1 Dependence of Rayleigh solution Φ upon dimensionless wave number $b_k a$.

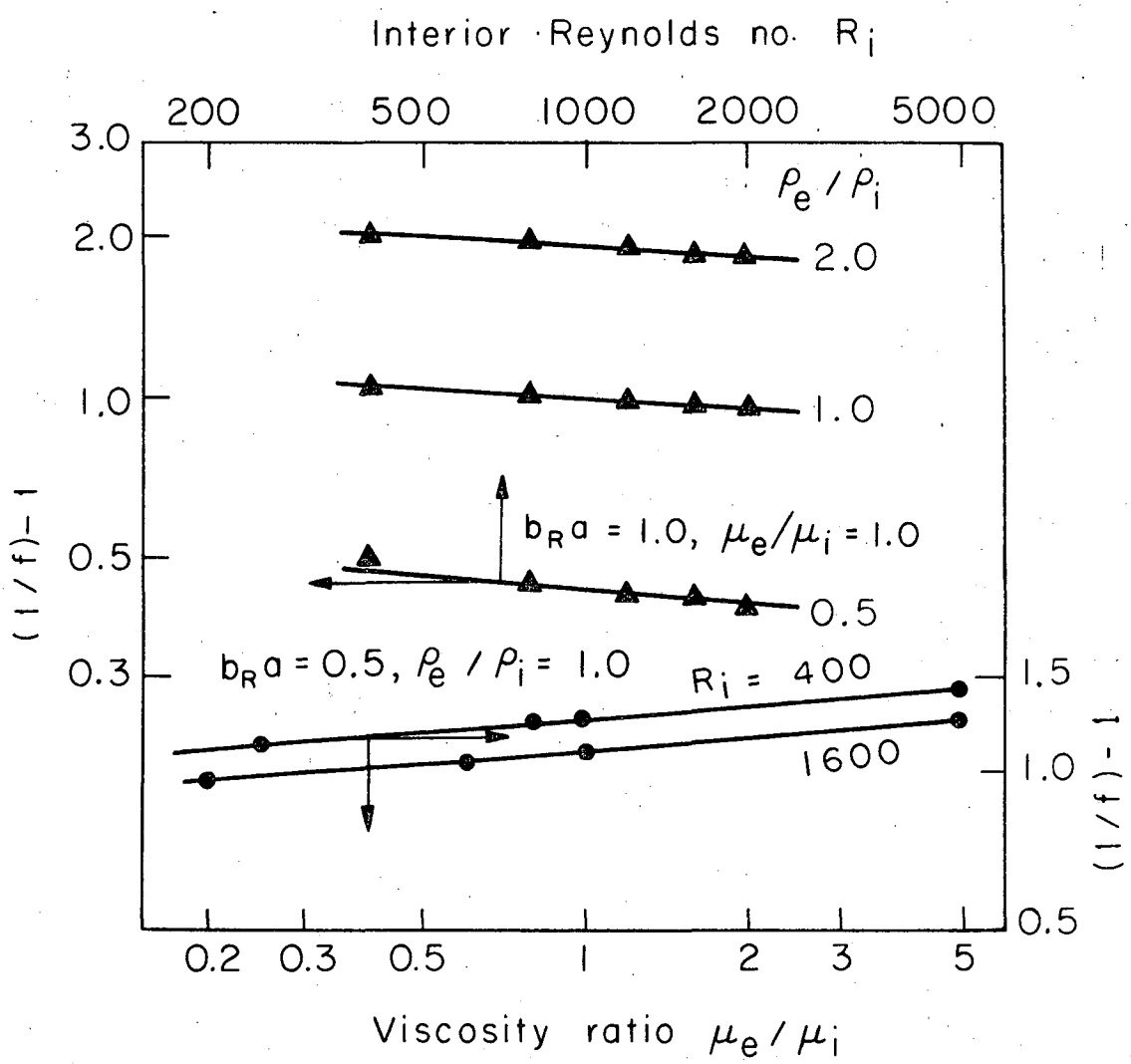

XBL6811-7197

Fig. 2 (1/f)- 1 vs. μ_e/μ_i and R_i.

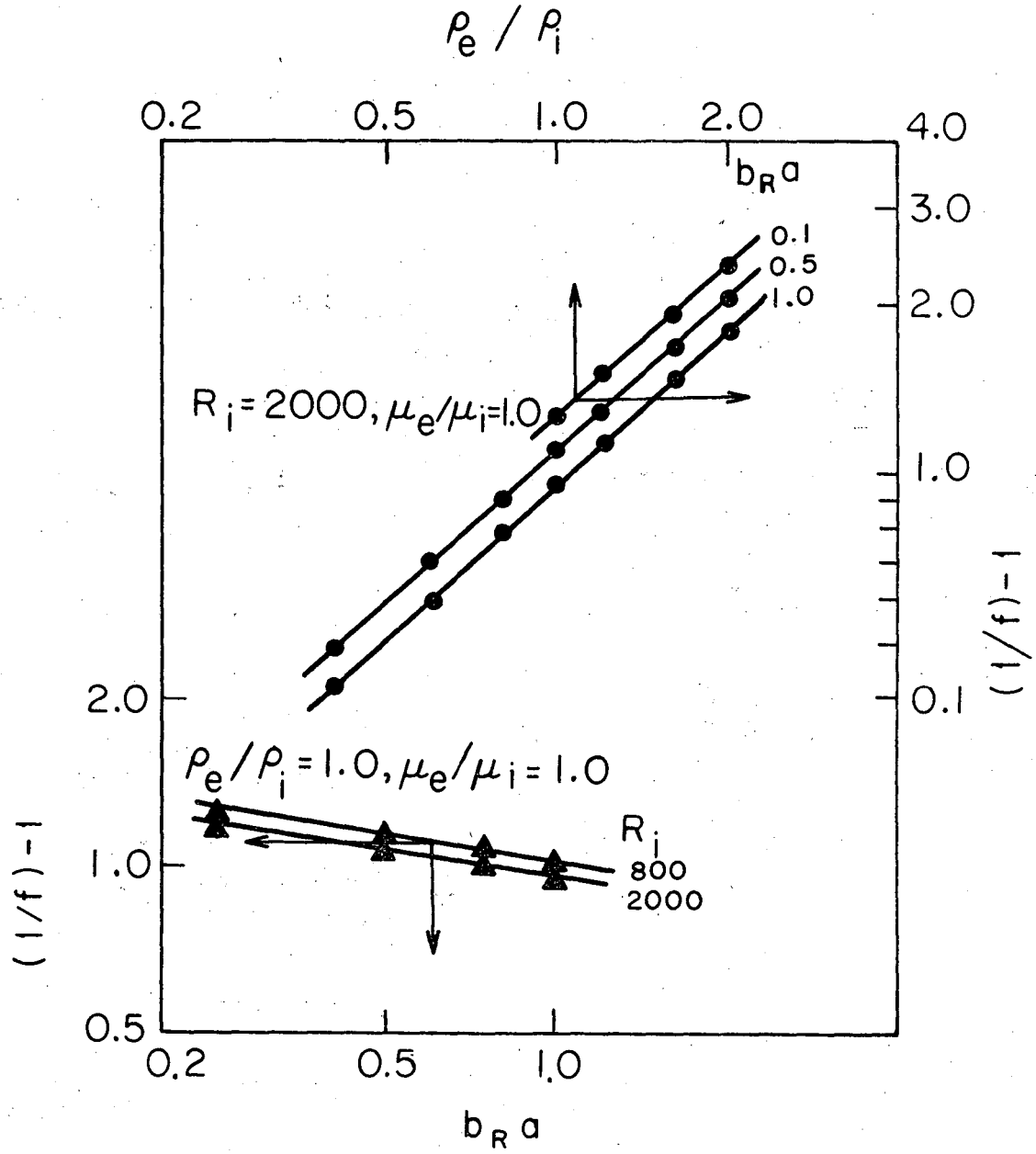

XBL6811-7198

Fig. 3 (1/f)- 1 vs ρ_e/ρ_i and $b_R a$.

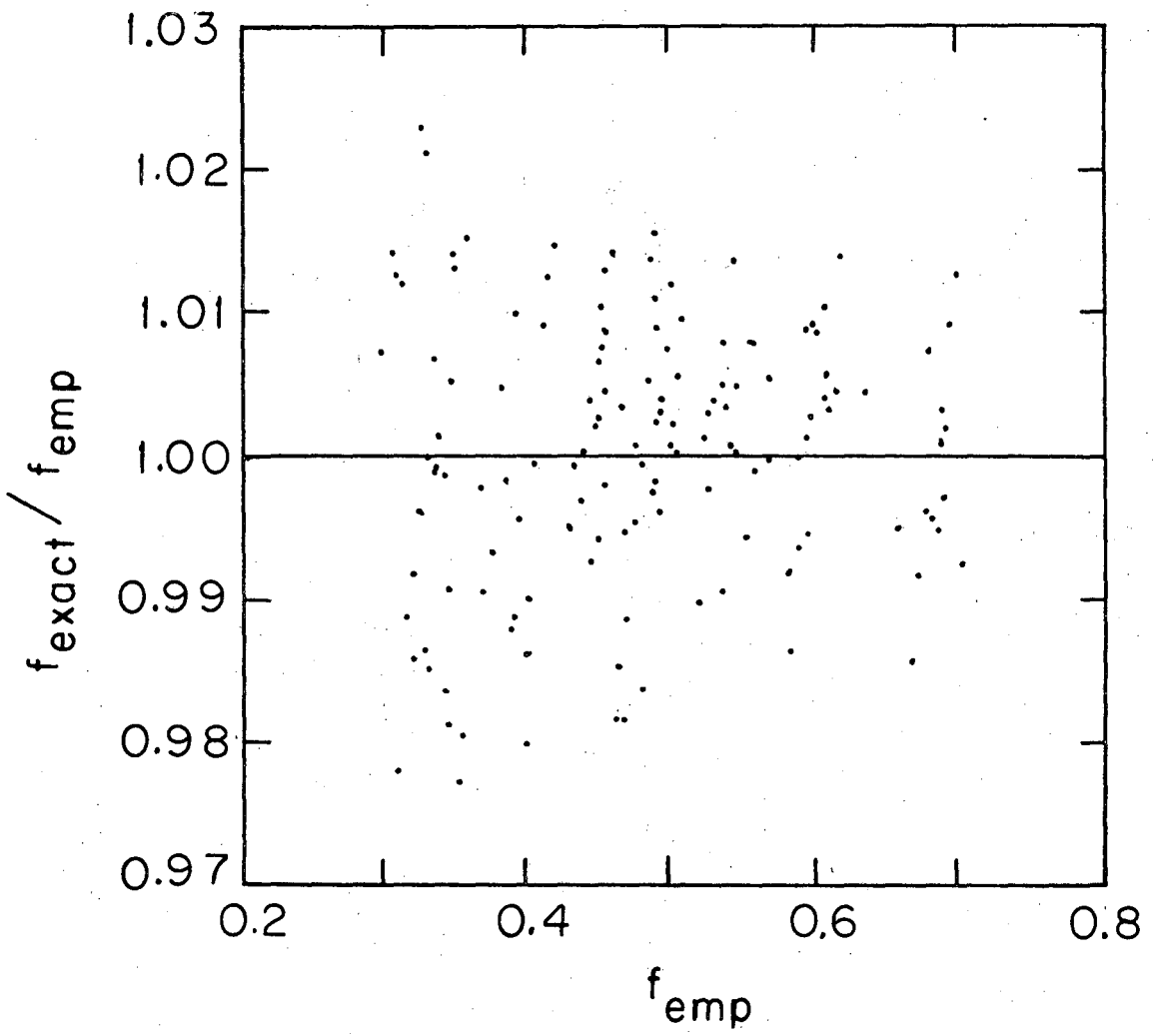

XBL6811-7206

Fig. 4 Comparison of empirical liquid-liquid correction function with exact computed values.

C. Experimental Study

1. Experimental

From the foregoing theoretical analysis, it is seen that the quantities that must be measured to calculate the interfacial tension are: the wavelength of the oscillations, the jet velocity, the maximum and minimum diameters of the jet at the place of measurement, and the densities and viscosities of the two liquids.

A schematic diagram of the flow system used to obtain the jet measurements is shown in Fig. 5. The valve in the line ahead of the nozzle allows for varying the flow rate without moving the reservoir. The jet fluid collected overflows from the bottom of the chamber, while the second-phase fluid is kept stationary. The wavelength and the maximum and minimum diameters of the jet were measured photographically. The photographs of the jet were taken with a 135-mm Pacemaker Graphic camera with a magnification of about 2×. The nozzle was used as a reference to determine the exact magnification ratio in the photographs. Measurement of the negatives thus obtained, which involved further magnification of 4×, was done with a Vanguard Motion Analyzer which was accurate to 0.001 in. However, there is a difficulty of determining the exact maximum or minimum of the wave, and the estimated error in the dimension measurements amounts to ±5%.

One of the more difficult problems is the preparation of the elliptical nozzle that conforms to a mathematically precise shape. Trials of several different methods indicated that the best nozzles could be made by heating glass capillary tubing in a flame, drawing it

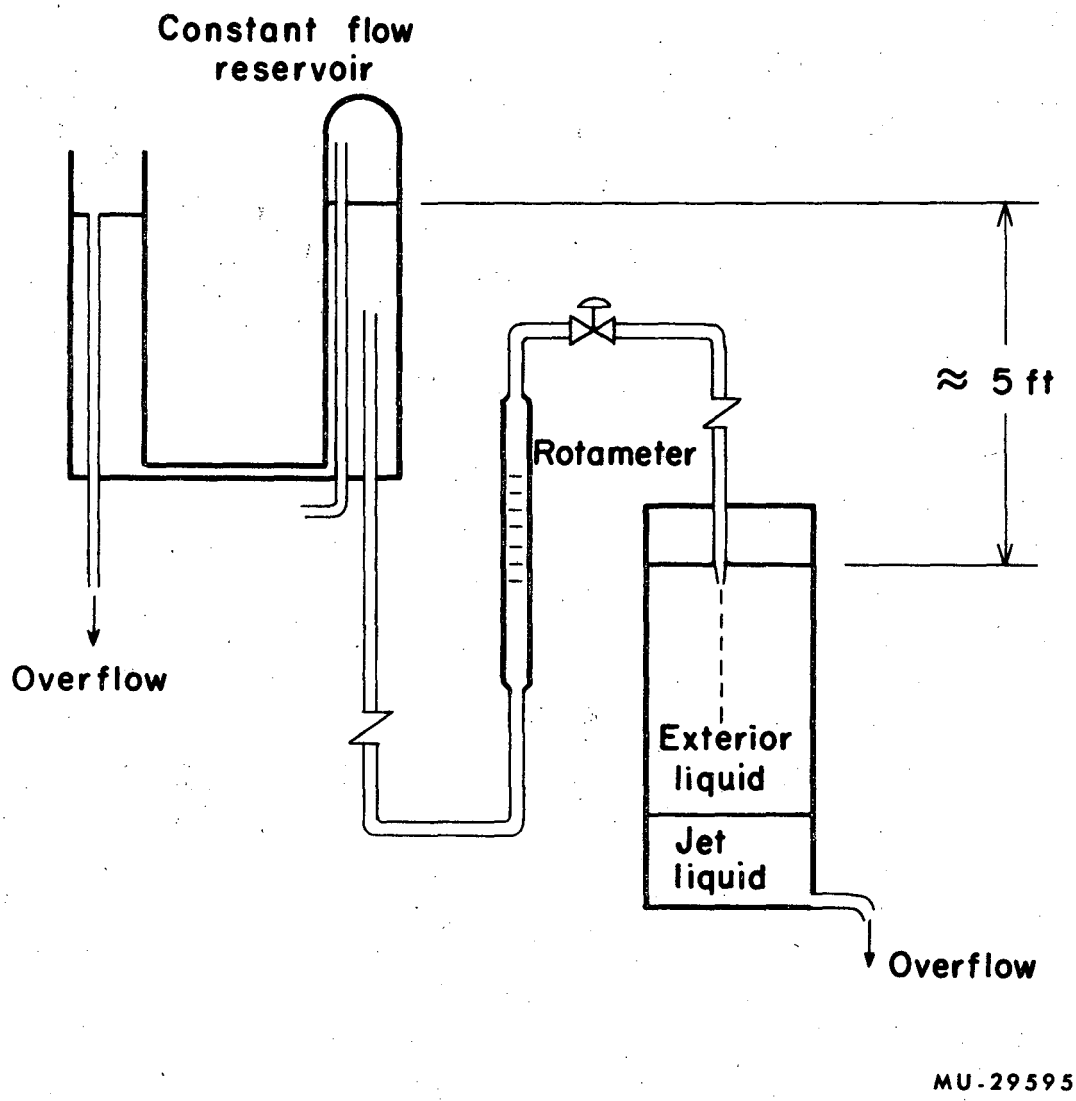

Fig. 5 Flow diagram.

to obtain a finer capillary, pressing the tip between flat graphite plates to form an elliptical cross section, and then removing part of the tip. The nozzles thus produced were as short as 4 cm; since the inside diameter of the tubing was about 0.05 cm, the length-to-diameter ratios were well above 50, which is sufficient to insure a fully developed flow at the Reynolds numbers which were used. The dimensions of the four nozzles are given in Table I. Figure 6 shows photographs of the nozzle cross-sections. Because of their large "shelf" errors these nozzles are not suitable for the study of a jet in a moving surrounding liquid, as discussed in the closing paragraph.

2. Physical Properties

The liquids that were used in the experiments were di-isobutyl ketone(DIBK), cumene (isopropyl benzene), normal heptane, carbon tetrachloride, isoamyl alcohol, and water. Water was always taken as one phase, and an organic compound as the other. The two phases were mutually saturated before the run so as to avoid any mass transfer between the phases during the run. The viscosities were measured with an Oswald viscometer, calibrated with water. Density measurements were made with a pycnometer. The interfacial tension was measured with a DuNouy ring tensiometer. The properties of the liquids used are given in Table II.

3. Results

As the theory would predict, the wavelength of the jet depends very strongly on the velocity and the interfacial tension. When the jet velocity was decreased, more waves - which were each shorter - became

Table I. Nozzle dimensions.

Nozzle No.	Max diam. (cm)	Min diam. (cm)	Area (cm^2) $\times 10^3$	Equivalent circular radius (cm)
1	0.109	0.061	5.19	0.0406
2	0.100	0.055	4.34	0.0371
3	0.108	0.061	5.17	0.0406
4	0.139	0.064	7.03	0.0472

Table II. Physical properties of liquids used.

Compound	Density (g/cm^3)	Viscosity (g/cm-sec)	Interfacial tension against water (25°C) (dyne/cm)
Water	1.00	0.0091	--
Cumene	0.86	0.0080	35.6
n-Heptane	0.68	0.0049	42.2
Carbon tetrachloride	1.59	0.0091	41.4
Di-isobutyl ketone	0.81	0.0086	21.5
Isoamyl alcohol	0.81	0.0360	6.1

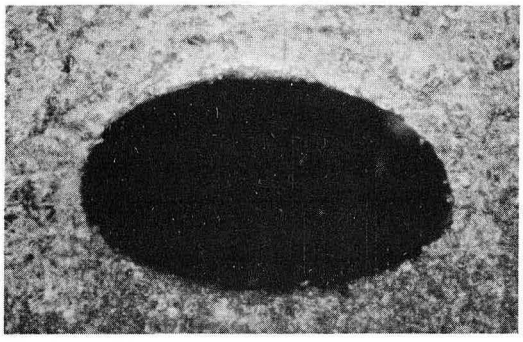

nozzle no. 1

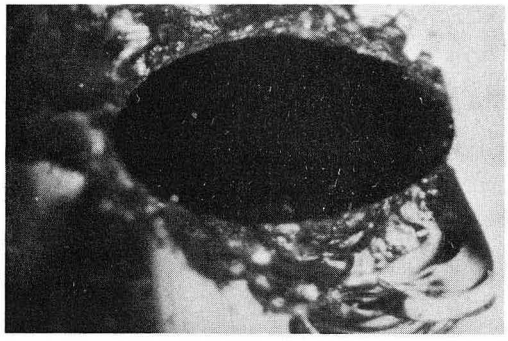

nozzle no. 2

0 5 1.0 1.5 mm

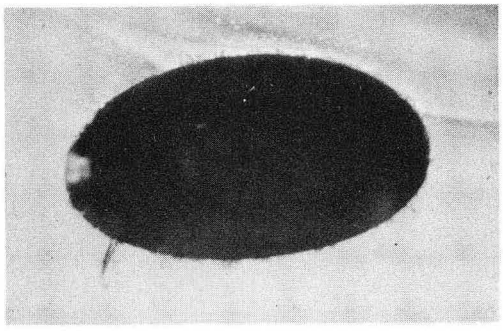

nozzle no. 3

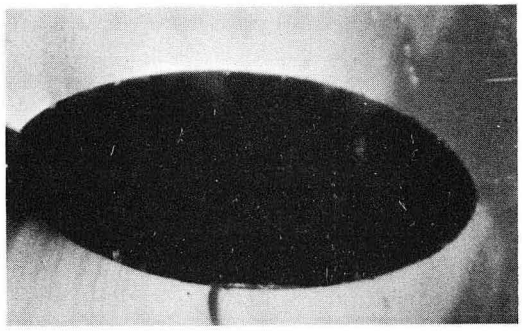

nozzle no. 4

XBB 6812-7391

Fig. 6. Nozzles used in experimental measurements.

visible. A still further decrease caused the waves to blur and disappear, giving a cylindrical jet with a diameter near that of the equivalent diameter of the nozzle. At the maximum velocity used, only about one-half wavelength remained visible before the jet broke up into droplets. Runs were generally made at or near the velocity at which the greatest number of waves was visible.

It is possible to use either the denser or the less dense liquid as the jet phase. Two of the systems used were run successfully both ways: DIBK-water and cumene-water. When the less dense liquid is the jet phase, the jet is directed vertically upward. The opposite is true with the more dense liquid as the jet phase. Theoretical considerations indicate, for the jet dimensions and flow conditions used, that gravity plays no measurable part in the oscillations.

There are two problems in applying the theory to interpret the experimental data.

First, because the jet is ejected into a stationary secondary phase, the bulk axial velocity profiles in each phase is not uniform as assumed in the theory. The velocity gradient near the interface is not zero and does not give a small "sleeve" as in a liquid-gas jet. Therefore one cannot simply take an interfacial velocity as representing a constant velocity for the jet.

Second, there is a change in the radius of a jet; initially contraction (termed the <u>vena contracta</u>) due to momentum relaxation, and then expansion due to the momentum diffusion into the fluid. Therefore, it is more suitable to use, as a constant jet radius, the

mean radius at the place where the wavelength is measured rather than the equivalent circular radius of the nozzle.

Experimental data obtained for seven sets of systems are given in Table III. Systems are numbered from 1 to 7, and the jet liquid is always named first. Distance is taken from the orifice plane to the plane at which wavelength and the maximum and minimum diameters are measured. The average velocity at the orifice is used as a reference velocity.

From a number of representative experimental data, a correlation was sought between a representative local jet velocity which corresponds to c and an interfacial velocity w_a at the point of measurement. The interfacial velocity w_a was calculated using a method developed by the present authors.[24] The representative local velocity c, which is termed an "effective plug-flow velocity," was calculated from the maximum and minimum diameters, wavelength, interior Reynolds number, viscosity ratio, and the actual interfacial-tension value, by use of Eq. (47). The calculated results indicate that the ratio of c/w_a is dependent on the viscosity ratio for the two liquids, but independent of the density ratios. The ratio c/w_a approaches 1 as the viscosity ratio diminishes to zero; this is consistent with the observation of others that the surface velocity can be adopted as the effective plug-flow velocity of a liquid-gas jet. Also c/w_a must approach 1 as the velocity profile becomes flat.

Therefore the following empirical equation was assumed:

$$c = w_a + \alpha\{w_o(a_o/a)^2 - w_a\}(\mu_e/\mu_i)^n \tag{48}$$

Table III. Oscillation data.

System	Nozzle no.	Max. diam. (cm)	Min. diam. (cm)	Wave-length (cm)	Flow-rate (cm^3/s)	Av. vel. at inlet (cm/s)	Calc. or actual σ (dyne/cm)
1	2	0.067	0.044	0.322	0.625	144	47.6
	2	0.063	0.055	0.308	0.505	116	33.3
	2	0.071	0.042	0.426	0.840	194	52.0
	1	0.088	0.057	0.535	0.995	192	50.0
	Actual						42.2
2	1	0.072	0.056	0.500	0.615	119	21.1
	1	0.071	0.055	0.408	0.515	99	21.0
	2	0.076	0.040	0.452	0.500	115	20.7
	3	0.069	0.064	0.452	0.530	102	19.1
	Actual						21.5
3	1	0.087	0.062	0.519	0.599	116	30.0
	1	0.085	0.069	0.364	0.448	86	31.5
	3	0.075	0.062	0.356	0.418	96	36.5
	3	0.085	0.054	0.439	0.500	115	37.8
	Actual						41.4
4	4	0.068	0.057	0.665	0.455	65	5.90
	1	0.086	0.038	1.086	0.600	116	5.68
	4	0.070	0.054	0.806	0.615	87	7.42
	1	0.078	0.052	0.802	0.485	94	5.81
	Actual						6.1
5	1	0.074	0.059	0.392	0.645	124	34.9
	2	0.075	0.050	0.384	0.605	139	37.2
	2	0.079	0.048	0.499	0.695	160	33.4
	4	0.094	0.080	0.623	0.990	141	32.7
	Actual						35.6
6	4	0.086	0.074	0.532	0.831	118	23.3
	1	0.083	0.063	0.559	0.746	114	15.0
	4	0.099	0.065	0.625	0.977	139	25.3
	2	0.083	0.060	0.715	0.887	204	25.7
	Actual						21.5
7	1	0.074	0.068	0.332	0.512	99	27.9
	4	0.085	0.067	0.445	0.823	117	33.1
	4	0.089	0.074	0.432	0.905	129	43.2
	2	0.076	0.053	0.520	0.834	192	36.6
	Actual						35.6

*) System:

1 Water - n-heptane
2 Water - DIBK
3 CCl_4 - water
4 Water - iso-amyl alc.
5 Water - cumene
6 DIBK - water
7 Cumene - water

Constants α and n were determined empirically as $\alpha = 0.3$, $n = 0.25$.

Using the effective plug-flow velocity obtained from the viscosity ratio and the calculated interfacial velocity in Eq. (48), the interfacial tension can be calculated by the exact computer program, or more efficiently by the empirical correlation of Eq. (47). The experimental data of Table III were analyzed in this manner to get the interfacial tension. Velocity data for the calculation are given in Table IV. The calculated interfacial tensions, also shown in Table III, are plotted against the actual values in Fig. 7.

Some investigators[13] who have studied the liquid-gas oscillating jets reported that each nozzle gives a wavelength that must be correlated for the nozzle's deviation from an ellipse. However, the present data do not seem to give such a definite trend. Comparison of the calculated interfacial tension with the actual value in Fig. 7 shows considerable scatter, especially when the jet fluid is lighter than the exterior fluid. The results are better for those systems in which it was possible to obtain four or more waves: water into DIBK, and water into cumene. Water into isoamyl alcohol gave only about 2.5 waves; however, because of extremely low interfacial tension, its long wavelength gave jets as long as the others, and it could be measured with high accuracy.

4. Discussion

Instead of adopting an effective plug-flow velocity, it might be possible to correlate the apparent increase in the wavelength that results from the radial gradient of axial velocity. However, since such a treatment would still be empirical, it is likely that similar accuracy would be obtained despite the greater numerical complexity.

Table IV. Velocity data.

System	Dimensionless distance, z	Interior Reynolds no., R_i	$(z/a_o R_i)$	Interfacial vel., w_a/w_o	c/w_a calc. from Eq.(48)
1	33.4	1180	0.0284	0.740	1.01
	24.5	946	0.0256	0.737	0.953
	23.3	1380	0.0169	0.703	0.965
	25.9	1710	0.0151	0.695	0.849
2	49.0	1030	0.0476	0.658	0.940
	49.8	884	0.0564	0.663	0.947
	50.9	940	0.0541	0.662	0.950
	54.7	891	0.0614	0.666	0.910
3	37.5	1650	0.0227	0.659	0.816
	35.7	1220	0.0293	0.676	0.806
	38.2	1250	0.0305	0.678	0.888
	32.8	1630	0.0201	0.651	0.865
4	42.6	675	0.0632	0.482	1.24
	53.9	1035	0.0520	0.482	0.963
	34.0	776	0.0438	0.480	1.21
	39.4	839	0.0470	0.481	0.938
5	37.7	1110	0.0340	0.660	0.901
	30.0	1130	0.0266	0.648	0.867
	53.1	1305	0.0407	0.669	0.871
	38.4	1470	0.0262	0.645	0.799
6	31.4	1530	0.0205	0.575	0.824
	40.7	872	0.0466	0.615	0.822
	20.0	1240	0.0161	0.559	0.791
	58.0	1425	0.0407	0.611	0.755
7	32.5	865	0.0376	0.591	0.814
	29.6	1190	0.0249	0.566	0.869
	27.2	1310	0.0208	0.561	0.803
	27.3	1530	0.0179	0.552	0.791

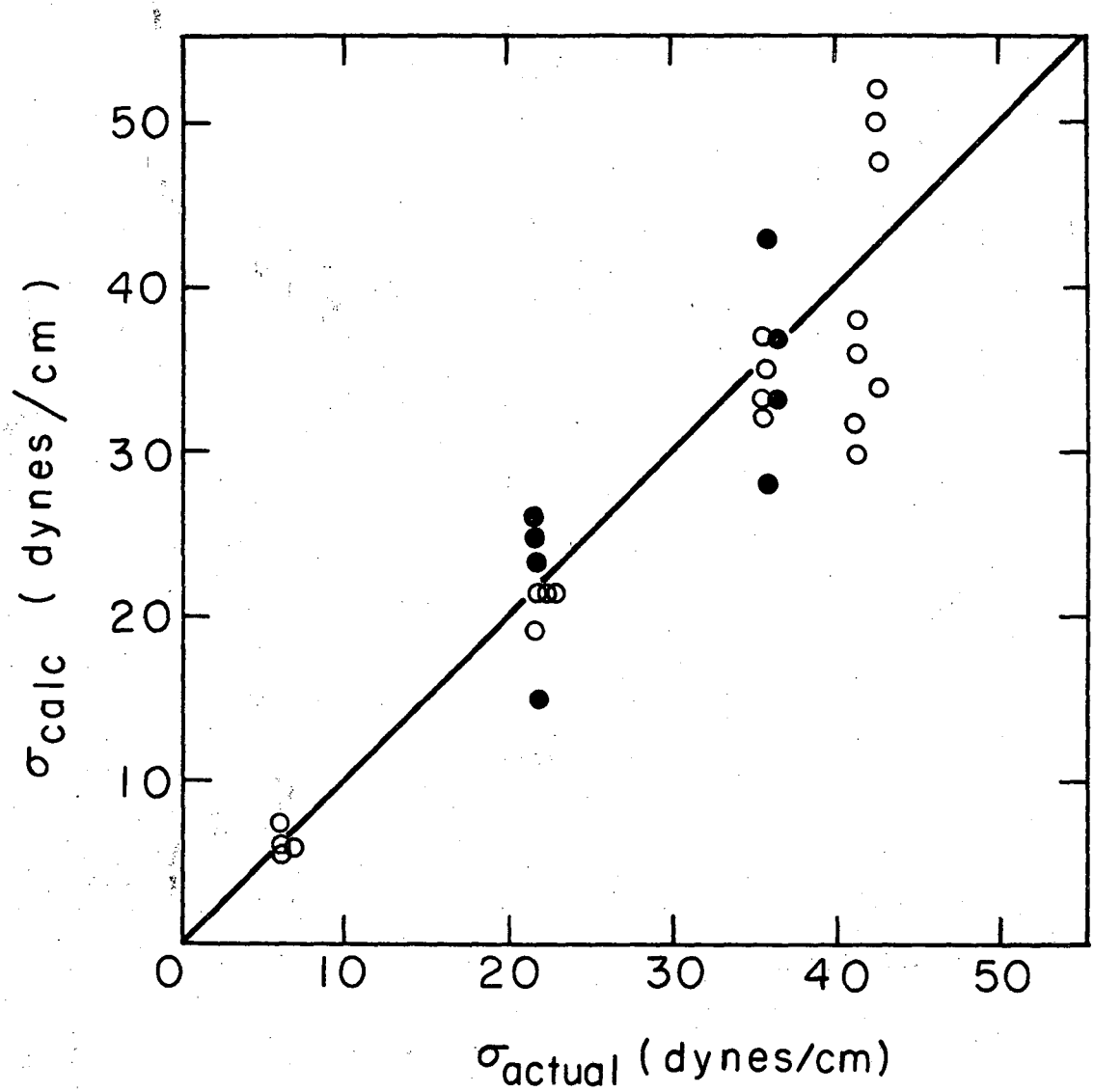

XBL6811-7207

Fig. 7 Comparison between actual and calculated interfacial tension. Open circles, jet fluid heavier; closed circles, jet fluid lighter.

In order to develop this method of measuring interfacial tension into a more accurate tool, there are two main areas in which more work is necessary.

First, better nozzles are needed. The work reported here indicates that at least four waves are necessary for reliable results. The length of such a jet is sufficient for a significant study of mass transfer, since it provides a contact time in the range of 10^{-3} to 10^{-2} sec.

The range of usable jet diameters and velocities is restricted by several factors. Foremost of these is the likelihood that the jet issuing from the orifice will have greater stability and a better defined velocity profile if the jet is laminar; i.e. if $R_i \leq 2000$, or $ac \leq 10$. Bohr has given a damping factor ϵ (per cm) dependent upon R_i and a:

$$\epsilon \sim (\text{const.})/aR_i$$

For a gas-liquid jet the theoretical value of constant is 12; for the liquid-liquid jet studied experimentally, the observed constant was about 25. For satisfactory measurements, $\epsilon z \leq 1$, hence $25z/aR_i \leq 1$. The distance required to measure dynamic interfacial-tension behavior resulting from mass transfer is of the order of 4λ. From Rayleigh's solution, the wavelength λ is approximately $3ca^{3/2}/\sigma^{1/2}$; hence for $\sigma \sim 30$, $\lambda \sim 0.5ca^{3/2}$. Therefore, the radius of a nozzle a must be $a > 0.03$ cm.

The desired contact time for mass transfer studies is generally less than 0.1 sec. Thus $z/c \sim 4\lambda/c \leq 0.1$; hence for $\lambda \sim 0.5ca^{3/2}$, $a \leq 0.14$ cm.

To limit the error of dimensional measurements of the jet within 5%, it is necessary to have the jet length at least 1 cm; hence $4\lambda \geq 1.0$, $ca^{3/2} \geq 0.5$. This limit is in the vicinity of $R_i = 500$.

Thus the above four conditions limit the operable region of an oscillating jet. A schematic diagram of the operable combinations of a and c is given in Fig. 8.

Second, in order to improve the stability of the jet, and also to approximate the flow conditions better to the theory derived, the use of a flowing external phase (instead of a stationary one) at a velocity near the mean velocity of the interior jet is proposed. The present authors also have solved the velocity-profile problem for this case.[24]

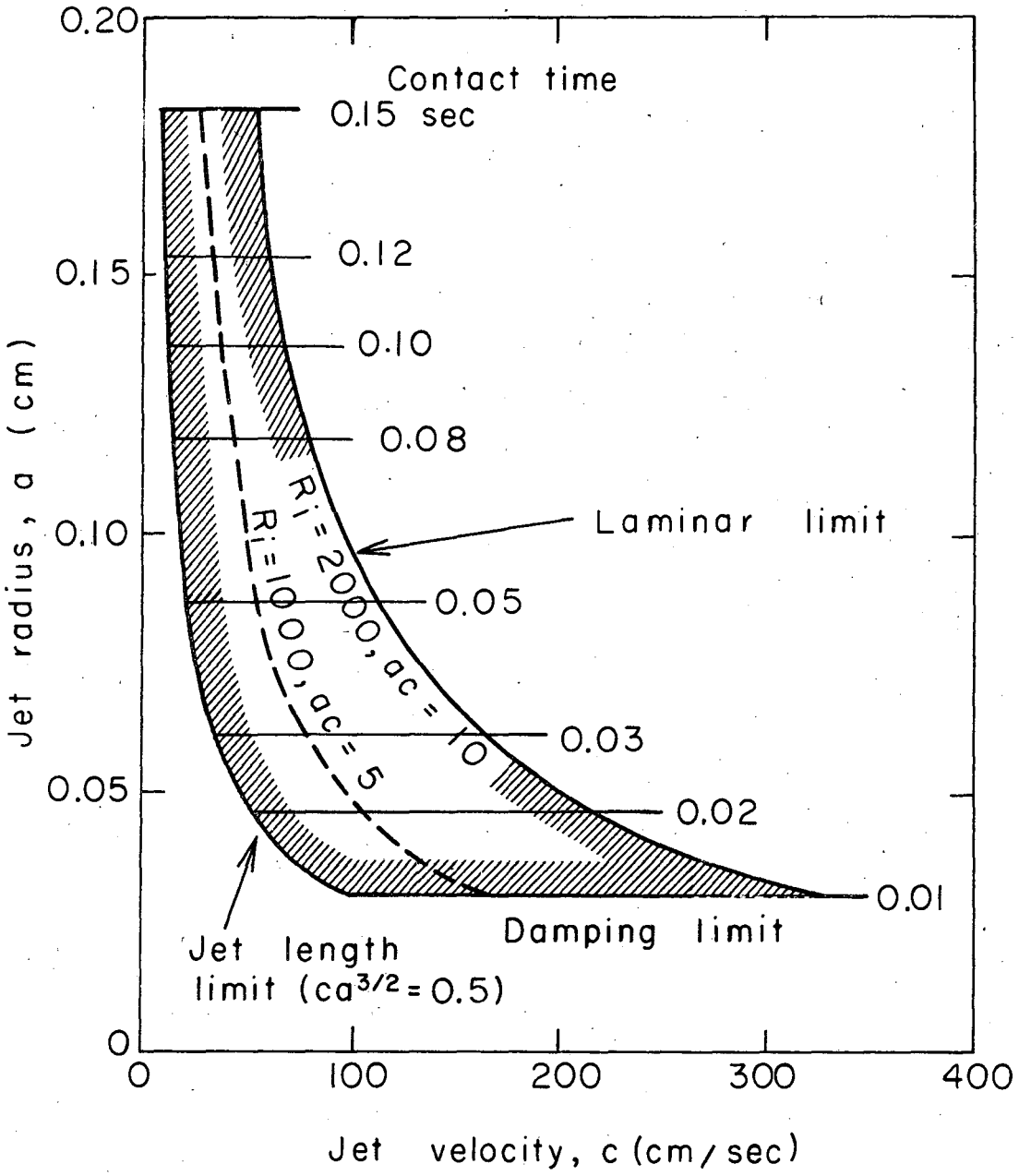

XBL6811-7208

Fig. 8 Operable region for oscillating jets.

REFERENCES

1. C. C. Addison, J. Chem. Soc. 535 (1943).
2. Ibid., 252 (1944).
3. Ibid., 477 (1944).
4. Ibid., 98 (1945).
5. Ibid., 354 (1945).
6. C. C. Addison, Phil. Mag. 36, 73 (1945).
7. G. Bidone, Expériences sur la Forme et la Direction des Veines et des Courants d'Eau lancés par diverses Ouvertures, 1829; Mémoires de l'Académie Royal de Sciences de Turin 34, 229 (1830).
8. E. J. Burcik, J. Colloid Sci. 6, 522 (1951).
9. Ibid., 5, 421 (1950).
10. Ibid., 8, 520 (1953).
11. N. Bohr, Phil. Trans. A209, 281 (1908-1909).
12. W. N. Bond and H. O. Puls, Phil. Mag. 24, (7) 864 (1937).
13. R. Defay and J. R. Hommelen, J. Colloid Sci. 13, 553 (1958).
14. Ibid., 14, 401 (1959), Erratum.
15. S. L. Goren and S. Wronski, J. Fluid. Mech. 25, 87 (1966).
16. R. S. Hansen, M. E. Purchase, T. C. Wallace, and R. W. Woody, J. Phys. Chem. 62, 210 (1958).
17. R. S. Hansen and T. C. Wallace, J. Phys. Chem. 62, 210 (1958).
18. P. Magnus, Pogg. Ann. 25, 95 (1855).
19. P. O. Pederson, Phil. Trans. A207, 341 (1906-1907).
20. Lord Rayleigh, Proc. Roy. Soc. (London) 29, 71 (1879).

21. H. Stocker, Z. Physik. Chem. 94, 149 (1920).

22. K. L. Sutherland, Rev. Pure and Appl. Chem. 1, 35 (1951).

23. K. L. Sutherland, Australian J. Chem. 7, 319 (1954).

24. S. Tada and T. Vermeulen, paper submitted to J. Fluid Mech.

25. A. E. Vandegrift, J. Colloid Sci., 23, 43 (1967).

26. A. E. Vandegrift , S. Tada, and T. Vermeulen, paper submitted to J. Fluid Mech.

III. VELOCITY PROFILE OF CYLINDRICAL LAMINAR LIQUID JETS ENTERING A STATIONARY SURROUNDING LIQUID

A. Introduction

Jets of a liquid into a second immiscible liquid are of particular interest for studies of mass transfer and heterogeneous reaction kinetics. In such systems, also, interfacial adsorption can be determined by means of an oscillating (elliptical) jet which measures the local interfacial tension along the length of the jet.

Several investigations have been made of laminar free jets, i.e., liquid jets issuing from an orifice or a capillary into an inviscid or zero-density medium. Scriven and Pigford[10] obtained an approximate solution using the boundary-layer theory to calculate the surface velocity, and found that the surface velocity increases as the cube root of the axial distance in the neighborhood of the orifice. Recently Goren[4] and Goren and Wronski[5] have derived formulas for the surface velocity and the change in the radius of the jet by the method of Meksyn,[9] with results very similar to those obtained by Scriven and Pigford. Middleman[8] has used a boundary-layer type analysis to calculate the velocity profile and jet diameter as functions of an axial variable, assuming a polynomial form for the jet velocity.

The nonlinearity of the Navier-Stokes equations gives considerable difficulty in obtaining the solutions, but the boundary conditions at the surface impose further difficulty even when one tries to solve the equations numerically: the exact location of the interface is not known until one has solved for the velocity profile. Duda and Vrentas[1] have overcome the difficulties of the free boundary by use of a coordinate system

in which the stream function is used as the variable in the radial direction; they obtain a boundary-layer solution at high Reynolds numbers and numerical solutions for several cases. Also they obtain an analytic solution by linearizing the equation of motion, and have shown good agreement between this result and one by numerical calculation. In principle their method can be applied to a liquid-liquid jet, but complexities caused by the involvement of the second-phase equations and the boundary conditions are not dealt with easily.

There are only a few studies available on the velocity profile of a liquid jet in another liquid. Garner and Mina[3] solved the problem for the case where the inertial terms are negligible compared with the viscous terms in the equation of motion. However, this case is entirely outside the scope of our present interest. Schlichting[11] solved the problem in which a viscous fluid issues from a point source into an infinite volume of the same fluid.

In this paper we seek an approximate solution for the problem, applying the governing relations to a pair of empirical velocity equations which describe the transition from parabolic to non-parabolic behavior.

B. Theory

We shall consider a steady axisymmetric liquid jet, flowing into another immiscible liquid which is stationary at infinite distance from the jet. The pressure in the z-direction is assumed constant; hence the total momentum in the z-direction is constant in all planes normal to the jet axis, downstream of the orifice. The axial flow of exterior fluid is supplied by inwardly (later, outwardly) directed radial flows of exterior fluid. At any cross-section, the momentum in the outlying exterior fluid being displaced by downstream axial flow is negligible compared to the momentum directly transferred into the near exterior fluid moving as part of the expanded jet. Momentum transfer provides a flow of mechanical energy, which in the steady state will undergo continual viscous dissipation into an equivalent quantity of thermal energy. We assume that this dissipation occurs at extremely large radial and axial distances, and thus does not affect the jet equations. Also, our analysis applies to real jets only in the stable region prior to breakup.

The Navier-Stokes equation for incompressible fluid under boundary-layer type approximations, in dimensionless form, is

$$W_p \frac{\partial W_p}{\partial z} + U_p \frac{\partial W_p}{\partial r} = \frac{2}{R_p} \cdot \frac{1}{r} \frac{\partial}{\partial r}\left(r \frac{\partial W_p}{\partial r} \right) \qquad (1)$$

$$(p = i, e)$$

The following notations are used:

$A, B, C, C_1, D, D_1; E, M$	coefficients which are functions of the axial-distance variable
A'	interface radius (cm)
A_0'	orifice radius (cm)
a	A'/A_0', dimensionless jet radius
F_r	$W_0'^2/2A_0'g$, Froude number
g	gravity constant
h	modified stream function
L	function defined by Eq. (31)
r	R'/A_0', dimensionless radial distance
R_i	$2A_0'W_0'\rho_i/\mu_i$, interior Reynolds number
R_e	$2A_0'W_0'\rho_e/\mu_e$, exterior Reynolds number
R'	radial distance (cm)
S	constant defined by Eq. (25)
U	U'/W_0', dimensionless radial velocity
U'	radial velocity (cm/sec)
W	W'/W_0', dimensionless axial velocity
W'	axial velocity (cm/sec)
W_0'	initial mean velocity of jet (cm/sec)
z	Z'/Z_0', dimensionless axial distance
i	interior phase
e	exterior phase
α	parabolic constant

β	$\mu_e\rho_e/\mu_i\rho_i$, viscosity-density constant
γ	function defined by Eq. (30)
ζ	z/R_i
η	similarity variable
μ	viscosity (g/cm sec)
ρ	density (g/cm^3)
$'$	superscript denoting dimensional variables
ϕ	stream function

In this analysis, radial velocity is assumed negligible compared with axial velocity, and the effect of interfacial tension is disregarded for the Reynolds-number range of interest (200 - 2,000).

Axial velocities are expressed with the use of five coefficients which are functions of the axial-distance variable, z. The problem is now reduced to one of solving for these functions and for the jet radius at each given axial distance, by satisfying the six following boundary conditions.

The first condition is that the radial velocity vanishes at the center of the jet. Equation (1) then simplifies to

$$\left(W_i \frac{\partial W_i}{\partial z}\right)_{r=0} = \frac{2}{R_i}\left[\frac{1}{r} \cdot \frac{\partial}{\partial r}\left(r \frac{\partial W_i}{\partial r}\right)\right]_{r=0} \tag{1a}$$

To avoid difficulty associated with the evaluation of an empirical velocity equation, which we shall discuss in the following section, Eq. (1a) has been integrated with respect to z:

$$\left(W_i^{\,2}\right)_{r=0} - 4 = \frac{4}{R_i}\int_0^z \left[\frac{1}{r}\cdot\frac{\partial}{\partial r}\left(r\cdot\frac{\partial W_i}{\partial r}\right)\right]_{r=0} dz \qquad (2)$$

The second condition is that the continuity of axial velocities at the interface:

$$\left(W_i\right)_{r=a} = \left(W_e\right)_{r=a} \qquad (3)$$

The third condition is the continuity of tangential stresses at the interface, in which again the term involving the radial-velocity component has been omitted.

$$\mu_i\left(\frac{\partial W_i}{\partial r}\right)_{r=a} = \mu_e\left(\frac{\partial W_i}{\partial r}\right)_{r=a} \qquad (4)$$

The fourth condition is the conservation of volume or mass for the jet phase. Given a parabolic profile at the orifice, the mass balance is

$$\int_0^a rW_i\,dr = \frac{1}{2} \qquad (5)$$

The fifth condition is the macroscopic momentum balance in the interior (jet) fluid, assuming that momentum is transferred between the two phases only through tangential stresses. Noting that there is no flow across the interface, we follow a Von Karman-type momentum integral.

For an initially parabolic velocity profile,

$$\int_0^a rW_i^2 dr = \frac{2}{3} + \frac{2}{R_i}\int_0^z a\left(\frac{\partial W_i}{\partial r}\right)_{r=a} dz \tag{6}$$

The sixth condition is the complementary momentum balance of the exterior fluid, which is taken to be stationary behind the nozzle plane,

$$\int_a^\infty rW_e^2 dr = -\frac{2}{R_e}\int_0^z a\left(\frac{\partial W_e}{\partial r}\right)_{r=a} dz \tag{7}$$

1. <u>Empirical Velocity Equation</u>

Now we assume suitable forms of axial-velocity expression for both interior and exterior phases. The forms selected are somewhat arbitrary. To approximate its initial parabola, the jet phase requires a form which combines a perturbing function with a parabola. This form allows the radial-velocity profile to change from a parabolic (the first term being dominant) to a nonparabolic form (the second term being dominant) with increasing axial distance. The perturbing function (the second term) can assume the same radial functionality as Schlichting's solution.[11] An exponential form has been adopted for the surrounding phase. The resulting equations are:

$$W_i = 2\alpha e^{-Mz}(a^2 - r^2) + B/(1 + Ar^2)^2 \tag{8}$$

$$W_e = De^{-Cr^2} \tag{9}$$

Here A, B, C, D, and M are functions of the axial variable z To initiate the calculation, the perturbing function B must be non-zero; hence the parabolic constant α cannot be set precisely at unity. Substituting W_i and W_e into Eqs. (2) and (7) gives us the following six equations which enable us to evaluate the unknown functions A, B, C, D, M, and the jet radius a.

Equation (2) becomes:

$$(2\alpha e^{-Mz}a^2)^2 + 4\alpha Ba^2e^{-Mz} + B^2 - 4 - \frac{32}{R_i}\int_0^z (\alpha e^{-Mz} + AB)dz = 0 \tag{10}$$

Equation (3):

$$B/(1 + Aa^2)^2 - De^{-Ca^2} = 0 \tag{11}$$

Equation (4):

$$\alpha e^{-Mz} + AB/(1 + Aa^2)^3 - 0.5(\mu_e/\mu_i)CDe^{-Ca^2} = 0 \tag{12}$$

Equation (5):

$$\alpha a^4e^{-Mz} + Ba^2/(1 + Aa^2) - 1 = 0 \tag{13}$$

Equation (6):

$$\frac{2}{3}\alpha^2a^6e^{-2Mz} + 2\alpha Be^{-Mz}[a^4/(1 + Aa^2) - \ln(1 + Aa^2)/A^2 + a^2/\{A(1 + Aa^2)\}]$$

$$+ \frac{1}{6}\cdot(B^2/A)\{1 - 1/(1 + Aa^2)^3\} - \frac{2}{3} - \frac{8}{R_i}\int_0^z \{\alpha e^{-Mz}a^2$$

$$+ ABa^2/(1 + Aa^2)^3\}dz = 0 \tag{14}$$

Equation (7):

$$\frac{1}{4} \cdot D^2 e^{-2Ca^2}/C - \frac{4}{R_e} \int_0^z CDa^2 e^{-Ca^2} dz = 0 \tag{15}$$

2. Computation Procedure

It is necessary to solve these six simultaneous equations for the six unknowns at each z value, even though no explicit solutions are available. These equations have been linearized in each of the six unknowns, relative to its preceding value, so as to obtain six linear simultaneous equations which can readily be solved for small increments of z.

Because of the high nonlinearity of the equations, a simple Euler-type method causes large truncation errors and gives meaningless results. A successful calculation has been achieved by use of a third-order Runge-Kutta method, the algorithm of which is as follows:

$$k_1 = hf(x_n, y_n)$$

$$k_2 = hf(x_n\ 2\ h/2,\ y_n + k_1/2) \qquad n = 0, 1, 2, \ldots.$$

$$k_3 = hf(x_n + h,\ y_n + 2k_2 - k_1)$$

$$y_{n+1} = y_n + (k_1 + 4k_2 + k_3)/6 \tag{16}$$

Near the orifice, C and D are unmanageably large, so in Eqs. (11), (12), and (15), the substitution is needed:

$$E = De^{-Ca^2} \tag{17}$$

If now we express the linear simultaneous equations as $\underset{\approx}{M}d\underset{\sim}{x} = \underset{\sim}{N}dz$, where $dx_1 = dA$, $dx_2 = dB$, $dx_3 = dC$, $dx_4 = dE$, $dx_5 = da$, $dx_6 = dM$, then M_{jk} and $N_j (j,k = 1,2,\ldots.6)$ are given as follows (zero-valued elements are omitted).

$$M_{12} = 4\alpha e^{-Mz}a^2 + 2B$$
$$M_{15} = 16\alpha^2 a^3 e^{-2Mz} + 8\alpha Bae^{-Mz}$$
$$M_{16} = -8\alpha^2 a^4 ze^{-2Mz} - 4\alpha Ba^2 ze^{-Mz}$$
$$N_1 = 8\alpha^2 a^4 Me^{-2Mz} + 4\alpha Ba^2 Me^{-Mz} - 32(\alpha e^{-Mz} + AB)/R_i$$
$$M_{21} = -2Ba^2/(1 + Aa^2)^2$$
$$M_{22} = 1/(1 + Aa^2)^2$$
$$M_{24} = -1$$
$$M_{25} = -4ABa/(1 + Aa^2)^3$$
$$M_{31} = B/(1 + Aa^2)^3 - 3ABa^2/(1 + Aa^2)^4$$
$$M_{32} = A/(1 + Aa^2)^3$$
$$M_{33} = -1/2(\mu_e/\mu_i)D$$
$$M_{34} = -1/2(\mu_e/\mu_i)C$$
$$M_{35} = -6A^2Ba/(1 + Aa^2)^4$$
$$M_{36} = -\alpha ze^{-Mz}$$
$$N_3 = \alpha Me^{-Mz}$$
$$M_{41} = -1/2(Ba^4)/(1 + Aa^2)^2$$
$$M_{42} = a^2/\{2(1 + Aa^2)\}$$
$$M_{45} = 2\alpha a^3 e^{-Mz} + Ba/(1 + Aa^2) - ABa^3/(1 + Aa^2)^2$$
$$M_{46} = -1/2(\alpha a^4 ze^{-Mz})$$
$$N_4 = 1/2(\alpha a^4 Me^{-Mz})$$

$$M_{51} = 2\alpha Be^{-Mz}[-a^6/(1 + Aa^2)^2 - a^4/\{A(1 + Aa^2)^2\}$$
$$- 2a^2/\{A^2(1 + Aa^2)\} + \ln(1 + Aa^2)/A^3]$$
$$- 1/6(B/A)^2\{1 - 1/(1 + Aa^2)^3\} + 1/2(Ba)^2/\{A(1 + Aa^2)^4\}$$
$$M_{52} = 2\alpha e^{-Mz}[a^4/(1 + Aa^2) - \ln(1 + Aa^2)/A^2$$
$$+ a^2/\{A(1 + Aa^2)\}] + 1/3(B/A)\{1 - 1/(1 + Aa^2)^3\}$$
$$M_{55} = 4\alpha^2 a^5 e^{-2Mz} + 4ABa^3 e^{-Mz}/(1 + Aa^2) + Ba^2/(1 + Aa^2)^4$$
$$M_{56} = -4/3(\alpha^2 a^6 ze^{-2Mz}) - 2\alpha Bze^{-Mz}[a^4/(1 + Aa^2)$$
$$- \ln(1 + Aa^2)/A^2 + a^2/\{A(1 + Aa^2)\}]$$
$$N_5 = 4/3(\alpha^2 a^6 ze^{-2Mz}) + 2\alpha BMe^{-Mz}[a^4/(1 + Aa^2)$$
$$- \ln(1 + Aa^2)/A^2 + a^2/\{A(1 + Aa^2)\} - 8/R_i(\alpha a^2 e^{-Mz}$$
$$+ ABa^2/(1 + Aa^2)^3]$$
$$M_{63} = -1/4(E/C)^2$$
$$M_{64} = 1/2(E/C)$$
$$N_6 = 4/R_e(CEa^2)$$

The numerical calculations have been done on a Control Data Corporation 6600 digital computer.

The choice of α is arbitrary; the closer it is to 1, the finer the z-increments required in order for the computation to remain stable. By trial we found that $\alpha = 0.95$ gives a reasonably good fit to the initial parabolic form, with z-increments initially 1×10^{-7}; any finer increment size would require double-precision arithmetic with an undesirable increase in computation time. Moreover, values nearer to 1 do not give appreciably different results.

The initial values for A and B are obtained from Eqs. (13) and (14) by use of a suitable root-finding method, for example, the Newton-Raphson method. The initial values of C and E are determined from Eqs. (11) and (12); they make the left-hand side of Eq. (15) equal to about 10^{-6}, which is well within the level of accuracy that has been retained. After z reaches 1×10^{-1}, C and D can be calculated separately and then Eq. (9) can be evaluated fully.

By using an integrated relation (2) we eliminate dB/dz, da/dz, and dM/dz, but it is still necessary to know the initial value of M. Fortunately, the product Mz near the origin is so small that any arbitrary initial value of M, after several steps, gives the same M values in the following steps.

In several calculations, for small viscosity or density ratio, the velocity profiles have completely switched to nonparabolic forms. As a result the terms involving M have dropped out, and the number of equations has become more than necessary to solve for five unknowns. Addition of Eq. (6) to Eq. (7) times density ratio, gives Eq. (6a), which is a total momentum balance for the jet. Therefore, in such cases, one can replace the fifth governing relation (6) by Eq. (6a), leaving out Eq. (7):

$$\int_0^a rw_i^2 dr + (\rho_e/\rho_i)\int_a^\infty rw_e^2 dr = \frac{2}{3} \tag{6a}$$

The following step-by-step calculation can be achieved by use of 5×5 matrix elements with new fifth-row elements corresponding to (6a). The changes in the fifth-row elements of the matrix expression are:

$$M_{53} = -1/4(E/C)^2(\rho_e/\rho_i)$$
$$M_{54} = 1/2(E/C)(\rho_e/\rho_i)$$
$$N_5 = 4/3(\alpha^2 a^6 z e^{-2Mz}) + 2\alpha BMe^{-Mz}[a^4/(1 + Aa^2) - \ln(1 + Aa^2)/A^2 + a^2/\{A(1 + Aa^2)\}]$$

C. Results

1. Comparison with Published Experimental Data

Kimura and Miyauchi[7] have measured the interfacial velocity for a benzene jet into water, using stroboflash photography. As tracers, they injected water bubbles into the benzene phase, and aluminum particles into the surrounding water phase. Their experimental parameters (viscosity ratio 1.54, density ratio 1.13, and interior Reynolds number 450) fall within the range of our model. The experimental results for interfacial velocity and the jet radius are plotted in Fig. 1, along with comparative calculated values.

For the calculation, the input data are an interior Reynolds number R_i, a viscosity ratio μ_e/μ_i, and a density ratio ρ_e/ρ_i. The values of interfacial velocity predicted from the present model are significantly higher, and the calculated jet-radius values are lower, than the experimental data. As discussed by Fosberg and Heideger,[2] such discrepancies can be attributed to fluid-dynamic end effects due to the receiver into which the interior jet impinges: the solid surface of the receiver hinders the flow of both the interior and exterior fluid.

A more realistic model requires a boundary condition at the downstream end of the jet, and also a pressure-gradient term in the equation of motion; thus the problem becomes one of boundary-value type rather than of initial-value type. At this stage so detailed a model seems too complicated to be solved, so a simpler correction method has been proposed. An additional resistance caused by the presence of a receiver may be viewed as equivalent to an increase in viscosity ratio,

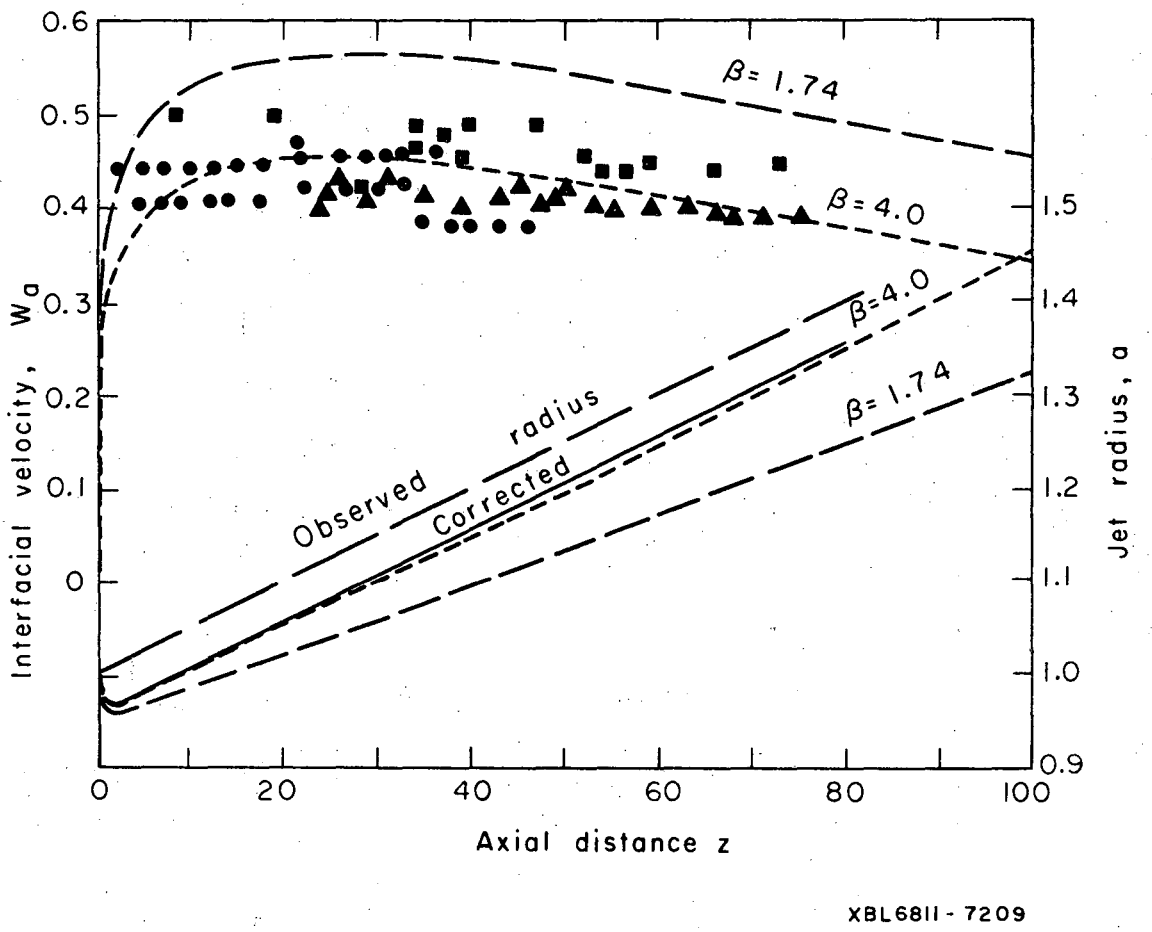

Fig. 1 Experimental and calculated jet radius and interface velocity, for benzene jet into stationary water. Circles and squares, tracer particles in benzene phase. Triangles, particles in water phase.

producing a commensurable increase in jet-radius change. Hence we propose to correct the velocity profile by matching a calculated jet-radius profile with an observed shape. Thereby we either (1) determine a new β value to be used in computing the interfacial velocity, or (2) simply divide the calculated velocity values by the square of the jet-radius ratios; method (1) has been applied here.

In the experimental-jet profile, there is no description of the vena contracta, which should occur very close to the orifice plane with a reduction of the jet radius by approximately 5%. An experimental photograph by Kimura[6] seems to show a vena contracta very near the orifice plane, hence the real initial radius could be about 5% larger than the given value; this correction has also been included. The jet radius corrected in this way has been found to fit a value of $(\mu_e/\mu_i)(\rho_e/\rho_i) = 4.0$, as shown in Fig. 1. This value, indicated as $\beta = 4.0$, also gives a good fit to the measured interfacial velocity. (Justification for using the parameter β follows directly.)

2. Generalized Behavior

Close examination of Eqs. (10-15) indicates that the functions A, B, and M and the jet radius a can be expressed concisely in terms of two collective parameters, composed of the four original variables R_i, μ_e/μ_i, ρ_e/ρ_i, and z.

The first parameter is the product of viscosity ratio and density ratio, designated by β:

$$\beta = \mu_e \rho_e / \mu_i \rho_i \tag{18}$$

The second parameter, which is exact within the framework of the present boundary-layer approximation, is a modified axial distance designated by ζ:

$$\zeta = z/R_i \tag{19}$$

The validity of these substitutions can be proved in the following way. Use of Eq. (19) involves replacing Mz by $MR_i\zeta$, with the subsequent finding that MR_i can be treated as a single variable. Separately, from Eqs. (11) and (12), we find that De^{-Ca^2} and $C\rho_i/\rho_e$ must each be functions of β. (From this, it follows that $D\rho_i/\rho_e$ depends upon β.) Finally, using these relations, Eq. (15) is shown to involve only functions of β and MR_i.

The functions A, B, and M and the jet radius a are plotted in Figs. 2 and 3. For the conditions used, A ranges between 0.3 and 0.85 ($A\beta^{1/3}$ between 0 and 1.8); B between 0.2 and 2.0; $MR_i\zeta$ (or Mz) between 0 and 8.0; a between 0.9 and 1.35. The functions $C\rho_i/\rho_e$ (or C_1) and D_1 (equal to D at $\rho_e/\rho_i = 1$) relating to the exterior fluid are plotted (as reciprocals) in Fig. 4. At any density ratio other than 1, at constant β, D is obtained from D_1, C_1, a, and ρ_e/ρ_i, as

$$D = D_1 \cdot \exp[C_1 a^2 (\frac{\rho_e}{\rho_i} - 1)] \tag{20}$$

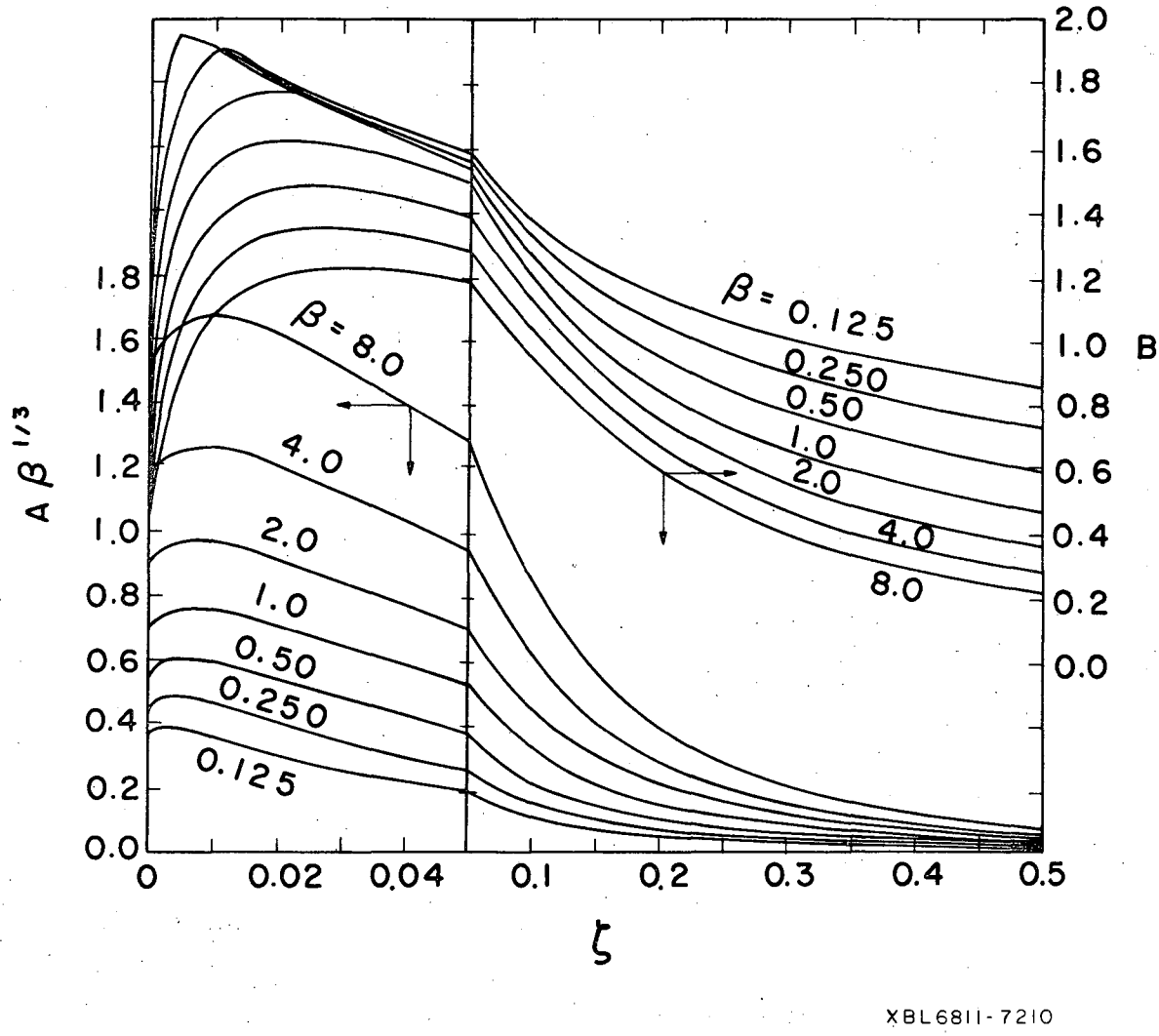

Fig. 2 Interior-jet parameters A and B as functions of ζ and β.

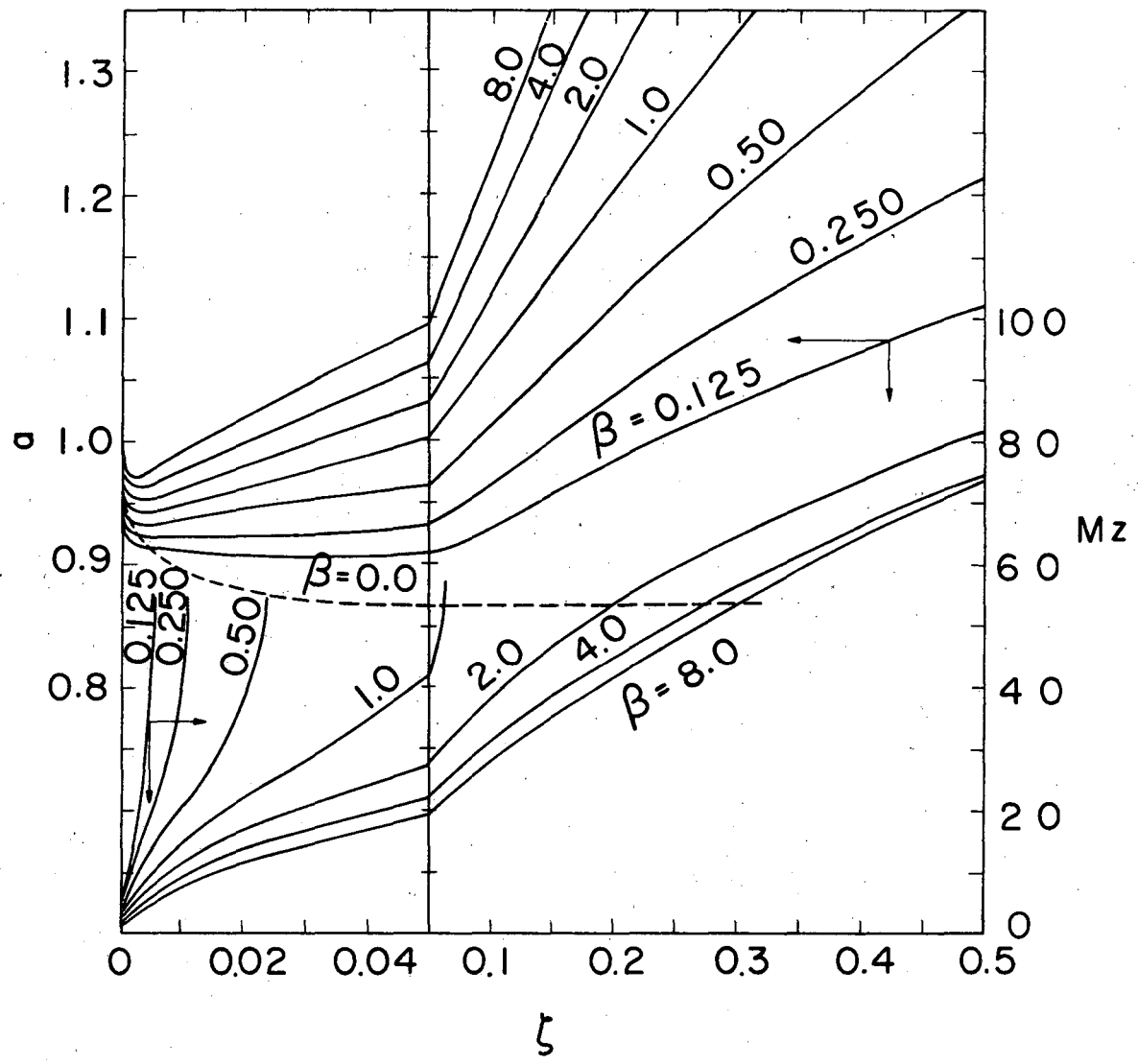

XBL6811-7202

Fig. 3 Jet radius a and parameter Mz as functions of ζ and β.

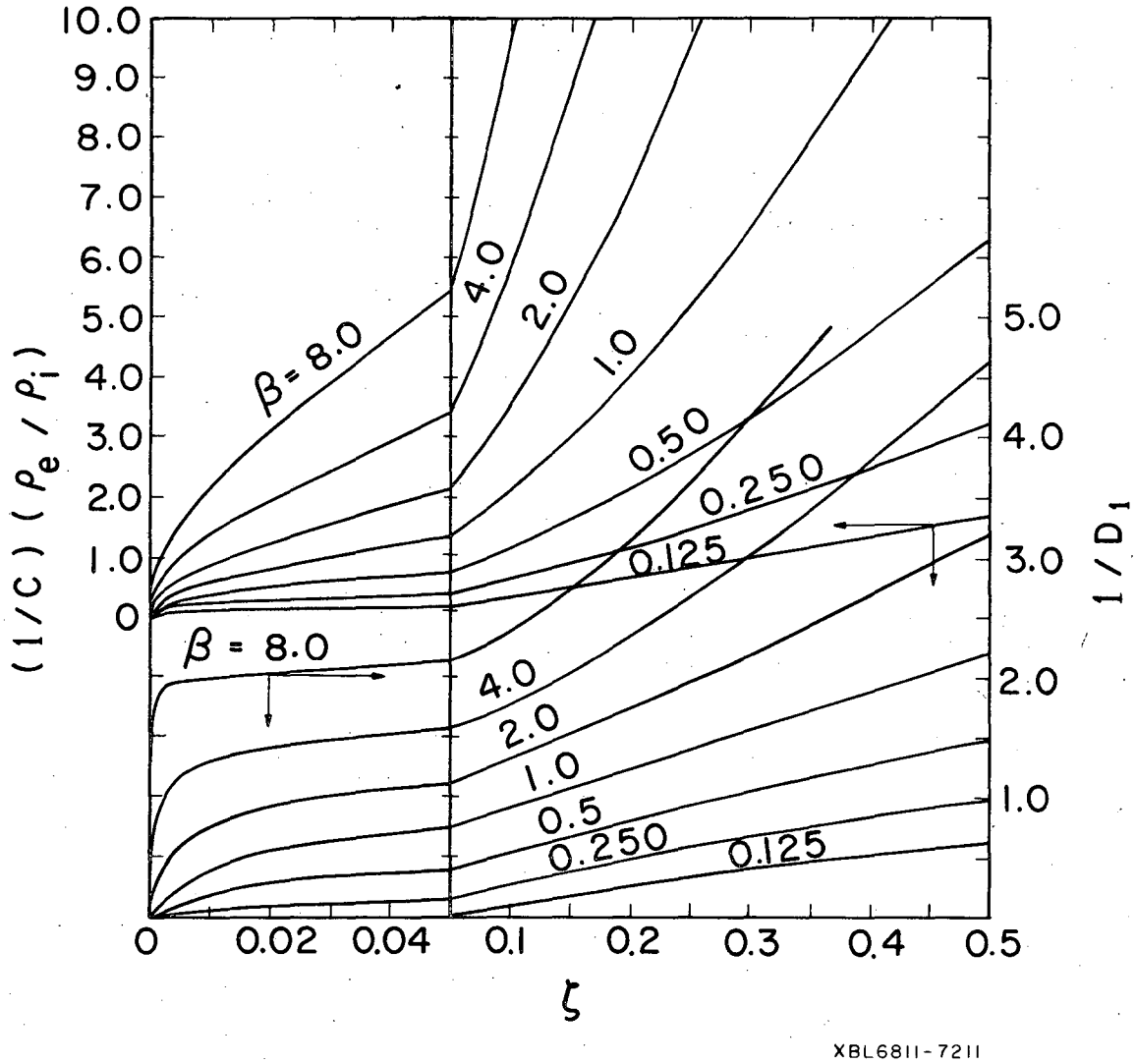

Fig. 4 Exterior jet parameters as functions of ζ and β.

The velocity profile of the jet can be reconstructed from the preceding plots, using Eqs. (8) and (9). The center-line velocity and the interfacial velocity (shown in Fig. 5) are also functions of β and ζ.

The center-line velocity curves for various β's collapse into a single line with a slope of -8α, as ζ diminishes to zero. This is because the initial radial profile of axial velocity is pseudo-parabolic.

The interfacial velocity and jet radius curves for a free jet (see below), which corresponds to $\beta = 0$, are calculated by Duda and Vrentas.[1] These curves are also plotted in Fig. 3 and Fig. 5 with broken lines.

Figure 6 shows a velocity profile radially with the axial distance z as a parameter for benzene-water system ($\mu_e/\mu_i = 1.54$, $\rho_e/\rho_i = 1.13$, and $R_i = 450$).

3. Comparison with Schlichting-Type Solution

A circular jet issuing from a point-source orifice and mixing with the surrounding fluid has been analyzed by Schlichting, in a boundary-layer approximation.[11] As in the preceding analysis, the pressure is considered constant. The total momentum provided in a "real" cylindrical jet with initially parabolic velocity profile can be equated to the momentum in the Schlichting jet. In the Schlichting jet the velocity through the point source is infinite, but the initial mass flow rate is zero and the momentum remains finite. Therefore a direct comparison only becomes possible at distances far downstream from the orifice.

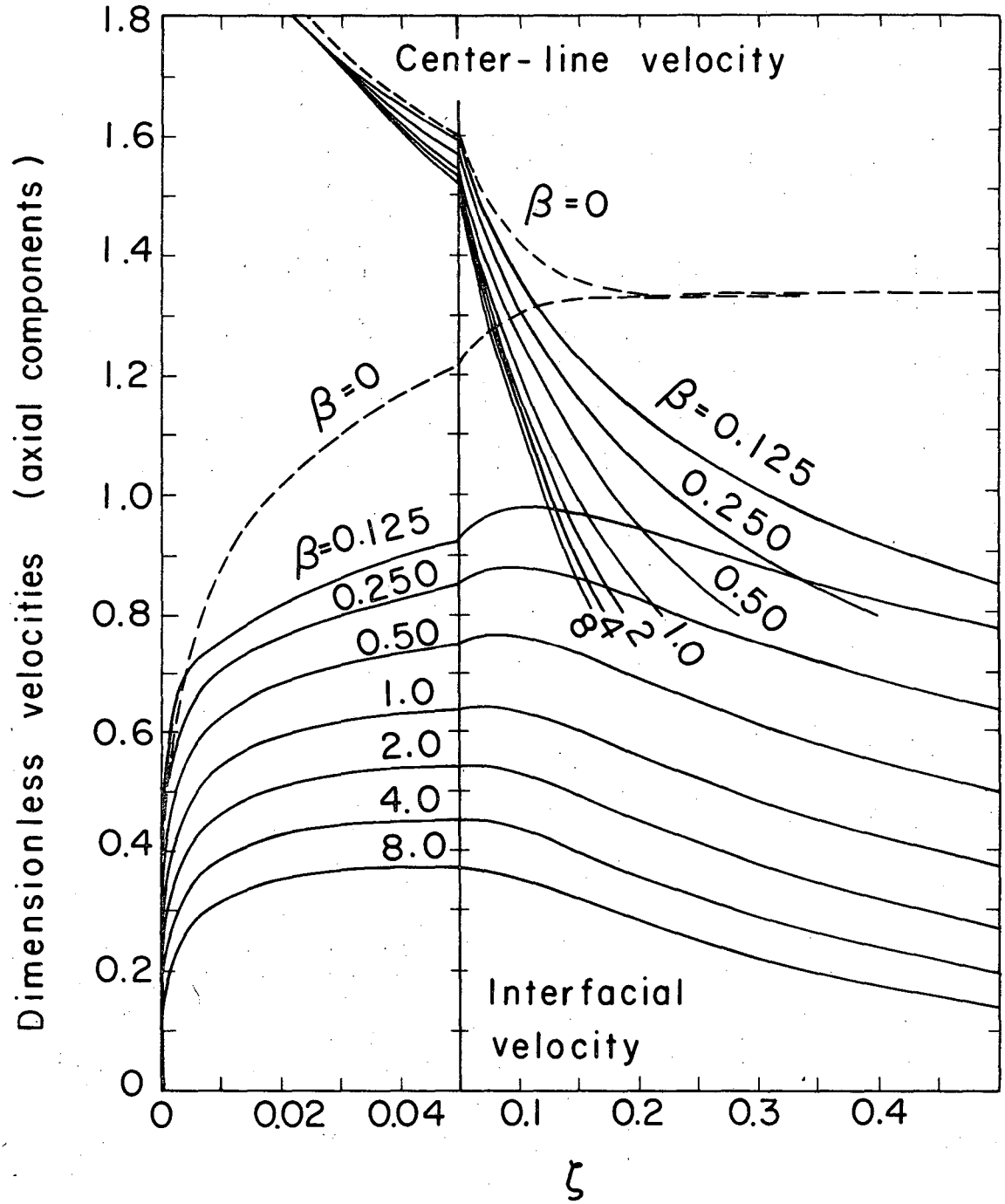

XBL6811-7201

Fig. 5 Center-line and interfacial velocities as functions of ζ and β.

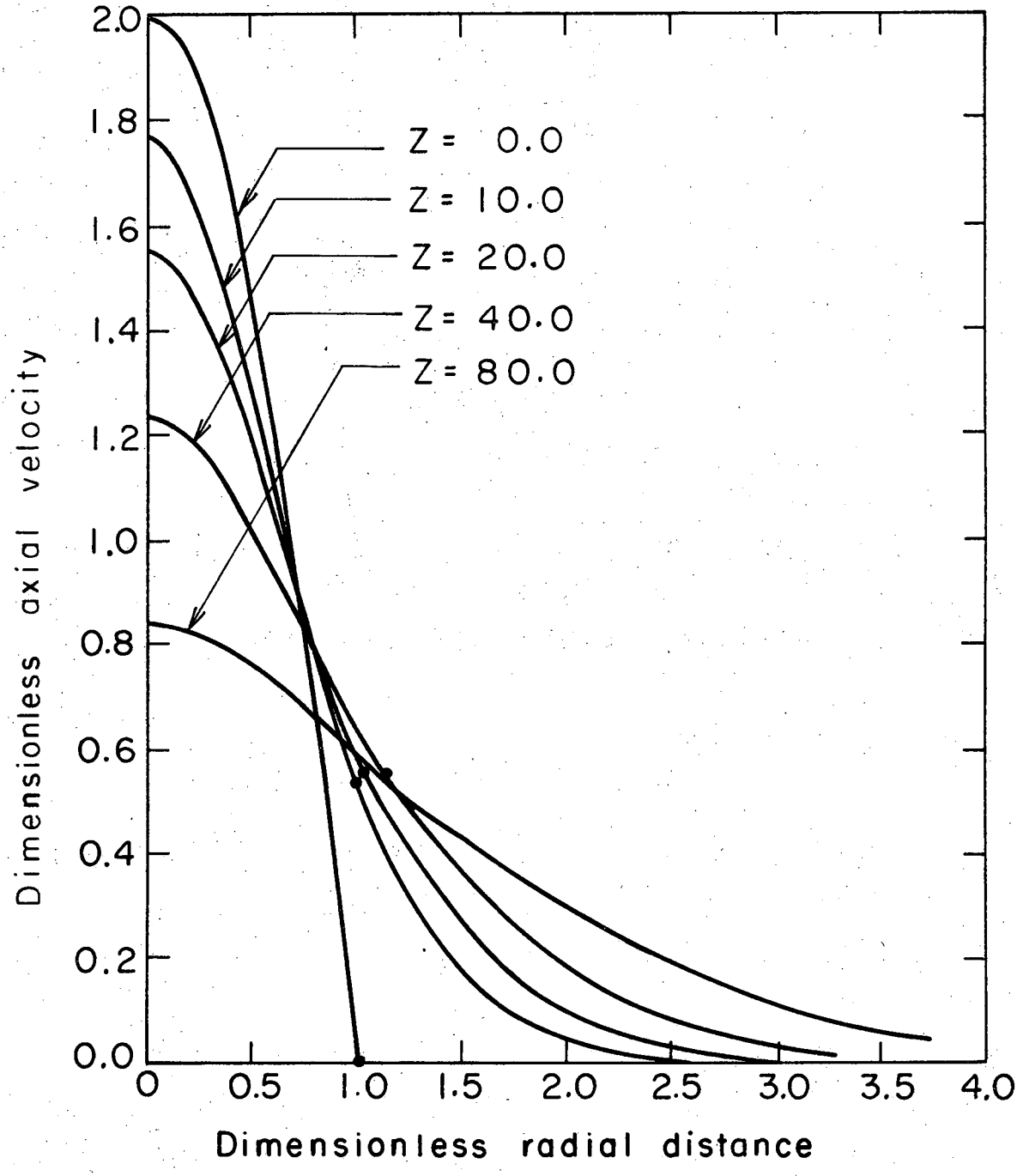

XBL6811-7203

Fig. 6. Axial-velocity profile for benzene-water system at R_i = 450.

To Eqs. (1) and (6a), for the case where the jet liquid and the exterior liquid are the same, or have the same densities and viscosities, we can apply the transformations equivalent to the following:

$$\phi = \frac{z}{R_i} h(\eta), \qquad \eta = R_i \frac{r}{z} \tag{21}$$

Here ϕ is the stream function, η is a "similarity variable," and R_i is the Reynolds number $2A_0'W_0'\rho_i/\mu_i$ as calculated for the real jet.

In terms of the real-jet variables, the velocities then become

$$W_i = \frac{32Sz^3}{(r^2R_i+2Sz^2)^2} \tag{22}$$

$$U_i = \frac{4r(2Sz^2 - r^2R_i)^2}{(r^2R_i + 2Sz^2)^2} \tag{23}$$

When the mass balance for the real interior jet phase is introduced, the jet radius (applicable only at large z, and with an orifice plane possibly different from that for the real jet) can be given as:

$$a^2 = \frac{2Sz^2}{16z - R_i} \tag{24}$$

When the total momentum is equated between the Schlichting jet and the real jet, a constant S is obtained:

$$S = 32/R_i \tag{25}$$

In terms of parameter $\zeta(=z/R_i)$, Eqs. (19) and (22) are then expressed as

$$W_i = \frac{1024\zeta^3}{(r^2 + 64\zeta^2)^2} \tag{26}$$

$$a^2 = \frac{64\zeta^2}{(16\zeta - 1)} \tag{27}$$

Figures 7-9 show the center velocity, interfacial velocity, and the jet radius calculated from the Schlichting model for ζ values between 0.0625 (a singular point) and 1.0, together with those from the real-jet model in the case of $\beta = 1.0$. As is expected, the curves become parallel in the vicinity of $\zeta = 1.0$. Since in the real-jet model the exterior-velocity profile is assumed to have an exponential form, the agreement is better in the neighborhood of $r = 0$.

Vandegrift[13] extended Schlichting's model to the case of two different fluids. His solution does not satisfy tangential-stress continuity at the interface, but does satisfy the total momentum balance for interior plus exterior fluid. The interior velocities and the jet radius can be expressed the same way as in Eqs. (22-24), but with a different value of S which is obtained from the numberical integration of the momentum balance for both phases described by Eq. (6a). The exterior velocities become:

$$W_e = \frac{4z}{r^2 R_e} \quad (r^2 - L^2) \tag{28}$$

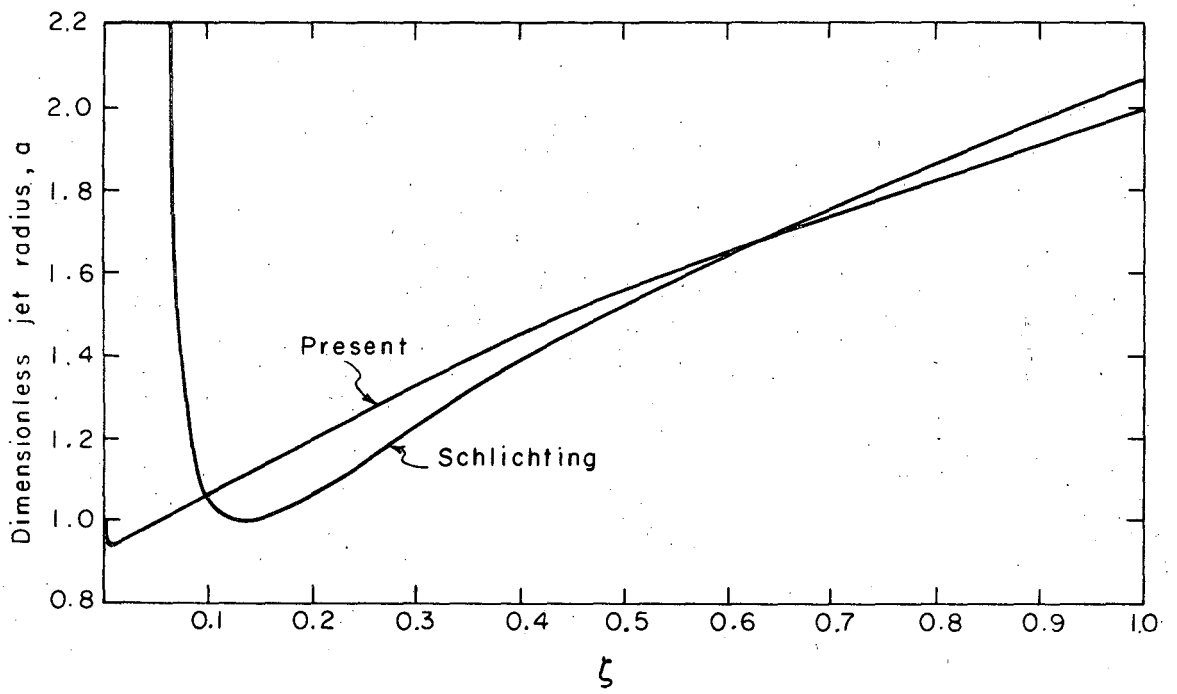

XBL 6811-7205

Fig. 7 Center-line velocity computed by empirical-fit technique and by Schlichting method.

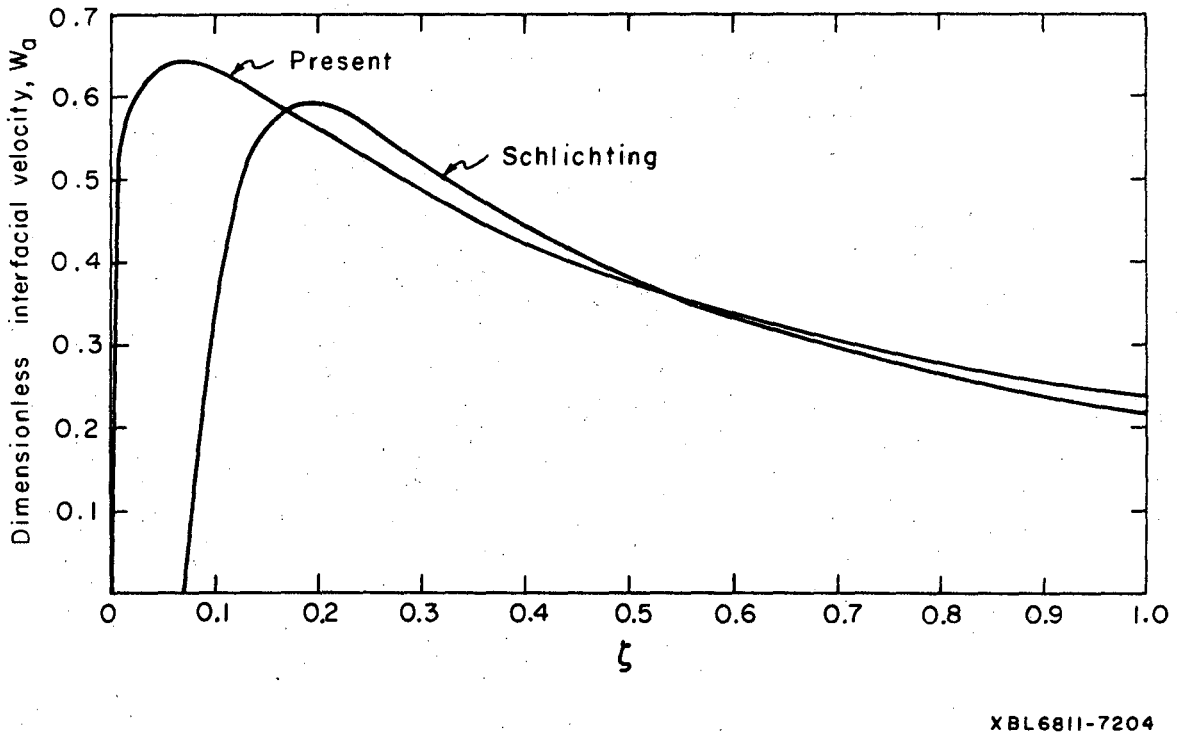

Fig. 8 Interfacial velocity computed by empirical-fit technique and by Schlichting method.

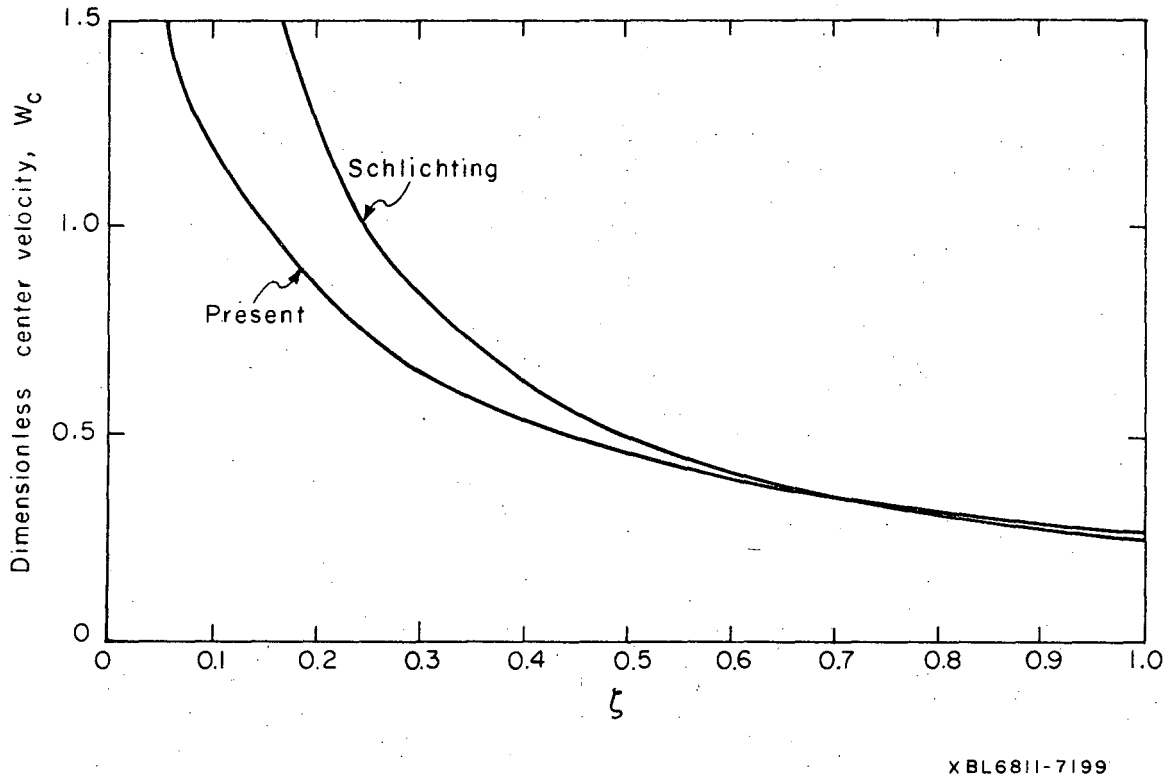

Fig. 9 Jet radius computed by empirical-fit technique and by Schlichting method.

$$U_e = \frac{4}{rR_e} \left(\gamma^2 - L^2 - L - 1\right) \tag{29}$$

where

$$\gamma^2 = \frac{4a^4 R_e (R_e - R_i)}{(2Sz^2 + a^2 R_i)^2} + 1 \tag{30}$$

$$L = \frac{2a^2 R_e}{2Sz^2 + a^2 R_i} - 1 \tag{31}$$

Profiles calculated by using these equations have been given by Vandegrift.[13] For this case, as for a single phase, the match on ζ is difficult to establish. Also the calculated and experimental velocity profiles can agree only at points rather far downstream from the real inlet.

4. Effect of Density Difference

The buoyancy effect due to a difference in fluid densities can be taken into account by introducing Froude-number terms into the equation of motion for center-line velocity and into interior and exterior momentum-balance equations. These equations then become:

$$(W_i^2)_{r=0} - 4 = 4/R_i \int_0^z \left[\frac{1}{r}\frac{\partial}{\partial r}\left(r\frac{\partial W_i}{\partial r}\right)\right]_{r=0} dz + \frac{z}{Fr} \tag{2a}$$

$$\int_0^a rW_i^2 dr = 2/3 + 2/R_i \int_0^z a\left(\frac{\partial W_i}{\partial r}\right)_{r=a} dz + 1/2F_r \int_0^z a^2 dz \tag{6b}$$

$$\int_a^\infty rW_e^2 dr = -2/R_e \int_0^z a\left(\frac{\partial W_e}{\partial r}\right)_{r=a} dz - 1/2F_r \int_0^z (\rho_i/\rho_e)a^2 dz \tag{7a}$$

where $F_r = W_0'^2/2A_0'g$, and the corresponding changes in the matrix elements are

$$N_1 = N_1 - 1/F_r$$

$$N_5 = N_5 - a^2/4F_r$$

$$N_6 = N_6 + (\rho_i/\rho_e)a^2/rF_r$$

The liquid-liquid jet of interest usually has a R_i/F_r of about 10, and for this case the numerical computation which includes Froude-number terms does not show any appreciable difference.

D. Summary

A calculational method for the velocity profile of a circular liquid jet in a stationary surrounding liquid has been developed. The assumed axial-velocity equations are made to satisfy six governing conditions.

Linearization and numerical integration by a third-order Runge-Kutta method has been used to obtain numerical values of velocity functions in terms of an axial distance variable. The velocity values and the jet radius, as well as the generating parameters in the velocity equations, are obtained as functions of a viscosity-density constant β and a dimensionless axial distance ζ. The effect of gravity, expressed by a ratio of Reynolds number to Froude number near 10, is found to be negligible.

The method has been applied to published experimental data, and shows fairly good agreement. Comparison with Schlichting's analytical solution of a circular jet is also fairly good at distances far downstream from the orifice plane. Comparison with values for a free jet indicates that the method is less accurate at β values below about 0.25.

REFERENCES

1. J. L. Duda and J. S. Vrentas, Chem. Eng. Sci. 22, 855 (1967).
2. T. M. Fosberg and W. J. Heideger, Can. J. Chem. Eng. 45, 82 (1967).
3. F. H. Garner, P. Mina, and V. G. Jenson, Trans. Faraday Soc. 55, 1627 (1959).
4. S. L. Goren, J. Fluid Mech. 25, 87 (1966).
5. S. L. Goren and S. Wronski, J. Fluid Mech. 25, 185 (1966).
6. S. Kimura, Ph.D. Thesis, University of Tokyo, Tokyo, Japan, 1963.
7. S. Kimura and T. Miyauchi, Chem. Eng. Sci. 21, 1057 (1966).
8. S. Middleman, Ind. Eng. Chem. Fundamentals 3, 118 (1964).
9. D. Meksyn, New Methods in Boundary-Layer Theory (Pergamon Press, Oxford, 1961).
10. L. E. Scriven and R. L. Pigford, A.I.Ch.E.J. 5, 397 (1959).
11. H. Schlichting, ZAMM 13, 260 (1933).
12. S. Tada, T. Vermeulen, and A. E. Vandegrift, A.I.Ch.E.J., in press.

IV. VELOCITY PROFILE OF CYLINDRICAL LAMINAR LIQUID JETS ENTERING A MOVING SURROUNDING LIQUID

A. Introduction

In cases where a laminar-flow liquid jet is injected axisymmetrically in an immiscible liquid flowing at uniform velocity, knowledge of the entry behavior is necessary to establish the actual velocity behavior of both liquids as governed by momentum transfer across the phase boundary. If the external flow also is laminar, the jet will be more stable than for injection into a stationary external liquid, due to the lower rate of momentum transfer. Moreover, whereas injection into a stationary external liquid may never reach a steady-state profile, the distance required for transition of the interior-jet velocity from its initially parabolic profile to a flat profile is relatively short.

One important experimental application of such jets is their use in studies of heat and mass transfer, the latter sometimes including chemical reaction. The theory of an oscillating jet[2] assumes a uniform axial-velocity profile, on which perturbed velocities due to the non-circular orifice are superposed. Therefore a closer approximation to the theory should be shown by a jet in a flowing external lqiuid than by one in a stationary external liquid.

Wygnanski[4] recently solved the problem of a two-dimensional laminar jet issuing co-directionally into a uniform stream of the same fluid. He developed a direct expansion to apply near the origin, and an asymptotic expansion valid only at large distances; the two expansions are joined along the center line of the jet. However, it appears that

no theory has yet been developed for the axisymmetric case, particularly for a pair of immiscible liquids having different viscosities and densities.

The present authors with Vandegrift[3] have developed a numerical stepwise empirical-fit technique for a cylindrical jet issuing into a stationary immiscible liquid. That method will be extended here to cases having a flowing external liquid.

B. Theory

We consider a liquid jet injected into another liquid flowing in the same direction, and confined in a cylindrical tube. Throughout the length of the system considered here, the exterior liquid flows within a relatively large cylindrical wall. Upstream of the orifice from which the interior jet emerges, its flow is also bounded by a central thin-wall orifice tube having the same diameter as the emerging jet (Fig. 1).

At the orifice, the velocity at the interface between interior and exterior fluids is zero. Immediately downstream, at radius values near the value of the orifice radius, both fluids are accelerated. If the interior-fluid velocity adjacent to the interface increases more rapidly, the interior jet can be termed a "strong" jet; conversely, if its acceleration is less rapid, it can be identified as "weak." Near the orifice a strong jet will impart momentum to the exterior fluid, whereas a weak jet will absorb momentum from the exterior fluid; further downstream, the direction of momentum transfer may reverse before the steady-state profile is attained. However, because of the mathematical forms of velocity equations, only a strong-jet behavior, which is our main concern, can be described by the following model.

The following notations are used;

$A, B, C, C_1, D, D_1, E, G, M$	coefficients which are functions of the axial-distance variable
A'	interfacial radius or jet radius (cm)
A_0'	orifice radius (cm)

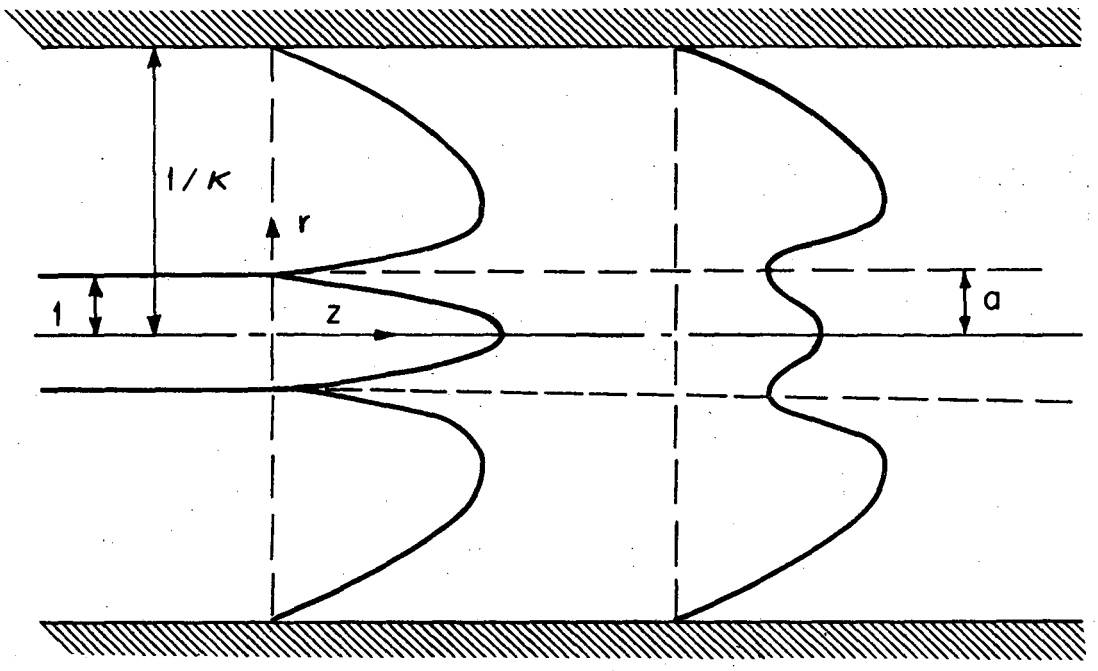

XBL6811-7228

Fig. 1 Flow-system geometry with representative velocity profile.

A_T'	tube radius (cm)
a	A'/A_0', dimensionless jet radius
K	$1 + \kappa^2 - (1 - \kappa^2)/\ln(1/\kappa)$
K_a	$(1 - \kappa^2 a^2)/\ln(\kappa a) = 2(1 - \eta)/\ln\eta$
R'	radial distance (cm)
r	R'/A_0', dimensionless radial distance
R_i	$2A_0'W_0'\rho_i/\mu_i$, interior Reynolds number
R_e	$2A_0'W_0'\rho_e/\mu_e$, exterior Reynolds number based on the interior-flow conditions
W'	axial velocity (cm/sec)
W	W'/W_0', dimensionless axial velocity
W_0'	initial mean velocity of jet (cm/sec)
W_{AF}'	initial mean annular velocity (cm/sec)
Z'	axial distance (cm)
z	Z'/A_0', dimensionless axial distance
i	interior phase
e	exterior phase
α	parabolic constant
β	$\mu_e\rho_e/\mu_i\rho_i$, viscosity density constant
γ	W_{AF}'/W_0', ratio of initial average velocities
η	$(\kappa a)^2$
κ	A_0'/A_T', ratio of orifice radius to outside-tube radius
ζ	z/R_i

1. Empirical Velocity Equations

In the case of a stationary surrounding fluid we added a perturbing function to a parabolic form to describe an interior jet-velocity profile. Here we shall add an exponential-type perturbing function to an annular-flow expression to give an exterior jet-velocity profile. However, since the outside-tube diameter is substantially larger than the orifice diameter, the exterior liquid can be viewed as essentially an infinite medium. This is equivalent to saying that the boundary layer that forms in the exterior liquid does not interact with the outside-tube wall within the flow-path interval in which the interior-jet profile changes from a parabolic to a flat form. Except for a very minor correction factor, G, which is introduced to satisfy the conservation of mass, our treatment is based upon the physical fact that the exterior jet-velocity profile far from the interface does not change.

The perturbing functions assumed for the interior and exterior jets are the same as in the stationary case. The velocity equations are:

$$W_i = 2\alpha e^{-Mz}(a^2 - r^2) + B/(1 + Ar^2)^2 \qquad (1)$$

$$W_e = 2\gamma G/K\{1 - (\kappa r)^2 - (1 - \kappa^2 a^2)\ln(\kappa r)/\ln(\kappa a)\} + De^{-Cr^2} \qquad (2)$$

where the first term in each equation represents the parabolic or annular-type profile[1] which applies at the orifice plane.

As in the related analysis for a jet in a stationary fluid, a boundary-layer approximation is made, and axial velocities can be expressed by use of six parametric functions plus the radius a.

The following seven governing equations are used: first, the integrated equation of motion on the center line,[3]

$$(W_i^2)_{r=0} - 4 = 4/R_i \int_0^z a\left(\frac{\partial W_i}{\partial r}\right)_{r=0} dz \tag{3}$$

The continuity of axial velocities at the interface,

$$(W_i)_{r=a} = (W_e)_{r=a} \tag{4}$$

The continuity of tangential stresses at the interface,

$$\mu_i\left(\frac{\partial W_i}{\partial r}\right)_{r=a} = \mu_e\left(\frac{\partial W_e}{\partial r}\right)_{r=a} \tag{5}$$

Mass balance for the interior jet,

$$\int_0^a rW_i dr = 1/2 \tag{6}$$

Mass balance for the exterior fluid, which is flowing and bounded by a cylindrical tube,

$$\int_a^{1/\kappa} rW_e dr = \int_1^{1/\kappa} rW_{AF} dr \tag{7}$$

where

$$W_{AF} = 2\gamma/K\{1 - (\kappa r)^2 - (1 - \kappa^2)\ln(\kappa r)/\ln\}$$

with $\gamma = W_{AF}'/W_0'$; $K = 1 + \kappa^2 - (1 - \kappa^2)/\ln(1/\kappa)$; and $1 \leq r \leq 1/\kappa$.

Momentum balance for the interior jet,

$$\int_0^{1/\kappa} rW_i^2 dr = \frac{2}{3} + \frac{2}{R_i}\int_1^{1/\kappa} a\left(\frac{\partial W_i}{\partial r}\right)_{r=a} dz \tag{8}$$

Momentum balance for the exterior fluid,

$$\int_a^{1/\kappa} rW_e^2 dr - \int_1^{1/\kappa} rW_{AF}^2 dr = -\frac{2}{R_e}\int_0^z a\left(\frac{\partial W_e}{\partial r}\right)_{r=a} dz \tag{9}$$

Substituting W_i and W_e into Eqs. (3) through (9), we obtain

$$(2\alpha e^{-Mz}a^2)^2 + 4\alpha Ba^2 e^{-Mz} + B^2 - 4 - \frac{32}{R_i}\int_0^z (\alpha e^{-Mz} + AB)dz = 0 \tag{10}$$

$$B/(1 + Aa^2)^2 - De^{-Ca^2} = 0 \tag{11}$$

$$Ae^{-Mz} + AB/(1 + Aa^2)^3 - 0.5(\mu_e/\mu_i)\ (\gamma G/K)(2\kappa^2 + K_a/a^2) + CDe^{-Ca^2} = 0 \tag{12}$$

$$\alpha a^4 e^{-Mz} + Ba^2/(1 + Aa^2) - 1 = 0 \tag{13}$$

$$2(\gamma G/K)\{(1/\kappa - a) - 0.25\kappa^2(1/\kappa^4 - a^4) + 0.5a^2(1 - \kappa_1)$$

$$+ 0.25(1 - \kappa_1)K_a/\kappa^2\} + 0.5De^{-Ca^2}/C \sim 0 \qquad (14)$$

$$\frac{2}{3}\alpha^2 a^6 e^{-2Mz} + 2\alpha Be^{-Mz}\,[a^4/(1 + Aa^2) - \ln(1 + Aa^2)/A^2$$

$$+ a^2/\{A(1 + Aa^2)\}] + \frac{1}{6}(B^2/A)\{1 - 1/(1 + Aa^2)^3\}$$

$$- \frac{2}{3} - \frac{8}{R_i}\int_a^z \{\alpha a^2 e^{-Mz} + ABa^2/(1 + Aa^2)^3\}dz = 0 \qquad (15)$$

$$MI - MI_0 = \frac{2}{R_e}\int_0^z \{(\gamma G/K)(2\eta + K_a) + CDa^2 e^{-Ca^2}\}dz \qquad (16)$$

where $MI = MI_1 + MI_2 + MI_3$ and $\eta = \kappa^2 a^2$

$$MI_0 = \int_1^{1/\kappa} rW_{AF}^2 dr = \text{const.} \qquad (17)$$

$$MI_1 = \int_a^{1/\kappa} (2\gamma G/K)^2\{1 - (\kappa r)^2 - K_a \ln(\kappa r)\}^2 r dr$$

$$= 2(\gamma G/K)^2[(1 - \eta)/\kappa^2 + (1 - \eta^3)/3\kappa^2$$

$$+ (K_a^2/4\kappa^2)\{2 - \eta(\ln\eta)^2 + 2\eta\ln\eta - 2\eta\}$$

$$- (1 - \eta^2)/\kappa^2 + (K_a/\kappa^2)(\eta^2/4 - \eta^2\ln\eta/2 - \tfrac{1}{4})$$

$$- (K_a/\kappa^2)(\eta - \eta\ln\eta - 1)] \qquad (18)$$

$$MI_2 = \int_a^{1/\kappa} (4\gamma G/K)\{1 - (\kappa r)^2 - K_a \ln(\kappa r)\} De^{-Cr^2} r dr$$

$$\sim \int_{a^2}^{\infty} (2\gamma G/K)(De^{-Ct} - \kappa^2 t De^{-Ct} - K_a De^{-Ct} \ln \kappa^2 t/2) dt$$

$$= (2\gamma G/K)[De^{-Ca^2}/C - \kappa^2 De^{-Ca^2}(1 + Ca^2)/C^2$$

$$- (K_a De^{-Ca^2}/2C\{\ln\eta + e^{Ca^2} E_1(Ca^2)\}] \tag{19}$$

$$MI_3 = D^2 e^{-2Ca^2}/4C \tag{20}$$

The last term in Eq. (19) is the exponential integral,

$$E_1(Ca^2) = \int_{Ca^2}^{\infty} (e^{-t}/t) dt$$

2. Computation Procedure

As in the case of stationary external liquid, the above seven equations are linearized, and the resulting seven linear equations are solved for seven incremental values of parameters at each increment of z. The third-order Runge-Kutta shceme is used to reduce truncation errors. The following substitution is also needed to avoid numerical difficulties at small z values:

$$E = De^{-Ca^2}$$

The elements of the linear simultaneous equations $\underset{\approx}{M}d\underset{\sim}{x} = \underset{\sim}{N}dz$ are given as follows (zero-valued elements are omitted), where $dx_1 = dA$, $dx_2 = dB$, $dx_3 = dC$, $dx_4 = dE$, $dx_5 = da$, $dx_6 = dG$, and $dx_7 = dM$:

$$M_{12} = 4\alpha a^2 e^{-Mz} + 2B$$
$$M_{15} = 16\alpha^2 a^3 e^{-2Mz} + 8\alpha Bae^{-Mz}$$
$$M_{17} = -8\alpha^2 a^4 e^{-2Mz} - 4\alpha Ba^2 ze^{-Mz}$$
$$N_1 = 8\alpha^2 a^4 Me^{-2Mz} + 4\alpha Ba^2 Me^{-Mz} - 32(\alpha e^{-Mz} + AB)/R_i$$
$$M_{21} = -2Ba^2/(1 + Aa^2)^3$$
$$M_{22} = 1/(1 + Aa^2)^2$$
$$M_{24} = -1$$
$$M_{25} = -4ABa/(1 + Aa^2)^3$$
$$M_{31} = B/(1 + Aa^2)^3 - 3ABa^2/(1 + Aa^2)^4$$
$$M_{32} = A/(1 + Aa^2)^3$$
$$M_{33} = -0.5(\mu_e/\mu_i)E$$
$$M_{35} = -6A^2Ba/(1 + Aa^2)^4 + 2(\mu_e/\mu_i)(\gamma G/K)(1 - \eta + \ln\eta)/a^3(\ln\eta)^2$$
$$M_{36} = -0.5(\mu_e/\mu_i)(\gamma/K)(2\kappa^2 + K_a/a^2)$$
$$M_{37} = -\alpha ze^{-Mz}$$
$$N_3 = \alpha ze^{-Mz}$$
$$M_{41} = -0.5Ba^4/(1 + Aa^2)^2$$
$$M_{42} = 0.5a^2/(1 + Aa^2)$$
$$M_{45} = 2\alpha a^3 e^{-Mz} + Ba/(1 + Aa^2) - ABa^3/(1 + Aa^2)^2$$
$$M_{47} = -0.5\alpha a^4 ze^{-Mz}$$
$$N_4 = 0.5\alpha a^4 Me^{-Mz}$$

$$M_{53} = -0.5E/C^2$$

$$M_{54} = 0.5/C$$

$$M_{55} = 2(\gamma G/K)\{(1 - \eta)a - 1 - 0.5aK_a + 0.5a(1 - \eta)dK_a/d\eta\}$$

$$M_{56} = 2(\gamma/K)\{ (1/\kappa - a) - 0.25\ ^2(1/\kappa^4 - a^4) + 0.5a\ ^2(1 - \eta + 0.25(1 - \eta)K_a/\kappa^2\}$$

$$M_{61} = 2\alpha B[-a^6/(1 + Aa^2)^2 - a^4/\{A(1 + Aa^2)^2\} - 2a^2/\{A^2(1 + Aa^2)\} + 2\ell n(1 + Aa^2)/A^3]e^{-Mz} - 1/6(B/A)^2\{1 - 1/(1 + Aa^2)^3\} + 0.5(Ba)^2/\{A(1 + Aa^2)^4\}$$

$$M_{62} = 2\alpha[a^4/(1 + Aa^2) - \ell n(1 + Aa^2)/A^2 + a^2/\{A(1 + Aa^2)\}]e^{-Mz} + 1/3(B/A)\{1 - 1/(1 + Aa^2)^3\}$$

$$M_{65} = 4\alpha^2a^5e^{-2Mz} + 4\alpha Ba^3e^{-Mz}/(1 + Aa^2) + B^2a/(1 + Aa^2)^4$$

$$M_{67} = -4/3\alpha^2a^6ze^{-2Mz} - 2\alpha Bz[a^4/(1 + Aa^2) - \ell n(1 + Aa^2)/A^2 + a^2/\{A(1 + Aa^2)\}]e^{-Mz}$$

$$N_6 = 4/3\alpha^2a^6Me^{-2Mz} + 2\alpha BM[a^4/(1 + Aa^2) - \ell n(1 + Aa^2)/A^2 + a^2/\{A(1 + Aa^2)\}]e^{-Mz} - 8\{\alpha a^2e^{-Mz} + ABa^2/(1 + Aa^2)^3\}/R_i$$

$$M_{73} = 2(\gamma G/K)[2\kappa^2E/C^3 + (\eta - 1)E/C^2 + 0.5K_a(E/C^2)\}\ell n\eta + e^{Ca^2}E_1(Ca^2)\}] + 0.5E/C$$

$$M_{75} = 4(\gamma G/K)^2\{T_1 + 0.5K_aT_2(dK_a/d\eta) - (K_a\ell n\eta)^2/4 - K_a(\eta - 1)\ell n\eta + T_3(dK_a/d\eta)\}a - 2(\gamma G/K)\{2\eta E/(Ca) + \kappa_1E\{\ell n\eta + e^{Ca^2}E_1(Ca^2)\}$$

$$M_{76} = 2MI_1/G + MI_2/G$$

$$N_7 = 4\{(\gamma G/K)(2\eta + K_a) + CEa^2\}/R_e$$

where

$$T_1 = -\eta^2 + 2\eta - 1$$

$$T_2 = 2 - \eta(\ell n\eta)^2 + 2\eta\ell n - 2\eta$$

$$T_3 = \eta^2/4 - \eta + 3/4 - (\eta^2/2 - \eta)\ln\eta$$
$$dK_a/d\eta = -2\{\ln\eta + (1 - \eta)/\eta\}/(\ln\eta)^2$$

As in the calculation for the stationary surrounding liquid, α is taken to be 0.95, $z_0 = 1.0\times10^{-6}$, and $a_0 = 1.0$. The initial values are then determined as before, except that G is set at 1.0. When the terms involving M shrink to negligible levels, a total momentum balance is used, adding Eq. (8) to Eq. (9) times the density ratio:

$$\int_0^a rW_i^2 dr + \frac{\rho_e}{\rho_i}\int_a^{1/\kappa} rW_e^2 ar = \frac{2}{3} + \frac{\rho_e}{\rho_i}\int_1^{1/\kappa} rW_{AF}^2 dr = \text{const.} \tag{8a}$$

The resulting 6×6 matrix has changes in the sixth-row elements, as follows:

$$M_{63} = (\rho_e/\rho_i)M_{73}$$
$$M_{64} = (\rho_e/\rho_i)M_{74}$$
$$M_{65} = M_{65} + (\rho_e/\rho_i)M_{75}$$
$$M_{66} = (\rho_e/\rho_i)M_{76}$$
$$N_6 = (\rho_e/\rho_i)N_7$$

3. <u>Generalized Behavior</u>

There are four input variables for the present calculation: viscosity ratio μ_e/μ_i, density ratio ρ_e/ρ_i, orifice-to-tube radius ratio κ, and average-velocity ratio γ. Once κ and γ are fixed, the the functions A, B, C ρ_i/ρ_e (or C_1), D_1 (equal to D at $\rho_e/\rho_i = 1$), a,

M, and G can be expressed in terms of two parameters β and ζ as for the stationary surrounding liquid.

$$\beta = \mu_e \rho_e / \mu_i \rho_i \tag{21}$$

$$\zeta = z/R_i \tag{22}$$

Therefore β, γ, and κ are the input variables to be specified so as to carry out the numerical integration by the third-order Runge-Kutta scheme. In order to explore the functional behavior, β has been varied from 1 to 16; γ from 0.125 to 2; κ from 0.025 to 0.20.

a. Effect of viscosities and densities. For $\gamma = 0.25$ and $\kappa = 0.1$, the profiles of center-line velocity, interfacial velocity, and jet radius are shown in Fig. 2. The curves for different β's show that higher values of β have a diminishing effect on the jet behavior.

At higher γ values, near or over 1, curves for different β's would combine into a single curve, indicating that β has little effect in such cases. Thus the behavior for different values of β, at γ near or over 1, can be determined from the curves for $\beta = 4$ given in Fig. 3.

b. Effect of average-velocity ratio. For $\beta = 4.0$ and $\kappa = 0.1$, profiles at different γ values are shown in Fig. 3. The γ values have the most pronounced effect on the behavior of the velocity and the jet radius. Naturally, higher γ's give higher center-line and interfacial

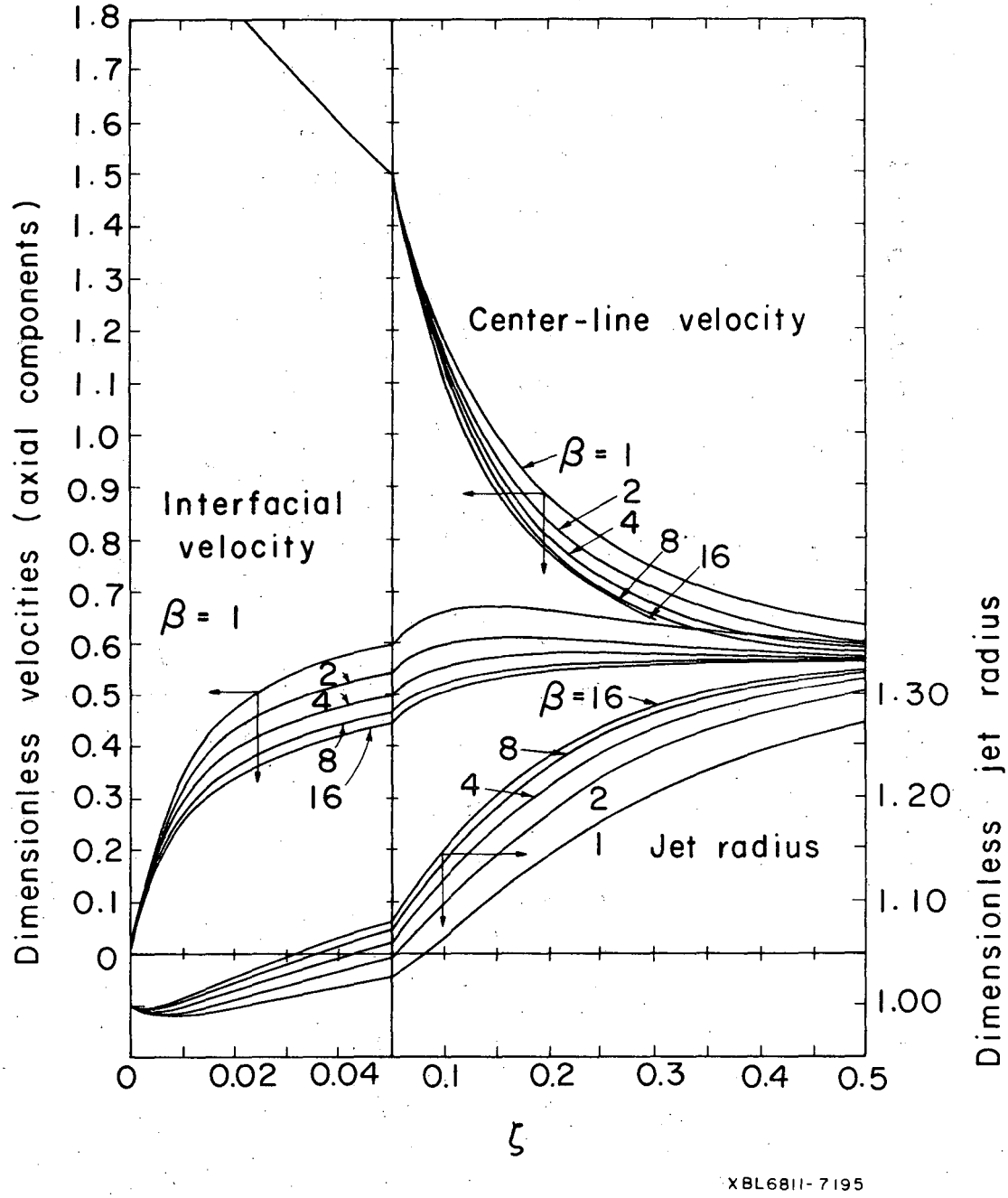

Fig. 2 Effect of β on jet velocities and radius for $\gamma = 0.25$ and $\kappa = 0.1$.

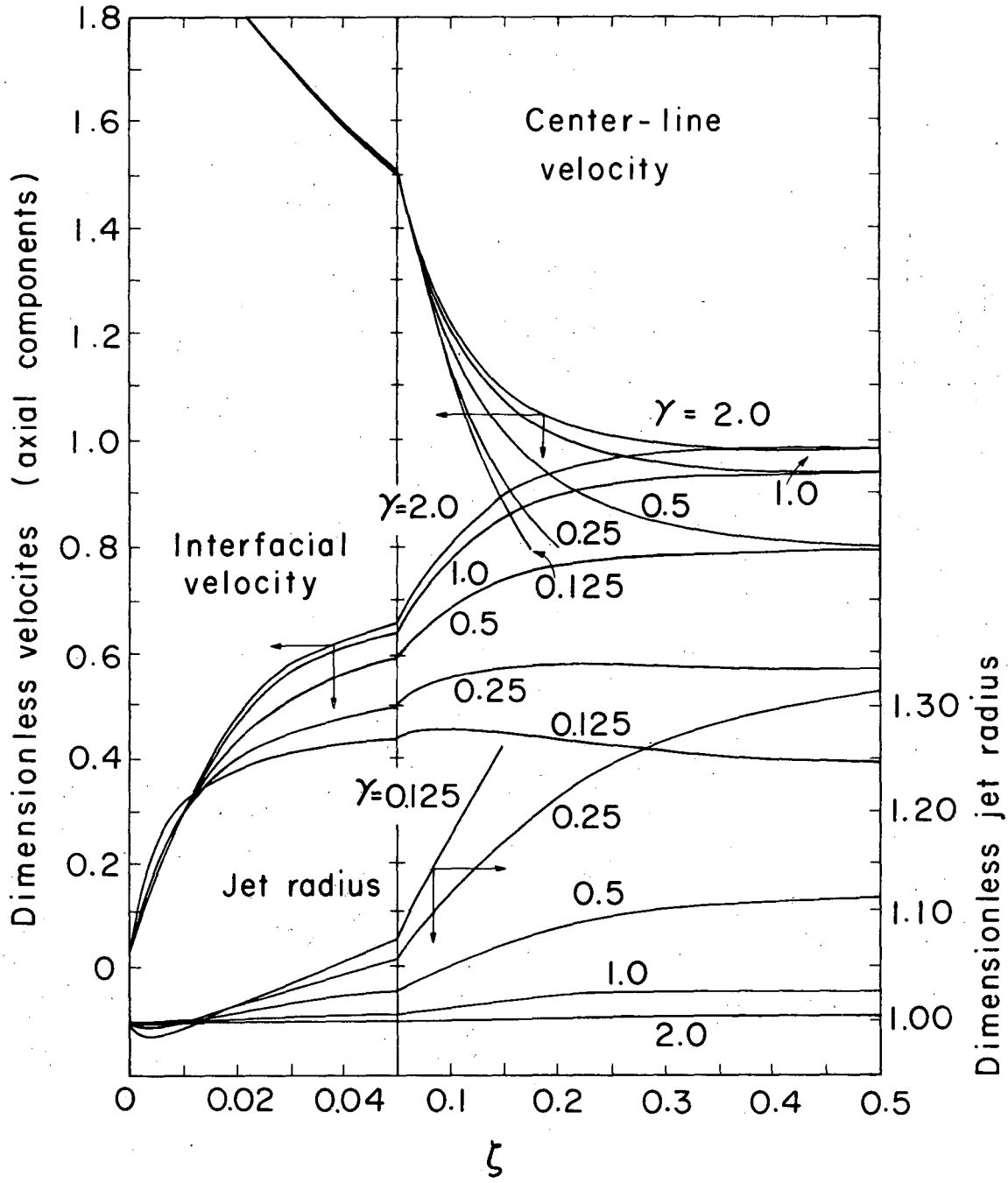

XBL6811-7194

Fig. 3 Effect of γ on jet velocities and radius, for $\beta = 4$ and $\kappa = 0.1$.

velocities for the interior jet, and smaller changes in the jet-radius profile.

For smaller γ, the velocity profiles level off at values above the original exterior average velocities, which they should ultimately approach. The present model fails to describe the entire eventual velocity profile. The equation of motion for the exterior phase has not been included, and only the region adjacent to the interior jet undergoes much change in velocity within the distance where the interior jet varies from parabolic to plug flow; the distance necessary for the exterior fluid to attain a true steady state is approximately 100 times that for the interior jet.

c. Effect of orifice-to-tube radius ratio. For $\beta = 4.0$ and $\gamma = 1.0$, profiles at different κ values are given in Fig. 4. Because of the approximations made in the mass and momentum balances for the exterior phase, Eqs. (14) and (16), the present calculational method does not apply for the κ values above 0.2. At γ values near or over 1, κ does not have much effect on the profiles, although it is quite significant at low γ values. The radius of maximum exterior velocity comes closer to the center-line of the tube, and the interior velocities attain higher values (with less increase in a), for smaller κ values.

d. Behavior of parameters. For reference, representative values of the parameters, as functions of ζ between 0.005 and 0.5, are tabulated in Table I.

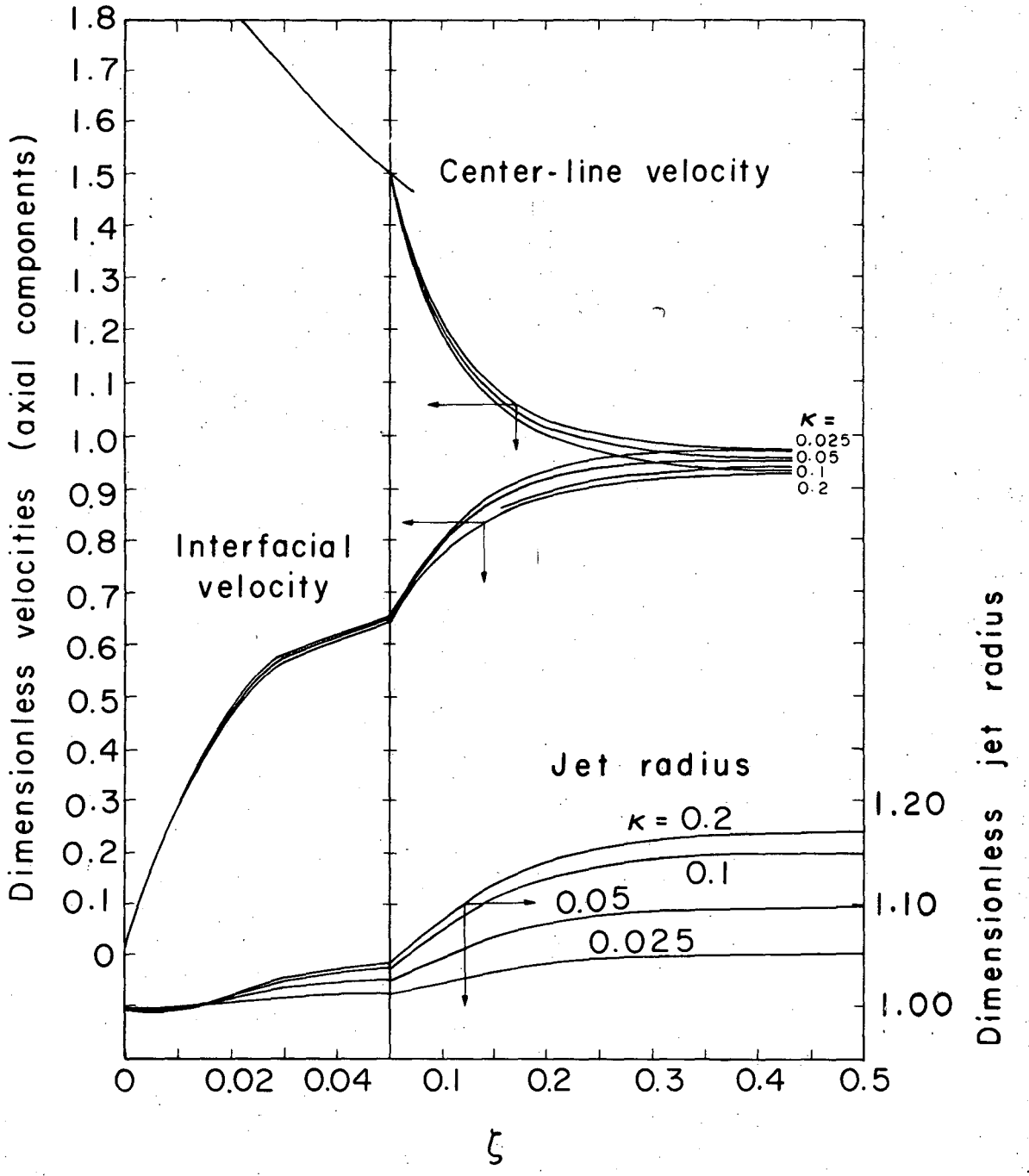

XBL6811-7196

Fig. 4 Effect of κ on jet velocities and radius, for $\beta = 4$ and $\gamma = 1.0$.

Table I. Behavior of Parameters

			A				B				M			
			$\zeta=$				$\zeta=$				$\zeta=$			
β	κ	γ	.0005	.005	.05	.5	.0005	.005	.05	.5	.0005	.005	.05	.5
1.0	0.10	0.25	1.314	0.908	0.550	0.019	0.225	0.739	1.495	0.635	0.421	0.401	0.771	--
1.0	0.10	1.0	1.392	0.967	0.519	0.0013	0.212	0.658	1.508	0.944	0.373	0.354	---	--
2.0	0.10	0.25	1.316	0.917	0.580	0.014	0.225	0.723	1.448	0.603	0.419	0.382	0.359	--
2.0	0.10	1.0	1.393	0.968	0.517	0.0011	0.212	0.659	1.502	0.943	0.373	0.353	---	--
4.0	0.05	1.0	1.396	0.971	0.520	0.0007	0.211	0.654	1.508	0.962	0.371	0.352	---	--
	0.10	0.25	1.320	0.931	0.597	0.0107	0.224	0.702	1.388	0.589	0.417	0.379	0.292	--
		0.5	1.377	0.961	0.546	0.0039	0.214	0.665	1.486	0.803	0.382	0.358	---	--
		1.0	1.393	0.969	0.515	0.0009	0.212	0.656	1.498	0.943	0.373	0.353	---	--
		2.0	1.397	0.971	0.485	0.0004	0.211	0.654	1.480	0.987	0.371	0.352	---	--
	0.20	1.0	1.387	0.965	0.514	0.0010	0.213	0.661	1.496	0.936	0.376	0.356	---	--
8.0	0.10	0.25	1.325	0.947	0.611	0.0089	0.223	0.679	1.347	0.582	0.414	0.366	0.264	--
		1.0	1.393	0.971	0.514	0.0008	0.212	0.655	1.496	0.943	0.373	0.352	---	--
16.0	0.10	0.25	1.330	0.963	0.621	0.0076	0.222	0.660	1.322	0.578	0.410	0.354	0.252	--
		1.0	1.393	0.971	0.514	0.0008	0.212	0.654	1.494	0.943	0.373	0.352	---	--

Table I. (continued)

			$C/(\rho_e/\rho_i)$				$D_1 = (D)_{\rho_e/\rho_i=1}$				G			
			$\rho=$				$\rho=$				$\rho=$			
β	κ	γ	.0005	.005	.05	.5	.0005	.005	.05	.5	.0005	.005	.05	.5
1.0	0.10	0.25	48.4	8.01	0.983	0.241	∞	544	1.69	0.883	1.00	1.00	1.01	1.01
		1.0	69.6	12.98	1.765	0.721	∞	72,750	3.86	2.02	1.00	1.00	1.00	1.00
2.0	0.10	0.25	26.4	4.60	0.709	0.216	∞	18.7	1.18	0.829	1.00	1.00	1.01	1.01
		1.0	44.4	8.59	1.422	0.718	∞	909.0	2.74	2.02	1.00	1.00	1.00	1.00
4.0	0.05	1.0	26.0	5.14	0.921	0.495	∞	28.8	1.65	1.61	1.00	1.00	1.00	1.00
	0.10	0.25	15.4	2.89	0.556	0.207	∞	3.35	0.929	0.811	1.00	1.00	1.01	1.01
		0.5	21.6	4.21	0.740	0.373	∞	11.52	1.31	1.27	1.00	1.00	1.00	1.01
		1.0	31.8	6.40	1.253	0.718	∞	101.4	2.30	2.02	1.00	1.00	1.00	1.00
		2.0	51.2	10.63	2.269	1.420	∞	6943.	6.53	4.16	1.00	1.00	1.00	1.00
	0.20	1.0	43.7	8.99	1.955	1.19	∞	1354.	4.72	3.32	1.00	1.00	1.00	1.01
8.0	0.10	0.25	9.90	2.03	0.468	0.203	808	1.35	0.796	0.803	1.00	1.00	1.01	1.01
		1.0	25.5	5.30	1.167	0.717	∞	33.8	2.11	2.01	1.00	1.00	1.00	1.00
16.0	0.10	0.25	7.15	1.58	0.420	0.201	51.7	0.832	0.725	0.800	1.00	1.00	1.01	1.01
		1.0	22.3	4.75	1.126	0.717	∞	19.5	2.03	2.01	1.00	1.00	1.00	1.00

REFERENCES

1. R. B. Bird, W. E. Stewart, and E. N. Lightfoot, Transport Phenomena (John Wiley and Sons, Inc., New York, 1960).

2. S. Tada, T. Vermeulen, and A. E. Vandegrift, in press, A.I.Ch.E.J.

3. A. E. Vandegrift, S. Tada, and T. Vermeulen, paper submitted to J. Fluid Mech.

4. I. Wygnanski, J. Fluid Mech. 27, 431 (1967).

V. CONCLUSIONS

The mathematical description of the oscillating jet has been divided into two parts: elliptical oscillation of a plug-flow jet, and relation of effective plug-flow velocities to actual velocity profiles and jet radii. A complete numerical solution for the oscillating wavelength has been obtained. Also, the cylindrical velocity profiles have have been calculated with an accuracy which should be adequate for interpreting experimental data on liquid-liquid jets.

Further study is needed of the effect of downstream obstructions producing pressure gradients along the jet path, and also of the correlation needed to define the effective plug-flow velocity on which the interfacial-tension determination is based.

The nozzles used in the reported experiments were made by drawing heated capillary glass tubing to obtain a taper and then pressing the tubing into an elliptical shape. Numerous other methods of producing satisfactory nozzles were attempted. In the most successful of them, heated Pyrex glass tubing (5 mm O.D.) was drawn to capillary dimensions (0.3-0.8 mm), and the resulting capillary was pressed into elliptical form. After breaking the tube squarely, 1 to 2 cm of nozzle tip thus obtained was attached to a stainless-steel hypodermic needle (No. 19) with epoxy glue. The effect of nozzle wall thickness should be much smaller than that of the nozzles constructed from thick-wall capillary tubing.

A study of additives for the exterior liquid (such as carboxymethyl cellulose) is necessary, to keep it in the laminar-flow region by increasing its viscosity without accompanying major changes in diffusivity.

ACKNOWLEDGMENTS

Thanks are due Professor Simon Goren and Professor Donald Olander for their invaluable aid and advice; to Peter Tennen and Dennis Iverson for help in the computer programming; and to Dr. A. E. Vandegrift for initiating this study, as reprinted in UCRL-10717.

The work described was performed in the Lawrence Radiation Laboratory under the auspices of the United States Atomic Energy Commission.

APPENDIXES: COMPUTER PROGRAMS

I. Wavelength--Interfacial-Tension Relation

The following programs were written to solve Eq. (38) to obtain the interfacial tension and the empirical multiplier, f.

A. Main Program (XINTES)

(1) Abstract

The object of this program is to evaluate a 6×6 complex matrix equation, the matrix being a function of a variable;

$$\underset{\approx}{A}(\sigma) \cdot \underset{\sim}{X} = 0$$

For nontrivial $\underset{\sim}{X}$, $\underset{\approx}{A}(\sigma) = 0$ must hold, which leads to solving the determinant equation for σ.

$$\sigma = - \frac{\det \underset{\approx}{D}}{\det \underset{\approx}{\Delta}}$$

(2) Usage

Input:

N	run no.
B	wave number, $2\pi/\lambda$
A	jet radius, a
RE1	one half of interior Reynolds no., ca ρ_i/μ_i
CMU1	interior-fluid viscosity

RMU	viscosity ratio, μ_e/μ_i
RRHO	density ratio, ρ_e/ρ_i
c	effective plug-flow velocity
Z(1), Z(2)	estimated initial-damping factors

Output:

DELR, DELI	real and imaginary parts of det $\underset{\approx}{\Delta}$
DETR, DETI	real and imaginary parts of det $\underset{\approx}{D}$
TR, TI	real and imaginary parts of interfacial tension
Z(L)	damping factor
WE	modified Weber no., $\mu_i c/\sigma$
RWE	reciprocal of modified Weber no.
RWE1	reciprocal of Weber no., $\sigma/c^2 a\rho_i$
F	empirical multiplier, f

B. <u>Gauss-Reduction Subprogram (GAUSS)</u>

(1) Abstract

This program gives a determinant of a matrix with complex variables.

(2) Usage

CALL GAUSS(M,BR,BI,DETR,DETI,FACTOR,JROW,ICOL)

M	no. of rows or columns of a matrix
BR	real part of element in A
BI	imaginary part of element in A
DETR	real part of determinant
DETI	imaginary part of determinant

FACTOR	scale factor to control overflow or underflow

(3) Restrictions

$M \leq 20$

(4) Method

The basic feature of the method is to convert the square determinant to triangular form, so that the determinant is simply the product of diagonal elements of the triangular matrix.

C. Bessel-Function Subprograms (BIS,BIL,BKS,BKL)

(1) Abstract

These programs give the functional values of modified Bessel functions with complex arguments.

(2) Usage

```
CALL BIS(N,RHO,PHI,BRIS,BIIS)
CALL BIL(N,RHO,PHI,BRIL,BIIL)
CALL BKS(N,RHO,PHI,BRKS,BIKS)
CALL BKL(N,RHO,PHI,BRKL,BIKL)
```

N	order of modified Bessel function
RHO	magnitude of argument
PHI	arg z = arctan(y/x)
BRIS,BIIS,BRIL,BIIL	real and imaginary parts of modified Bessel function of the first kind
BRKS,BIKS,BRKL,BIKL	real and imaginary parts of modified Bessel function of the second kind

(3) Restrictions

BIS,BKS for RHO $\leq$ 10

BIL,BKL for RHO > 10

(4) Method

BIS and BKS are summations of series (9.6.10), (9.6.11) up to the twentieth term. BIL and BKL are summations of series (9.7.1) and (9.7.2) up to the thirtieth term. These series are given in Handbook of Mathematical Functions.*

---

* Abramowitz and Stegun, Handbook of Mathematical Functions, Natl. Bureau of Standards, Appl. Math. Series No. 55, U.S. Govt. Printing Office (1964).

```
      PROGRAM XINTES(INPUT,OUTPUT,TAPE5 = INPUT,TAPE6 = OUTPUT)
      COMMON AR(20,20),AI(20,20),JROW(20),ICOL(20),IROW(20),JCOL(20),
     1          BR(20,20),BM(20,20),AAR(6),AAI(6),CR(20,20),CI(20,20),
     2          TR(25),TI(25),Z(25)

C     N = RUN NO., B = REAL-WAVE NO., A = AV. JET RADIUS, RE1 = ONE HALF
C     OF INTERIOR REYNOLDS NO., CMU1 = INTERIOR-FLUID VISCOSITY, RMU =
C     VISCOSITY RATIO, RRHO = DENSITY RATIO, C = CONSTANT AXIAL VELOCITY
C     , Z = DAMPING FACTOR, TR = REAL-PART INTERFACIAL TENSION,
C     TI = IMAGINARY-PART INTERFACIAL TENSION, WE = MODIFIED WEBER NO.,
C     RWE = 1./WE, RWE1 = 1./(WEBER NO.), F = EMPIRICAL MULTIPLIER TO
C     RAYLEIGH SOLUTION.

C     GIVEN BA, RE1,RMU, RRHO, AND Z OF 1ST AND 2ND APPROXIMATION, WE
C     OBTAIN TR WITH TI = 0., WEBER NO.S, AND F. WHEN IT OVERFLOWS, TR =
C     TI = WE = F = 0. WHEN TI DOES NOT CONVERGE TO 0, TR, TI, WE, AND
C     F WILL BE SET TO 100.

    8 READ (5,1) N,B,A,RE1,CMU1,RMU,RRHO,C
      IF(N.EQ.99) STOP
      READ (5,11) Z(1),Z(2)
      CMU2 = RMU*CMU1
      RE2 = RE1*(RRHO/RMU)
      WRITE (6,2) N,B,A,RE1,CMU1,RMU,RRHO,C
      L= 1
      BAR = B*A
    7 BAI = Z(L)*A
      U1 = BAR**2 - BAI**2 - BAI*RE1
      U2 = BAR**2 - BAI**2 - BAI*RE2
      V1 = 2.*BAR*BAI + BAR*RE1
      V2 = 2.*BAR*BAI + BAR*RE2
      Y12 = (-U1 + SQRT(U1**2 + V1**2))/2.
      Y22 = (-U2 + SQRT(U2**2 + V2**2))/2.
```

```
      X12 = Y12 + U1
      X22 = Y22 + U2
      D1AR = SQRT(X12)
      D1AI = SQRT(Y12)
      D2AR = SQRT(X22)
      D2AI = SQRT(Y22)
      RBA = SQRT(BAR**2 + BAI**2)
      PHIB = ATAN(BAI/BAR)
      R1 = SQRT(D1AR**2 + D1AI**2)
      PHI1 = ATAN(D1AI/D1AR)
      R2 = SQRT(D2AR**2 + D2AI**2)
      PHI2 = ATAN(D2AI/D2AR)
      RBAR = BAR/(BAR**2 + BAI**2)
      RBAI = -BAI/(BAR**2 + BAI**2)
      SBAR = BAR**2 -BAI**2
      SBAI = 2.*BAR*BAI
      RSBAR = SBAR/(SBAR**2 + SBAI**2)
      RSBAI = -SBAI/(SBAR**2 + SBAI**2)
      RD1AR = D1AR/((D1AR**2)+(D1AI**2))
      RD1AI = -D1AI/((D1AR**2)+(D1AI**2))
      RD2AR = D2AR/((D2AR**2)+(D2AI**2))
      RD2AI = -D2AI/((D2AR**2)+(D2AI**2))
      SD1AR = U1
      SD1AI = V1
      SD2AR = U2
      SD2AI = V2
      RSD1AR = SD1AR/((SD1AR**2)+(SD1AI**2))
      RSD1AI = -SD1AI/((SD1AR**2)+(SD1AI**2))
      RSD2AR = SD2AR/((SD2AR**2)+(SD2AI**2))
      RSD2AI = -SD2AI/((SD2AR**2)+(SD2AI**2))
      CALL BIS(1,RBA,PHIB,BI1R,BI1I)
      CALL BIS(2,RBA,PHIB,BI2R,BI2I)
      CALL BKS(1,RBA,PHIB,BK1R,BK1I)
      CALL BKS(2,RBA,PHIB,BK2R,BK2I)
      IF (R1-10.) 300,310,310
  300 CALL BIS(1,R1,PHI1,DI1R,DI1I)
      CALL BIS(2,R1,PHI1,DI2R,DI2I)
      GO TO 315
```

```
310 CALL BIL(1,R1,PHI1,DI1R,DI1I)
    CALL BIL(2,R1,PHI1,DI2R,DI2I)
315 IF (R2-10.) 320,330,330
320 CALL BKS(1,R2,PHI2,DK1R,DK1I)
    CALL BKS(2,R2,PHI2,DK2R,DK2I)
    GO TO 335
330 CALL BKL(1,R2,PHI2,DK1R,DK1I)
    CALL BKL(2,R2,PHI2,DK2R,DK2I)
335 BI2PR = BI1R - 2.*(RBAR*BI2R - RBAI*BI2I)
    BI2PI = BI1I - 2.*(RBAI*BI2R+RBAR*BI2I)
    BI2PPR = (1.+6.*RSBAR)*BI2R-6.*RSBAI*BI2I-RBAR*BI1R+RBAI*BI1I
    BI2PPI = (1.+6.*RSBAR)*BI2I+6.*RSBAI*BI2R-RBAI*BI1R-RBAR*BI1I
    BK2PR = -BK1R -2.*(RBAR*BK2R - RBAI*BK2I)
    BK2PI = -BK1I - 2.*(RBAI*BK2R + RBAR*BK2I)
    BK2PPR = (1.+6.*RSBAR)*BK2R-6.*RSBAI*BK2I+RBAR*BK1R-RBAI*BK1I
    BK2PPI = (1.+6.*RSBAR)*BK2I+6.*RSBAI*BK2R+RBAI*BK1R+RBAR*BK1I
    DI2PR = DI1R - 2.*(RD1AR*DI2R - RD1AI*DI2I)
    DI2PI = DI1I - 2.*(RD1AI*DI2R + RD1AR*DI2I)
    DI2PPR= (1.+6.*RSD1AR)*DI2R-6.*RSD1AI*DI2I-RD1AR*DI1R+RD1AI*DI1I
    DI2PPI= (1.+6.*RSD1AR)*DI2I+6.*RSD1AI*DI2R-RD1AI*DI1R-RD1AR*DI1I
    DK2PR = -DK1R - 2.*(RD2AR*DK2R - RD2AI*DK2I)
    DK2PI = -DK1I - 2.*(RD2AI*DK2R + RD2AR*DK2I)
    DK2PPR= (1.+6.*RSD2AR)*DK2R-6.*RSD2AI*DK2I+RD2AR*DK1R-RD2AI*DK1I
    DK2PPI= (1.+6.*RSD2AR)*DK2I+6.*RSD2AI*DK2R+RD2AI*DK1R+RD2AR*DK1I
    ELR = -(RBAI*(3.+SBAR)+SBAI*RBAR)/C
    ELI = (RBAR*(3.+SBAR)-SBAI*RBAI)/C
    AR(1,1) = BI2R
    AI(1,1) = BI2I
    AR(1,2) = -BK2R
    AI(1,2) = -BK2I
    AR(1,3) = -DI2R
    AI(1,3) = -DI2I
    AR(1,4) = DK2R
    AI(1,4) = DK2I
    AR(1,5) = 0.
    AI(1,5) = 0.
```

```
      AR(1,6) = 0.
      AI(1,6) = 0.
      AR(2,1) = -BI2PI
      AI(2,1) = BI2PR
      AR(2,2) = BK2PI
      AI(2,2) = -BK2PR
      AR(2,3) = (BAR*RD1AR-BAI*RD1AI)*DI2PI+(BAR*RD1AI+BAI*RD1AR)*DI2PR
      AI(2,3) =-(BAR*RD1AR-BAI*RD1AI)*DI2PR-(BAR*RD1AI+BAI*RD1AR)*DI2PI
      AR(2,4)=-(BAR*RD2AR-BAI*RD2AI)*DK2PI-(BAR*RD2AI+BAI*RD2AR)*DK2PR
      AI(2,4)= (BAR*RD2AR-BAI*RD2AI)*DK2PR+(BAR*RD2AI+BAI*RD2AR)*DK2PI
      AR(2,5) = DI2R
      AI(2,5) = DI2I
      AR(2,6) = -DK2R
      AI(2,6) = -DK2I
      AR(3,1)=2.*(RBAR*BI2R - RBAI*BI2I)
      AI(3,1)= 2.*(RBAR*BI2I + RBAI*BI2R)
      AR(3,2)= -2.*(RBAR*BK2R - RBAI*BK2I)
      AI(3,2)= -2.*(RBAR*BK2I + RBAI*BK2R)
      AR(3,3)=-2.*((BAR*RSD1AR-BAI*RSD1AI)*DI2R-(BAR*RSD1AI+BAI*RSD1AR)*
     1DI2I)
      AI(3,3)=-2.*((BAR*RSD1AR-BAI*RSD1AI)*DI2I+(BAR*RSD1AI+BAI*RSD1AR)*
     1DI2R)
      AR(3,4)= 2.*((BAR*RSD2AR-BAI*RSD2AI)*DK2R-(BAR*RSD2AI+BAI*RSD2AR)*
     1DK2I)
      AI(3,4)= 2.*((BAR*RSD2AR-BAI*RSD2AI)*DK2I+(BAR*RSD2AI+BAI*RSD2AR)*
     1DK2R)
      AR(3,5) =(D1AR*DI2PI + D1AI*DI2PR)/2.
      AI(3,5) = -(D1AR*DI2PR - D1AI*DI2PI)/2.
      AR(3,6) = -(D2AR*DK2PI + D2AI*DK2PR)/2.
      AI(3,6) =(D2AR*DK2PR - D2AI*DK2PI)/2.
      AR(4,1) = -2.*CMU1*(BAR*BI2PPI+BAI*BI2PPR) - CMU1*RE1*BI2R
      AI(4,1) = 2.*CMU1*(BAR*BI2PPR-BAI*BI2PPI) - CMU1*RE1*BI2I
      AAR(1) = (ELR*BI2PI + ELI*BI2PR)
      AAI(1) = -(ELR*BI2PR - ELI*BI2PI)
      AR(4,2) = 2.*CMU2*(BAR*BK2PPI+BAI*BK2PPR) + CMU2*RE2*BK2R
      AI(4,2) = -2.*CMU2*(BAR*BK2PPR-BAI*BK2PPI) + CMU2*RE2*BK2I
```

```
      AAR(2)  = 0.
      AAI(2)  = 0.
      AR(4,3)  = 2.*CMU1*(BAR*DI2PPI+BAI*DI2PPR)
      AI(4,3)  =-2.*CMU1*(BAR*DI2PPR-BAI*DI2PPI)
      AAR(3)  = (BAR*ELR-BAI*ELI)*(RD1AR*DI2PI+RD1AI*DI2PR)
     1         +(BAR*ELI+BAI*ELR)*(RD1AR*DI2PR-RD1AI*DI2PI)
      AAI(3)  = -(BAR*ELR-BAI*ELI)*(RD1AR*DI2PR-RD1AI*DI2PI)
     1          +(BAR*ELI+BAI*ELR)*(RD1AR*DI2PI+RD1AI*DI2PR)
      AR(4,4)  = -2.*CMU2*(BAR*DK2PPI+BAI*DK2PPR)
      AI(4,4)  = 2.*CMU2*(BAR*DK2PPR-BAI*DK2PPI)
      AAR(4)  = 0.
      AAI(4)  = 0.
      AR(4,5)  = 2.*CMU1*(D1AR*DI2PR - D1AI*DI2PI - DI2R)
      AI(4,5)  = 2.*CMU1*(D1AR*DI2PI + D1AI*DI2PR - DI2I)
      AAR(5)  = -(ELR*DI2R - ELI*DI2I)
      AAI(5)  = -(ELR*DI2I + ELI*DI2R)
      AR(4,6)  = -2.*CMU2*(D2AR*DK2PR-D2AI*DK2PI-DK2R)
      AI(4,6)  = -2.*CMU2*(D2AR*DK2PI+D2AI*DK2PR-DK2I)
      AAR(6)  = 0.
      AAI(6)  = 0.
      AR(5,1)  = 2.*CMU1*(BAR*BI2PR - BAI*BI2PI)
      AI(5,1)  = 2.*CMU1*(BAR*BI2PI + BAI*BI2PR)
      AR(5,2)  = -2.*CMU2*(BAR*BK2PR - BAI*BK2PI)
      AI(5,2)  = -2.*CMU2*(BAR*BK2PI + BAI*BK2PR)
      AR(5,3)  = -CMU1*((D1AR+SBAR*RD1AR-SBAI*RD1AI)*DI2PR
     1           -(D1AI+SBAR*RD1AI+SBAI*RD1AR)*DI2PI)
      AI(5,3)  = -CMU1*((D1AR+SBAR*RD1AR-SBAI*RD1AI)*DI2PI
     1           +(D1AI+SBAR*RD1AI+SBAI*RD1AR)*DI2PR)
      AR(5,4)  =  CMU2*((D2AR+SBAR*RD2AR-SBAI*RD2AI)*DK2PR
     1           -(D2AI+SBAR*RD2AI+SBAI*RD2AR)*DK2PI)
      AI(5,4)  =  CMU2*((D2AI+SBAR*RD2AR-SBAI*RD2AI)*DK2PI
     1           +(D2AI+SBAR*RD2AI+SBAI*RD2AR)*DK2PR)
      AR(5,5)  = CMU1*(BAR*DI2I + BAI*DI2R)
      AI(5,5)  = -CMU1*(BAR*DI2R - BAI*DI2I)
      AR(5,6)  = -CMU2*(BAR*DK2I + BAI*DK2R)
      AI(5,6)  = CMU2*(BAR*DK2R - BAI*DK2I)
```

```
      AR(6,1) = 4.*CMU1*(BI2PR - (RBAR*BI2R - RBAI*BI2I))
      AI(6,1) = 4.*CMU1*(BI2PI - (RBAR*BI2I + RBAI*BI2R))
      AR(6,2) = -4.*CMU1*(BK2PR - (RBAR*BK2R - RBAI*BK2I))
      AI(6,2) = -4.*CMU2*(BK2PI - (RBAR*BK2I + RBAI*BK2R))
      AR(6,3) = -4.*CMU1*((BAR*RD1AR-BAI*RD1AI)*DI2PR-(BAR*RD1AI
     1          +BAI*RD1AR)*DI2PI-(BAR*RSD1AR-BAI*RSD1AI)*DI2R
     2          +(BAR*RSD1AI + BAI*RSD1AR)*DI2I)
      AI(6,3) = -4.*CMU1*((BAR*RD1AR-BAI*RD1AI)*DI2PI+(BAR*RD1AI
     1          +BAI*RD1AR)*DI2PR-(BAR*RSD1AR-BAI*RSD1AI)*DI2I
     2          -(BAR*RSD1AI + BAI*RSD1AR)*DI2R)
      AR(6,4) = 4.*CMU2*((BAR*RD2AR-BAI*RD2AI)*DK2PR-(BAR*RD2AI
     1          +BAI*RD2AR)*DK2PI-(BAR*RSD2AR-BAI*RSD2AI)*DK2R
     2          +(BAR*RSD2AI + BAI*RSD2AR)*DK2I)
      AI(6,4) = 4.*CMU2*((BAR*RD2AR-BAI*RD2AI)*DK2PI+(BAR*RD2AI
     1          +BAI*RD2AR)*DK2PR-(BAR*RSD2AR-BAI*RSD2AI)*DK2I
     2          -(BAR*RSD2AI + BAI*RSD2AR)*DK2R)
      AR(6,5)= CMU1*((SD1AR*DI2PPI+SD1AI*DI2PPR)/2.-(D1AR*DI2PI
     1          +D1AI*DI2PR)/2.+2.*DI2I)
      AI(6,5) = -CMU1*((SD1AR*DI2PPR-SD1AI*DI2PPI)/2.-(D1AR*DI2PR
     1          -D1AI*DI2PI)/2.+2.*DI2R)
      AR(6,6) = -CMU2*((SD2AR*DK2PPI+SD2AI*DK2PPR)/2.-(D2AR*DK2PI
     1          +D2AI*DK2PR)/2.+2.*DK2I)
      AI(6,6) = CMU2*((SD2AR*DK2PPR-SD2AI*DK2PPI)/2.-(D2AR*DK2PR
     1          -D2AI*DK2PI)/2.+2.*DK2R)
      ITEST = 0
      DO 211 J = 1,6
      IF (ABS(AR(3,J)) - .1 E 11) 200,210,210
  210 ITEST = 1
  200 IF (ITEST) 211,211,212
  211 CONTINUE
      GO TO 250
  212 LJ = J
      DO 215 I = 1,6
      AR(I,LJ) = AR(I,LJ)*.1 E-11
      AI(I,LJ) = AI(I,LJ)*.1 E-11
  215 CONTINUE
```

```
      AAR(LJ) = AAR(LJ)*.1 E-11
      AAI(LJ) = AAI(LJ)*.1 E-11
      IF (ABS(AR(3,LJ)) - .1 E 11) 216,217,217
  216 ITEST = 0
      GO TO 200
  217 ITEST = 1
      GO TO 200
  250 DO 20 I = 1,6
      DO  20  I = 1,6
      DO  20  J = 1,6
      BR(I,J) = AR(I,J)
   20 BM(I,J) = AI(I,J)
      SCALE = 1.0
      CALL GAUSS(6,AR,AI,DETR,DETI,SCALE,JROW,ICOL)
      IF (DETR-.1 E 50) 105,105,125
  105 IF (DETI-.1 E 50) 107,107,125
  107 DO  10  I = 1,6
      DO  10  J = 1,6
      AR(I,J) = BR(I,J)
   10 AI(I,J) = BM(I,J)
      DO  16  J  =  1,6
      AR(4,J) = AAR(J)
   16 AI(4,J) = AAI(J)
      DO  30  I = 1,6
      DO  30  J = 1,6
      CR(I,J) = AR(I,J)
   30 CI(I,J) = AI(I,J)
      DDETR = DETR
      DDETI = DETI
      CALL GAUSS (6,AR,AI,DETR,DETI,SCALE,JROW,ICOL)
      DELR = DETR
      DELI = DETI
      DETR = DDETR
      DETI = DDETI
      DO  15  I = 1,6
      DO  15  J = 1,6
      AR(I,J) = BR(I,J)
```

```
 15 AI(I,J) = BM(I,J)
    IF (DELR-.1 E 50) 120,120,125
120 IF (DELI-.1 E 50) 126,126,125
125 TR(L) = 0.
    TI(L) = 0.
    WE = 0.
    DELR = 0.
    DELI = 0.
    F = 0.
    RWE = 0.
    RWE1 = 0.
    GO TO 60
126 SSQ = DELR**2 + DELI**2
    TR(L) = -(DETR*DELR + DETI*DELI)/SSQ
    TI(L) = -(DETI*DELR + DETR*DELI)/SSQ
    WE = CMU1*C/TR(L)
    CALL BIS(2,BAR,0.0,BI2R,BI2I)
    CALL BIS(1,BAR,0.0,BI1R,BI1I)
    BI2PR = BI1R - (2./BAR)*BI2R
    DENO = BI2PR/BI2R*(3. + BAR**2)/BAR
    F = WE*RE1/DENO
    RWE = 1./WE
    RWE1 = 1./(WE*RE1)
    IF (L-1) 50,70,50
 60 WRITE (6,3) L
    WRITE (6,61)
    DO 62 I = 1,6
    WRITE (6,4) AR(I,1),AR(I,2),AR(I,3),AR(I,4),AR(I,5),AR(I,6)
 62 CONTINUE
    WRITE (6,63)
    DO 64 I = 1,6
    WRITE (6,4) AI(I,1),AI(I,2),AI(I,3),AI(I,4),AI(I,5),AI(I,6)
 64 CONTINUE
    WRITE (6,65)
    WRITE (6,4) AAR(1),AAR(2),AAR(3),AAR(4),AAR(5),AAR(6)
    WRITE (6,66)
    WRITE (6,6) AAI(1),AAI(2),AAI(3),AAI(4),AAI(5),AAI(6)
```

```
      WRITE (6,5) DETR,DETI,DELR,DELI,TR(L),TI(L),Z(L),WE,RWE,RWE1,F
      GO TO 8
   70 WRITE (6,3) L
      WRITE (6,61)
      DO 72 I = 1,6
      WRITE (6,4) AR(I,1),AR(I,2),AR(I,3),AR(I,4),AR(I,5),AR(I,6)
   72 CONTINUE
      WRITE (6,63)
      DO 74 I = 1,6
      WRITE (6,4) AI(I,1),AI(I,2),AI(I,3),AI(I,4),AI(I,5),AI(I,6)
   74 CONTINUE
      WRITE (6,65)
      WRITE (6,4) AAR(1),AAR(2),AAR(3),AAR(4),AAR(5),AAR(6)
      WRITE (6,66)
      WRITE (6,6) AAI(1),AAI(2),AAI(3),AAI(4),AAI(5),AAI(6)
      WRITE (6,5) DETR,DETI,DELR,DELI,TR(L),TI(L),Z(L),WE,RWE,RWE1,F
      IF (ABS(TI(L)) - 0.001) 8,8,90
   90 L = 2
      GO TO 7
   50 IF (ABS(TI(L)) - 0.001) 60,60,35
   35 WRITE (6,3) L
      WRITE (6,5) DETR,DETI,DELR,DELI,TR(L),TI(L),Z(L),WE,RWE,RWE1,F
      L = L+1
      Z(L) = Z(L-1) - (TI(L-1)/(TI(L-1)-TI(L-2))*(Z(L-1) - Z(L-2)))
      IF (L-25) 40,40,34
   40 GO TO 7
   34 TR(L) = 100.
      TI(L) = 100.
      WE = 100.
      F = 100.
      RWE = 100.
      RWE1 = 100.
      GO TO 60
    1 FORMAT (I2,F8.4,F10.4,F10.2,F10.5,F10.5,F10.5,F6.2)
    2 FORMAT (//20H INTERFACIAL TENSION,4X,7HRUN NO.I3/11H INPUT DATA/5H
```

```
  1 B = F8.4,12X,5H A = F8.4/7H RE1 = F10.4,7X,7HCMU1 = F10.6/7H RMU
  2= F10.6,7X,7HRRHO = F10.6/6H  C  =F10.3)
 3 FORMAT (/4H L =I3/)
11 FORMAT (2F10.6)
61 FORMAT (/17H THE VALUES OF AR)
63 FORMAT (/17H THE VALUES OF AI)
65 FORMAT (/18H THE VALUES OF AAR)
66 FORMAT (/18H THE VALUES OF AAI)
 4 FORMAT (1X,6(E12.4,4X))
 5 FORMAT (1H ,4X,9HD        =2E16.8,9X,9HDELTA    =2E16.8//
  114H      T        =2E16.8,10X,8H Z      =E16.8//14H      WE       =E16.
  28,26X,8H RWE    =E16.8//14H      RWE1     =E16.8,26X,8H F      =E16.8/
  3)
 6 FORMAT (1X,6(E12.4,4X)//)
   END
```

```
CBIS
      SUBROUTINE BIS(N,RHO,PHI,BRIS,BIIS)
      XN = N
      R = RHO/2.0
      RSQ = R**2
      FP = R**N/FACN(XN)
      BRIS = FP*COS(XN*PHI)
      BIIS = FP*SIN(XN*PHI)
      DO 1 K = 1,20
      XK = K
      FA = FP*(RSQ/(XK*(XK+XN)))
      FP = FA
      BRIS = FA*COS((2.0*XK+XN)*PHI) + BRIS
    1 BIIS = FA*SIN((2.0*XK+XN)*PHI) + BIIS
      RETURN
      END

CBIL
      SUBROUTINE BIL(N,RHO,PHI,BRIL,BIIL)
      PI = 3.141592654
      XN = N
      XMU = 4.*(XN**2)
      R = RHO*8.0
      PF = 1.
      PFR = 1.
      PFI = 0.0
      SUMPR = PFR
      SUMPI = PFI
      DO 1 K = 1,30
      XK = K
      XM = 2*K - 1
      PF = -((XMU - (XM**2))/(XK*R))*PF
      PFR = PF*COS(-XK*PHI)
      PFI = PF*SIN(-XK*PHI)
      SUMPR = SUMPR + PFR
      SUMPI = SUMPI + PFI
    1 CONTINUE
```

```
      ALPHA = COS(PHI)
      BETA = SIN(PHI)
      X = RHO*ALPHA
      Y = RHO*BETA
      SR =(EXP(X)/SQRT(2.*PI*RHO))*(COS(-PHI/2.)*COS(Y)-SIN(-PHI/2.)*SIN
     1(Y))
      SI =(EXP(X)/SQRT(2.*PI*RHO))*(COS(-PHI/2.)*SIN(Y)+SIN(-PHI/2.)*COS
     1(Y))
      BRIL = SUMPR*SR - SUMPI*SI
      BIIL = SUMPR*SI + SUMPI*SR
      RETURN
      END

CBKL
      SUBROUTINE BKL(N,RHO,PHI,BRKL,BIKL)
      PI=3.141592654
      XN = N
      XMU = 4.*(XN**2)
      R = RHO*8.0
      PF = 1.0
      PFR = 1.0
      PFI = 0.0
      SUMPR = PFR
      SUMPI = PFI
      DO 1 K = 1,30
      XK = K
      XM = 2*K - 1
      PF = ((XMU - (XM**2))/(XK*R))*PF
      PFR = PF*COS(-XK*PHI)
      PFI = PF*SIN(-XK*PHI)
      SUMPR = SUMPR + PFR
      SUMPI = SUMPI + PFI
    1 CONTINUE
      ALPHA = COS(PHI)
      BETA = SIN(PHI)
      X = -RHO*ALPHA
```

```
      Y = -RHO*BETA
      SR =(EXP(X)*SQRT(PI/(2.*RHO)))*(COS(-PHI/2.)*COS(Y)-SIN(-PHI/2.)*S
     1IN(Y))
      SI =(EXP(X)*SQRT(PI/(2.*RHO)))*(COS(-PHI/2.)*SIN(Y)+SIN(-PHI/2.)*C
     1OS(Y))
      BRKL = SUMPR*SR - SUMPI*SI
      BIKL = SUMPR*SI + SUMPI*SR
      RETURN
      END
      FUNCTION PHY(XL)
      SUM = -0.577215665
      IF(XL-1.0) 1,1,2
    1 PHY = SUM
      RETURN
    2 L = XL
      LL = L-1
      SOMME = 0.
      DO 3 M = 1,LL
      XM = M
      SOMME = SOMME + 1.0/XM
    3 CONTINUE
      PHY = SUM + SOMME
      RETURN
      END

CBKS
      SUBROUTINE BKS(N,RHO,PHI,BRKS,BIKS)
      XN = N
      R = RHO/2.0
      RSQ = R**2
      FIRST = FACN(XN-1.0)
      FIRSTR = FACN(XN-1.0)
      FIRSTI = 0.0
      SUM1R = FIRSTR
      SUM1I = FIRSTI
      M = N-1
      IF (M) 4,4,3
    3 DO 1 K = 1,M
```

```
      XK = K
      FIRST =(FACN(XN-XK-1.)/FACN(XK))*((-RSQ)**K)
      FIRSTR = FIRST*COS(2.*XK*PHI)
      FIRSTI = FIRST*SIN(2.*XK*PHI)
      SUM1R = SUM1R + FIRSTR
      SUM1I = SUM1I + FIRSTI
    1 CONTINUE
    4 SUM1R=(0.5/(R**N))*(SUM1R*COS(-XN*PHI)-SUM1I*SIN(-XN*PHI))
      SUM1I = (0.5/(R**N))*(SUM1R*SIN(-XN*PHI) + SUM1I*COS(-XN*PHI))

      CALL BIS(N,RHO,PHI,BRI,BII)
      SUM2R = ((-1.)**(N+1))*(ALOG(R)*BRI-PHI*BII)
      SUM2I = ((-1.)**(N+1))*(ALOG(R)*BII + PHI*BRI)
      THIRD=(-0.577215665 + PHY(XN+1.0))/FACN(XN)
      THIRDR = THIRD
      THIRDI = 0.0
      SUM3R = THIRDR
      SUM3I = THIRDI
      DO 2 L = 1,20
      XL = L
      THIRD=(PHY(XL+1.0)+PHY(XN+XL+1.0))*(RSQ**L)/(FACN(XL)*FACN(XN+XL))
      THIRDR=THIRD*COS(2.0*XL*PHI)
      THIRDI=THIRD*SIN(2.0*XL*PHI)
      SUM3R = SUM3R + THIRDR
      SUM3I = SUM3I + THIRDI
    2 CONTINUE
      SUM3R=((-1.)**N)*(0.5*(R**N)*(SUM3R*COS(XN*PHI)-SUM3I*SIN(XN*PHI))
     1)
      SUM3I=((-1.)**N)*(0.5*(R**N)*(SUM3R*SIN(XN*PHI)+SUM3I*COS(XN*PHI))
     1)
      BRKS = SUM1R + SUM2R + SUM3R
      BIKS = SUM1I + SUM2I + SUM3I
      RETURN
      END
```

```
      FUNCTION FACN(XN)
      IF(XN-2.0) 1,2,3
    1 FACN = 1.0
      RETURN
    2 FACN = 2.0
      RETURN
    3 N = XN
      FACN = 2.0
      DO 4 I = 3,N
      XI = I
    4 FACN = FACN*XI
      RETURN
      END
```

```
      SUBROUTINE GAUSS(M,BR,BI,DETR,DETI,FACTOR,JROW,ICOL)
      DIMENSION AR(20,20),AI(20,20),JROW(20),ICOL(20),BR(20,20),
     1BI(20,20)
      N = M
      DO 33 I=1,N
      DO 33 J=1,N
      AR(I,J) = BR(I,J)
      AI(I,J) = BI(I,J)
   33 CONTINUE
      SCALE = FACTOR
      DO 11 IT = 1,N
      JROW(IT) = IT
   11 ICOL(IT) = IT
      NN = N-1
      DO 4 L = 1,NN
      K = L+1
      AMAX = 0.
      DO 20 J= L,N
      DO  20  I = L,N
      SSQ = AR(J,I)**2 + AI(J,I)**2
      IF(AMAX-SSQ) 10,20,20
   10 JR = J
      IR = I
      AMAX = SSQ
   20 CONTINUE
      SSQ = AMAX
      IF(SSQ) 21,100,21
   21 IF(JR-L) 30,40,30
   30 DO 31 I = 1,N
      CR = AR(JR,I)
      CI = AI(JR,I)
      AR(JR,I) = AR(L,I)
      AI(JR,I) = AI(L,I)
      AR(L,I) = CR
   31 AI(L,I) = CI
      SCALE = -SCALE
```

```
      JRO = JROW(JR)
      JROW(JR) = JROW(L)
      JROW(L) = JRO
   40 IF (IR-L) 60,50,60
   60 DO 61 J = 1,N
      CR = AR(J,IR)
      CI = AI(J,IR)
      AR(J,IR) = AR(J,L)
      AI(J,IR) = AI(J,L)
      AR(J,L) = CR
   61 AI(J,L) = CI
      SCALE = -SCALE
      ICO = ICOL(IR)
      ICOL(IR) = ICOL(L)
      ICOL(L) = ICO
   50 DO  4 I = K,N
      SQ = AR(I,L)**2 + AI(I,L)**2
      IF(SQ) 3,4,3
    3 DO 14 JJ = L,N
      J = N+L-JJ
      AX = AR(I,J)-(AR(I,L)*AR(L,J)*AR(L,L)+AR(I,L)*AI(L,J)*AI(L,L)
     1     +AI(I,L)*AR(L,J)*AI(L,L)-AI(I,L)*AI(L,J)*AR(L,L))/SSQ
      AI(I,J) = AI(I,J)-(AI(I,L)*AI(L,J)*AI(L,L)+AI(I,L)*AR(L,J)*AR(L,L)
     1          +AR(I,L)*AI(L,J)*AR(L,L)-AR(I,L)*AR(L,J)*AI(L,L))/SSQ
   14 AR(I,J) = AX
    4 CONTINUE
      IF(SCALE) 7,9,7
    9 SCALE = 1.
    7 DETR = SCALE
      DETI = 0.
      DO 95 I = 1,N
      DR = DETR
      DETR = DETR*AR(I,I)-DETI*AI(I,I)
   95 DETI = DETI*AR(I,I)+DR*AI(I,I)
      RETURN
  100 DETR = 0.
```

```
      DETI = 0.
      RETURN
      END
```

II. Velocity Profile in a Stationary Surrounding Liquid

The following programs were made to calculate the axial-velocity components and the jet radius as functions of axial distance.

A. Main Program (ESGJET)

(1) Abstract

The object of the program is to solve for increments of the six empirical parameters in Eqs. (8) and (9) at each axial-distance z. The matrix elements are given in the section for computation procedure.

(2) Usage

Input:

N	run number
RE1	interior Reynolds number
RMU	viscosity ratio
RRHO	density ratio
RFR	reciprocal of Froude number

Output:

A,B,C,D,E,M,z	functional values of parameters at each z.
F(1),F(2),F(3), F(4),F(5),F(6)	numerical values of Eqs. (10) through (15)
VC	dimensionless center-line velocity
VI	dimensionless interfacial velocity
SUMF	$\sum_{i=i}^{6} \{F(i)\}^2$, summation of the square of errors
z	dimensionless axial distance

(3) Restrictions

$z \leq 100$

(4) Method

Runge-Kutta third-order integration method.

B. Linearization Subprogram (LINIAL)

(1) Abstract

This program provides numerical evaluation of z-derivatives of given functions. Thus, the elements of the matrix in the main program can be evaluated without algebraic calculation. However, computation by this method is several times slower than the use of algebraically derived elements, therefore, this program was used only for a checking purpose.

(2) Usage

CALL LINIAL(Y,LS,A,B,LT,DF,F,SUMF,DSF,SUMO,SUM1,SUM2)

Input:

Y	magnitude of variables
LS	number of variables
LT	number of functions to be differentiated
F,SUMF,SUMO, SUM1,SUM2	to be called from a function subprogram
Output:	denoting the linearized matrix equations as $\underset{\approx}{A}d\underset{\sim}{Y} = \underset{\sim}{B}$;
A(I,J)	$\partial F(I)/\partial Y(J)$ $(1 \leq I \leq LT,\ 1 \leq J \leq LS)$
B(I)	$-(\partial F(I)/\partial z)dz$ $(1 \leq I \leq LT)$
DF(I,J)	$\partial F(I)/\partial Y(J)$ $(1 \leq I \leq LT,\ 1 \leq J \leq LS)$
DSF	$\partial(SUMF)/\partial Y(J)$ $(1 \leq J \leq LS)$

(3) Method

Numerical differentiation:

$$\partial F_i/\partial x_j \sim \{F_i(x_j+\Delta x_j) - F_i(x_j-\Delta x_j)\}/(2\Delta x_j)$$

C. Simplified Program for Solving Linear Simultaneous Equations (EQLIN)

(1) Abstract

This program solves linear simultaneous equations $\underset{\approx}{A}\underset{\sim}{x} = \underset{\sim}{B}$ by the elimination method.

(2) Usage:

CALL EQLIN (A,B,M,X)

Input:

A	coefficient-matrix element
B	constant vector
M	number of rows or columns in $\underset{\approx}{A}$

Output:

X	roots of the equations

(3) Restrictions

No provision has been made for underflow or overflow. A LRL library tape, LINIT, is used to replace EQLIN for cases where underflow or overflow occurs; it was not generally used because it had about twice the execution time of EQLIN.

D. Function Subprogram (FUNC)

(1) Abstract

This program furnishes magnitudes of functions for given variables. Thus, this can be used for the checking of errors generated by numerical integration.

(2) Usage

```
CALL FUNC(Y,LS,F,LT,SUMF,SUMO,SUM1,SUM2)
```

Input:

Y	magnitude of variables
LS	number of variables
LT	number of functions
SUMO,SUM1,SUM2	integral values in functions

Output:

F	magnitude of functions
SUMF	summation of square of F's

```
      PROGRAM ESGJET(INPUT,OUTPUT)
      DIMENSION A(6,6),B(6),X(6),F(6),Y(7),X0(6),X1(6),X2(6),Y1(6),YY(7)
     1,DF(6,7),DSF(7),SCR(6,20)
      COMMON     EX,RMU,DELZ,ALPHA,DEL1,DEL2,F1(6),F2(6),F3(6),F4(6),WCO
     1,ND,RRHO,FF3
      LOGICAL SINGUL

C     THIS IS AN EXPONENTIAL-SCHLICHTING TYPE VELOCITY MODEL.
C     VELOCITY PROFILE OF INTERIOR JET ASSUMES TWO FORMS.  AT FIRST
C     APPROXIMATE PARABOLA, THEN SCHLICHTING TYPE.

   24 READ 1, N,RE1,RMU,RRHO,RFR
      IF (N.EQ.99) STOP
    1 FORMAT (I2,4(F12.6))
      PRINT 4
    4 FORMAT (1H1)
      PRINT5, N,RE1,RMU,RRHO,RFR
    5 FORMAT (19H COMPUTATION NO. = I2,//,19H INSIDE RE        = F12.6,4X
     1,19H VISCOSITY RATIO = F12.6/19H DENSITY RATIO    = F12.6,4X,19H 1.
     2/FROUDE NO.    = F12.6//)

C     ALPHA IS A PARABOLIC CONSTANT.
C     ALPHA = 1.0 CORRESPONDS TO A PARABOLIC FORM.
C     HOWEVER,TOO HIGH A VALUE OF ALPHA MAY CAUSE A BREAKDOWN OF THE
C     CALCULATION.
C     RFR IS A RECIPROCAL FROUDE NO., WHICH IS POSITIVE WHEN THE
C     INTERIOR JET FLOW IS IN THE DIRECTION OF THE GRAVITY.


      ALPHA = 0.95
C     INITIAL VALUES OF PARAMETERS

      Y(1) = 1.8037
      Y(2) = 0.14019
      Y(3) = 1.0
      Y(4) = 1.0
```

```
      Y(5) = 1.0
      Y(6) = 0.
      Y(7) = 1.0E-06
      X(6) = 0.
      SUM0 = 0.
      SUM1 = 0.
      SUM2 = 0.
      DELZ = 0.
      WC0 = 2.0
      FF3 = 0.
      NB = 1
      ND = 999
      NP = 0
      NQ = 0
      MA = 6
      IT = 0
      DEL1 = 1.0E-05
      DEL2 = 0.5E-05
      RE2 = RE1*RRHO/RMU
      PRINT 300, ALPHA
  300 FORMAT (1X,9H ALPHA = F6.4//)
      PRINT 150
  150 FORMAT (4X,3H S1,9X,5H F(1),7X,5H F(2),7X,5H F(3),7X,5H F(4),7X,
     15H F(5),7X,5H F(6))
   31 EX = EXP(-Y(6)*Y(7))
      CALL LINIAL(Y,7,A,B,6,DF,F,SUMF,DSF,SUM0,SUM1,SUM2)
      IF (NB.GT.20) STOP
      S1 = F(4)**2 + F(5)**2
      PRINT 110, S1,F(1),F(2),F(3),F(4),F(5),F(6)
      IF (S1.LT.2.0E-12) GO TO 100
      DENO = DF(4,1)*DF(5,2) - DF(4,2)*DF(5,1)
      EPA = (F(4)*DF(5,2) - F(5)*DF(4,2))/DENO
      EPB = (F(5)*DF(4,1) - F(4)*DF(5,1))/DENO
      Y(1) = Y(1) - EPA
      Y(2) = Y(2) - EPB
      NB = NB + 1
```

```
      GO TO 31
  100 R1 = ALPHA + Y(1)*Y(2)/(1. + Y(1))**3
      Y(4) = Y(2)/(1. + Y(1))**2
      R2 = 0.5*RMU*Y(4)
      Y(3) = R1/R2
      EX = EXP(-Y(6)*Y(7))
      CALL FUNC(Y,7,F,6,SUMF,SUM0,SUM1,SUM2)
      PRINT 110,S1,F(1),F(2),F(3),F(4),F(5),F(6)
C     VC = CENTER VELOCITY, VI = INTERFACIAL VELOCITY
      PRINT 13
   13 FORMAT(/ 4X,2H Z,10X,2H A,10X,2H B,10X,2H C,10X,2H D,10X,2H R,10X,
     12H M,10X,3H VC,10X,3H VI,8X,5H SUMF/)
      VC = 2.*ALPHA*EXP(-Y(6)*Y(7))*Y(5)**2 + Y(2)
      WC0 = VC
      VI = Y(2)/(1. + Y(1)*Y(5)**2)**2
      VIE = Y(4)
      PRINT 14, Y(7),(Y(I),I=1,6),VC,VI,SUMF
      PRINT 110, VIE,(F(I),I=1,6)
      DELZ = 1.0E-07
      ID = 1
   55 X(6) = 0.
      IF (NP.NE.0.AND.ND.EQ.999) NQ = NQ + 1
      IF (ID.GE.ND) GO TO 56
      IF (EXP(-Y(6)*Y(7)).LT.5.0E-04) ND = ID
      IF (ID.EQ.ND) PRINT 3,ID,Y(7),EX
    3 FORMAT (I3,2E12.4)
      IF (ID.EQ.ND) PRINT 6
    6 FORMAT(5HID IN)
   56 IF (Y(7).LT.100.) GO TO 59
      PRINT 530, ID,Y(7)
  530 FORMAT(1H0,21HTOTAL NO. OF STEPS = I3,/////,11HMAX Y(7) = E12.4)
      GO TO 24
   59 IF (NP.NE.0.AND.NQ.LT.10) GO TO 60
      IF (ID.EQ.90) DELZ = 10.*DELZ
      IF (ID.EQ.180) DELZ = 10.*DELZ
      IF (ID.EQ.270) DELZ = 10.*DELZ
```

```
      IF (ID.EQ.360) DELZ = 10.*DELZ
      IF (ID.EQ.450) DELZ = 10.*DELZ
      IF (ID.EQ.540) DELZ = 10.*DELZ
      IF (ID.EQ.630) DELZ = 10.*DELZ
   60 IF (ND.NE.999) DELZ = 1.0
      IF (NQ.EQ.10) DELZ = 1.0
      IF (NQ.EQ.11) NP = 0
      IF (NP.EQ.0) NQ = 0
      NS = 1
      DO 73 I = 1,7
      YY(I) = Y(I)
   73 CONTINUE
  403 DO 400 I = 1,6
      DO 401 J = 1,6
      A(I,J) = 0.
  401 CONTINUE
      B(I) = 0.
  400 CONTINUE
      EX = EXP(-Y(6)*Y(7))
      IF (ND.NE.999) EX = 0.
      FX = 1. + Y(1)*Y(5)**2
      IF (FX.LT.0.0) PRINT 16
   16 FORMAT(9HFX.LT.0.0)
      IF (FX.LT.0.0) GO TO 24
      A(1,2) = 4.*ALPHA*EX*Y(5)**2 + 2.*Y(2)
      A(1,5) = 16.*ALPHA**2*Y(5)**3*EX**2 + 8.*ALPHA*Y(2)*Y(5)*EX
      A(1,6) = -8.*ALPHA**2*Y(5)**4*Y(7)*EX**2 - 4.*ALPHA*Y(2)*Y(5)**2*Y
     1(7)*EX
      B(1) = EX*(8.*ALPHA**2*Y(6)*Y(5)**4*EX + 4.*ALPHA*Y(2)*Y(6)*Y(5)**
     12)*DELZ
      A(2,1) = -2.*Y(2)*Y(5)**2/FX**3
      A(2,2) = 1./FX**2
      A(2,4) = -1.
      A(2,5) = -4.*Y(1)*Y(2)*Y(5)/FX**3
      A(3,1) = Y(2)/FX**3 - 3.*Y(1)*Y(2)*Y(5)**2/FX**4
      A(3,2) = Y(1)/FX**3
```

```
      A(3,3)  = -0.5*RMU*Y(4)
      A(3,4)  = -0.5*RMU*Y(3)
      A(3,5)  = -6.*Y(1)**2*Y(2)*Y(5)/FX**4
      A(3,6)  = -ALPHA*Y(7)*EX
      B(3)  = ALPHA*Y(6)*EX*DELZ
      A(4,1)  = -0.5*Y(2)*Y(5)**4/FX**2
      A(4,2)  = 0.5*Y(5)**2/FX
      A(4,5)  = 2.*ALPHA*Y(5)**3*EX + Y(2)*Y(5)/FX - Y(1)*Y(2)*Y(5)**3/FX
     1**2
      A(4,6)  = -0.5*ALPHA*Y(5)**4*Y(7)*EX
      B(4)  = 0.5*ALPHA*Y(6)*Y(5)**4*EX*DELZ
      A(5,1)  = 2.*ALPHA*Y(2)*EX*(-Y(5)**6/FX**2 - Y(5)**4/(Y(1)*FX**2) -
     12.*Y(5)**2/(Y(1)**2*FX) + 2.*ALOG(FX)/Y(1)**3) - 1./6.*(Y(2)/Y(1))
     2**2*(1. - 1./FX**3) + 0.5*(Y(2)*Y(5))**2/(Y(1)*FX**4)
      A(5,2)  = 2.*ALPHA*EX*(Y(5)**4/FX - ALOG(FX)/Y(1)**2 + Y(5)**2/(Y(1
     1)*FX)) + 1./3.*(Y(2)/Y(1))*(1. - 1./FX**3)
      A(5,5)  = 4.*ALPHA**2*Y(5)**5*EX**2 + 4.*ALPHA*Y(2)*EX*Y(5)**3/FX +
     1 Y(2)**2*Y(5)/FX**4
      A(5,6)  = -4./3.*ALPHA**2*Y(5)**6*Y(7)*EX**2 - 2.*ALPHA*Y(2)*Y(7)*E
     1X*(Y(5)**4/FX - ALOG(FX)/Y(1)**2 + Y(5)**2/(Y(1)*FX))
      B(5)  = (4./3.*ALPHA**2*Y(6)*Y(5)**6*EX**2 + 2.*ALPHA*Y(2)*Y(6)*EX*
     1(Y(5)**4/FX - ALOG(FX)/Y(1)**2 + Y(5)**2/(Y(1)*FX)))*DELZ
      A(6,3)  = -0.25*(Y(4)/Y(3))**2
      A(6,4)  = 0.5*Y(4)/Y(3)
      IF (ND.EQ.999) GO TO 402
      A(5,3)  = A(5,3) + RRHO*A(6,3)
      A(5,4)  = A(5,4) + RRHO*A(6,4)
      MA = 5
  402 IF (NS.EQ.2) GO TO 406
      IF (NS.EQ.3) GO TO 407
      IF (ID.NE.1) GO TO 700
      U1  = 32.*(ALPHA*EX + Y(1)*Y(2))/RE1 - RFR
      V1  = 8./RE1*(ALPHA*EX*Y(5)**2 + Y(1)*Y(2)*Y(5)**2/(1.
     1 + Y(1)*Y(5)**2)**3) - 0.25*Y(5)**2*RFR
      W1  = 4./RE2*Y(3)*Y(4)*Y(5)**2 - 0.25*Y(5)**2*RFR/RRHO
      GO TO 701
```

```
700 U1 = U4
    V1 = V4
    W1 = W4
701 B(1) = B(1) - U1*DELZ
    B(5) = B(5) - V1*DELZ
    B(6) = B(6) + W1*DELZ
    IF (ND.NE.999) B(5) = B(5) + RRHO*B(6)
    IF (ND.NE.999) GO TO 550
    CALL EQLIN(A,B,MA,X)
    GO TO 551
550 CALL LINIT(A,B,X,MA,1,DET,IEX,CNR,SINGUL,6,SCR)
    IF (SINGUL) PRINT 15
 15 FORMAT(13HA IS SINGULAR)
    IF (SINGUL) GO TO 24
551 DO 71 I = 1,6
    XO(I) = X(I)
 71 CONTINUE
    DO 74 I = 1,6
    Y(I) = YY(I) + XO(I)*0.5
 74 CONTINUE
    Y(7) = Y(7) + 0.5*DELZ
    NS = 2
    GO TO 403
406 U2 = 32.*(ALPHA*EX + Y(1)*Y(2))/RE1 - RFR
    V2 = 8./RE1*(ALPHA*EX*Y(5)**2 + Y(1)*Y(2)*Y(5)**2/(1.
   1 + Y(1)*Y(5)**2)**3) - 0.25*Y(5)**2*RFR
    W2 = 4./RE2*Y(3)*Y(4)*Y(5)**2 - 0.25*Y(5)**2*RFR/RRHO
    B(1) = B(1) - U2*DELZ
    B(5) = B(5) - V2*DELZ
    B(6) = B(6) + W2*DELZ
    IF (ND.NE.999) B(5) = B(5) + RRHO*B(6)
    IF (ND.NE.999) GO TO 552
    CALL EQLIN(A,B,MA,X)
    GO TO 553
552 CALL LINIT(A,B,X,MA,1,DET,IEX,CNR,SINGUL,6,SCR)
    IF (SINGUL) PRINT 15
```

```
      IF (SINGUL) GO TO 24
  553 DO 75 I = 1,6
      X1(I) = X(I)
   75 CONTINUE
      DO 76 I = 1,6
      Y(I) = YY(I) + 2.*X1(I) - X0(I)
   76 CONTINUE
      Y(7) = Y(7) + 0.5*DELZ
      NS = 3
      GO TO 403
  407 U3 = 32.*(ALPHA*EX + Y(1)*Y(2))/RE1 - RFR
      V3 = 8./RE1*(ALPHA*EX*Y(5)**2 + Y(1)*Y(2)*Y(5)**2/(1.
     1 + Y(1)*Y(5)**2)**3) - 0.25*Y(5)**2*RFR
      W3 = 4./RE2*Y(3)*Y(4)*Y(5)**2 - 0.25*Y(5)**2*RFR/RRHO
      B(1) = B(1) - U3*DELZ
      B(5) = B(5) - V3*DELZ
      B(6) = B(6) + W3*DELZ
      IF (ND.NE.999) B(5) = B(5) + RRHO*B(6)
      IF (ND.NE.999) GO TO 554
      CALL EQLIN(A,B,MA,X)
      GO TO 555
  554 CALL LINIT(A,B,X,MA,1,DET,IEX,CNR,SINGUL,6,SCR)
      IF (SINGUL) PRINT 15
      IF (SINGUL) GO TO 24
  555 DO 77 I = 1,6
      X2(I) = X(I)
   77 CONTINUE
      DO 78 I = 1,6
      Y1(I) = 1./6.*(X0(I) + 4.*X1(I) + X2(I))
   78 CONTINUE
      DO 81 I = 1,6
      Y(I) = YY(I) + Y1(I)
   81 CONTINUE
      Y(7) = YY(7) + DELZ
      EX = EXP(-Y(6)*Y(7))
      IF (ND.NE.999) EX = 0.
```

```
      IF (SINGUL) GO TO 24
  553 DO 75 I = 1,6
      X1(I) = X(I)
   75 CONTINUE
      DO 76 I = 1,6
      Y(I) = YY(I) + 2.*X1(I) - X0(I)
   76 CONTINUE
      Y(7) = Y(7) + 0.5*DELZ
      NS = 3
      GO TO 403
  407 U3 = 32.*(ALPHA*EX + Y(1)*Y(2))/RE1 - RFR
      V3 = 8./RE1*(ALPHA*EX*Y(5)**2 + Y(1)*Y(2)*Y(5)**2/(1.
     1 + Y(1)*Y(5)**2)**3) - 0.25*Y(5)**2*RFR
      W3 = 4./RE2*Y(3)*Y(4)*Y(5)**2 - 0.25*Y(5)**2*RFR/RRHO
      B(1) = B(1) - U3*DELZ
      B(5) = B(5) - V3*DELZ
      B(6) = B(6) + W3*DELZ
      IF (ND.NE.999) B(5) = B(5) + RRHO*B(6)
      IF (ND.NE.999) GO TO 554
      CALL EQLIN(A,B,MA,X)
      GO TO 555
  554 CALL LINIT(A,B,X,MA,1,DET,IEX,CNR,SINGUL,6,SCR)
      IF (SINGUL) PRINT 15
      IF (SINGUL) GO TO 24
  555 DO 77 I = 1,6
      X2(I) = X(I)
   77 CONTINUE
      DO 78 I = 1,6
      Y1(I) = 1./6.*(X0(I) + 4.*X1(I) + X2(I))
   78 CONTINUE
      DO 81 I = 1,6
      Y(I) = YY(I) + Y1(I)
   81 CONTINUE
      Y(7) = YY(7) + DELZ
      EX = EXP(-Y(6)*Y(7))
      IF (ND.NE.999) EX = 0.
```

```
      U4 = 32.*(ALPHA*EX + Y(1)*Y(2))/RE1 - RFR
      V4 = 8./RE1*(ALPHA*EX*Y(5)**2 + Y(1)*Y(2)*Y(5)**2/(1.
     1 + Y(1)*Y(5)**2)**3) - 0.25*Y(5)**2*RFR
      W4 = 4./RE2*Y(3)*Y(4)*Y(5)**2 - 0.25*Y(5)**2*RFR/RRHO

C     INTEGRATION BY TRAPEZOIDAL RULE

      SUMO = SUMO + DELZ*(U1 + U4)/2.
      SUM1 = SUM1 + DELZ*(V1 + V4)/2.
      SUM2 = SUM2 + DELZ*(W1 + W4)/2.

      CALL FUNC(Y,7,F,6,SUMF,SUMO,SUM1,SUM2)
      IF (ID.EQ.10) FF3 = F(3)
      DX = 0.
      CX = EXP(-Y(3)*Y(5)**2)
      IF (CX.LT.1.0E-08) GO TO 84
      DX = Y(4)/CX
   84 VC = 2.*ALPHA*EX*Y(5)**2 + Y(2)
      IF (ID.LE.10) WC0 = VC
      VI = Y(2)/(1. + Y(1)*Y(5)**2)**2
      VIE = Y(4)
      PRINT 14,    Y(7),(Y(I),I= 1,6),VC,VI,SUMF
   14 FORMAT (10E12.4)
      PRINT 110, VIE,(F(I),I=1,6)
  110 FORMAT (7E12.4)
      PRINT 110, (Y1(I),I=1,6),DX
      IF (ND.NE.999) GO TO 111
      IF (ID.LT.20) GO TO 111
      IF (SUMF.LT.1.0E-06) GO TO 114
      NP = NP + 1
C     REDUCE THE SIZE OF DELZ WHEN APPROACHING A CRITICAL POINT.
      IF (NP.EQ.1) PRINT 113
  113 FORMAT(7HSKIP ID)
      IF (NP.EQ.10) GO TO 24
      DO 112 I = 1,6
      Y(I) = Y(I) - Y1(I)
```

```
112 CONTINUE
    Y(7) = Y(7) - DELZ
    SUM0 = SUM0 - DELZ*(U1 + U4)/2.
    SUM1 = SUM1 - DELZ*(V1 + V4)/2.
    SUM2 = SUM2 - DELZ*(W1 + W4)/2.
    DELZ = 0.5*DELZ
    GO TO 55
114 IF (NP.NE.0.AND.NQ.LT.10) GO TO 55
    IF (NQ.EQ.10) PRINT 6
111 ID = ID + 1
    GO TO 55
    END
```

```
      SUBROUTINE  LINIAL(Y,LS,A,B,LT,DF,F,SUMF,DSF,SUM0,SUM1,SUM2)
      DIMENSION Y(LS),A(LT,LT),B(LT),DF(LT,LS),F(LT),DSF(LS)
      COMMON      EX,RMU,DELZ,ALPHA,DEL1,DEL2,F1(6),F2(6),F3(6),F4(6),WC0
     1,ND,RRHO,FF3
      CALL FUNC(Y,7,F,6,SUMF,SUM0,SUM1,SUM2)
      SUMF1 = SUMF
      DO 102 J = 1,LT
      F1(J) = F(J)
  102 CONTINUE
      DO 101 I = 1,LS
      Y(I) = Y(I) - DEL1
      CALL FUNC(Y,7,F,6,SUMF,SUM0,SUM1,SUM2)
      DO 104 J = 1,LT
      F2(J) = F(J)
  104 CONTINUE
      Y(I) = Y(I) + 2.*DEL1
      CALL FUNC(Y,7,F,6,SUMF,SUM0,SUM1,SUM2)
      DO 124 J = 1,LT
      F3(J) = F(J)
  124 CONTINUE
      Y(I) = Y(I) - DEL1
  110 Y(I) = Y(I) - DEL2
      CALL FUNC(Y,7,F,6,SUMF,SUM0,SUM1,SUM2)
      DO 125 J = 1,LT
      F4(J) = F(J)
  125 CONTINUE
      SUMF2 = SUMF
      Y(I) = Y(I) + 2.*DEL2
      CALL FUNC(Y,7,F,6,SUMF,SUM0,SUM1,SUM2)
      Y(I) = Y(I) - DEL2
      DO 103 K = 1,LT
      DF1 = (F3(K) - F2(K))/(2.*DEL1)
      DF(K,I) = (F(K) - F4(K))/(2.*DEL2)
      DEF = ABS(DF(K,I) - DF1)
      IF (DEF.LT.1.0E-04) GO TO 103
      IF (DEL2.LT.1.0E-08) GO TO 103
```

```
      DO 116 J = 1,LT
      F3(J) = F(J)
      F2(J) = F4(J)
  116 CONTINUE
      DEL1 = DEL2
      DEL2 = DEL2*0.5
      GO TO 110
  103 CONTINUE
      DSF(I) = (SUMF - SUMF2)/(2.*DEL2)
  101 CONTINUE
      DO 107 I = 1,LT
      DO 105 J = 1,LT
      A(I,J) = DF(I,J)
  105 CONTINUE
  107 CONTINUE
      DO 106 I = 1,LT
      B(I) = -DF(I,LS)*DELZ
  106 CONTINUE
      DO 108 I = 1,LT
      F(I) = F1(I)
  108 CONTINUE
      SUMF = SUMF1
      RETURN
      END
```

```
      SUBROUTINE EQLIN(A,B,M,X)
      DIMENSION A(M,M),B(M),X(M)
      COMMON     EX,RMU,DELZ,ALPHA,DEL1,DEL2,F1(6),F2(6),F3(6),F4(6),WCO
     1,ND,RRHO,FF3
      DO 1 K=1,M
      W=0
      DO 5 J=K,M
      Y=ABS(A(J,K))
      IF (Y.LE.W) GO TO 5
      W = Y
      JM=J
    5 CONTINUE
      IF (W.LT.1.0E-150) GO TO 7
      DO 6 J=K,M
      W=A(K,J)
      A(K,J)=A(JM,J)
    6 A(JM,J)=W
      W=B(K)
      B(K)=B(JM)
      B(JM)=W
      W=A(K,K)
      DO 2 J = K,M
    2 A(K,J)=A(K,J)/W
      B(K)=B(K)/W
      DO 3 I=1,M
      IF(I.EQ.K) GO TO 3
      W=A(I,K)
      DO 4 J=K,M
    4 A(I,J)=A(I,J)-W*A(K,J)
      B(I)=B(I)-W*B(K)
    3 CONTINUE
    1 CONTINUE
      DO 9 J=1,M
    9 X(J)=B(J)
      GO TO 8
    7 PRINT 100
```

```
100 FORMAT (1H1,18HSYSTEM IS SINGULAR)
    STOP
  8 RETURN

    END
```

```
      SUBROUTINE FUNC(Y,LS,F,LT,SUMF,SUMO,SUM1,SUM2)
      DIMENSION Y(LS),F(LT)
      COMMON     EX,RMU,DELZ,ALPHA,DEL1,DEL2,F1(6),F2(6),F3(6),F4(6),WCO
     1,ND,RRHO,FF3
      IF (ND.NE.999) EX = 0.
      FX = 1. + Y(1)*Y(5)**2
      IF (FX.LT.0.0) GO TO 1
C     EX = EXP(-Y(6)*Y(7))

C     COMBINATION OF PARABOLA AND NONPARABOLA.
C     THE FOLLOWING EQUATIONS ARE,

C     1. EQUATION OF MOTION AT R = 0
      F(1) = (2.*ALPHA*EX*Y(5)**2)**2 + 4.*ALPHA*Y(2)*Y(5)**2*EX + Y(2)*
     1*2 - WCO**2 + SUMO

C     2. THE MATCHING OF VELOCITIES AT AN INTERFACE
      F(2) = Y(2)/FX**2 - Y(4)

C     3. THE MATCHING OF TANGENTIAL STRESSES AT AN INTERFACE
      F(3) = ALPHA*EX + Y(1)*Y(2)/FX**3 - 0.5*RMU*Y(3)*Y(4) - FF3

C     4. MASS BALANCE FOR A JET
      F(4) = 0.5*ALPHA*Y(5)**4*EX + 0.5*Y(2)*Y(5)**2/FX - 0.5

C     5. MOMENTUM BALANCE FOR A JET
      F(5) = 2./3.*ALPHA**2*Y(5)**6*EX**2 + 2.*ALPHA*Y(2)*EX*(Y(5)**4/FX
     1 - ALOG(FX)/Y(1)**2 + Y(5)**2/(Y(1)*FX)) + 1./6.*(Y(2)**2/Y(1))*(1
     2. - 1./FX**3) - 2./3. + SUM1

C     6. MOMENTUM BALANCE FOR A SURROUNDING FLUID
      F(6) = 0.25*Y(4)**2/Y(3) - SUM2

      IF (ND.NE.999) F(5) = F(5) + RRHO*F(6)

      SUMF = F(1)**2 + F(2)**2 + F(3)**2 + F(4)**2 + F(5)**2 + F(6)**2
```

```
      IF (ND.NE.999) SUMF = SUMF - F(6)**2

      RETURN
    1 PRINT 2
    2 FORMAT(9HFX.LT.0.0)
      END
```

III. Velocity Profile in a Moving Surrounding Liquid

The programs are designed to calculate the axial-velocity components and the jet radius as functions of axial distance.

A. The Main Program (ANUJET)

(1) Abstract

The object of the program is to solve for increments of the seven parameters in Eqs. (1) and (2) at each axial-distance z. The matrix elements are given in the section for computation procedure.

(2) Usage

Input:

N	run number
RE1	interior Reynolds number
GAMA	average velocity ratio
RMU	viscosity ratio
RRHO	density ratio
SK	orifice-to-tube radius ratio

Output:

A,B,C,D,E,G,M,a	functional values of parameters at each z
F(1),F(2),F(3),F(4), F(5),F(6),F(7)	numerical values of Eqs. (10) through (16)
VC	dimensionless center-line velocity
VI	dimensionless interfacial velocity
SUMF	summation of the square of errors
z	dimensionless axial distance

(3) Restrictions

$z \leq 100$

(4) Runge-Kutta third-order integration method

B. Function Subprogram (FUNC)

(1) Abstract

This program gives the numerical values of functions for given variables.

(2) Usage

CALL FUNC(Y,LS,F,LT,SUMF,SUMO,SUM1,SUM2)

Input:

Y	magnitude of variables
LS	number of variables
LT	number of functions
SUMO,SUM1,SUM2	integral values in functions

Output:

F	magnitude of functions
SUMF	summation of square of F's
LINIAL and EQLIN	are the same as given before

```
      PROGRAM ANUJET(INPUT,OUTPUT)
      DIMENSION A(7,7),B(7),X(7),F(7),Y(8),X0(7),X1(7),X2(7),Y1(7),YY(8)
     1,DF(7,8),DSF(8),SCR(7,20)
      COMMON      EX,RMU,DELZ,ALPHA,DEL1,DEL2,F1(7),F2(7),F3(7),F4(7),WCO
     1,ND,RRHO,GAMA,CK,SK,CKA,SK1,EE1,FF3,FF5,FF7
      LOGICAL SINGUL

C     THIS IS A PROGRAM DES+GNED FOR A JET IN A CIRCULAR TUBE.
C     THIS IS AN EXPONENTIAL-SCHLICHTING TYPE VELOCITY MODEL.
C     VELOCITY PROFILE OF INTERIOR JET ASSUMES TWO FORMS.  AT FIRST
C     APPROXIMATE PARABOLA, THEN SCHLIC+TING TYPE.

   24 READ 1,N,RE1,GAMA,RMU,RRHO,SK
    1 FORMAT(I2,5F12.6)
      IF (N.EQ.9 ) STOP
      PRINT 4
    4 FORMAT (1H1)
      PRINT 5, N,RE1,GAMA,RMU,RRHO
    5 FORMAT (19H COMPUTATION NO. = I2,//,19H INSIDE RE        = F12.6,4X
     1,19H AVE. VEL. RATIO = F12.6/19H VISCOSITY RATIO = F12.6,4X,19H DE
     2NSITY RATIO    = F12.6//)

C     ALPHA IS A PARABOLIC CONSTANT.
C     ALPHA = 1.0 CORRESPONDS TO A PARABOLIC FORM.
C     HOWEVER,TOO HIGH A VALUE OF ALPHA MAY CAUSE A BREAKDOWN OF THE
C     CALCULATION.
C     GAMA IS A RATIO OF AVERAGE VELOCITIES OF INTERIOR AND EXTERIOR
C     JETS.


      ALPHA = 0.95
C     INITIAL VALUES OF PARAMETERS

      Y(1) = 1.8037
      Y(2) = 0.14019
      Y(3) = 1.0
      Y(4) = 1.0
```

```
      Y(5) = 1.0
      Y(6) = 1.0
      Y(7) = 0.
      Y(8) = 1.0E-06
      X(7) = 0.
      SUM0 = 0.
      SUM1 = 0.
      SUM2 = 0.
      DELZ = 0.
      WC0 = 2.0
      FF3 = 0.
      FF5 = 0.
      FF7 = 0.
      NB = 1
      ND = 999
      NP = 0
      NQ = 0
      MA = 7
      IT = 0
      DEL1 = 1.0E-05
      DEL2 = 0.5E-05

      RE2 = RE1*RRHO/RMU
C     RE2 IS AN EXTER+-R REYNOLDS NO. BASED ON THE ORIFICE DIA.

      CK = 1. + SK**2 - (1. - SK**2)/ALOG(1./SK)
      EE1 = 0.
      SK1 = SK**2
      CKA = (1. - SK**2)/(ALOG(SK))
      PRINT 308, SK
  308 FORMAT (1X,18H RAT+O OF RADII = F6.4//)
      PRINT 300, ALPHA
  300 FORMAT (1X,9H ALPHA = F6.4//)
   31 EX = EXP(-Y(7)*Y(8))
      CALL LINIAL(Y,8,A,B,7,DF,F,SUMF,DSF,SUM0,SUM1,SUM2)
      IF (NB.GT.20) STOP
```

```
      S1 = F(4)**2 + F(6)**2
      PRINT 110, S1, (F(I),I=1,7)
  110 FORMAT (8E11.3)
      IF (S1.LT.2.0E-12) GO TO 100
      DENO = DF(4,1)*DF(6,2) - DF(4,2)*DF(6,1)
      EPA = (F(4)*DF(6,2) - F(6)*DF(4,2))/DENO
      EPB = (F(6)*DF(4,1) - F(4)*DF(6,1))/DENO
      Y(1) = Y(1) - EPA
      Y(2) = Y(2) - EPB
      NB = NB + 1
      GO TO 31
  100 R1 = ALPHA + Y(1)*Y(2)/(1. + Y(1))**3 - 0.5*RMU*GAMA/CK*(2.*SK*-2
     1 + CKA/Y(5)**2)
      Y(4) = Y(2)/(1. + Y(1))**2
      R2 = 0.5*RMU*Y(4)
      Y(3) = R1/R2
      EX = EXP(-Y(7)*Y(8))
      CALL FUNC(Y,8,F,7,SUMF,SUMO,SUM1,SUM2)
      FF5 = F(5)
      FF7 = F(7)
      PRINT 110, S1, (F(I),I=1,7)
C     VC = CENTER VELOCITY, VI = INTERFACIAL VELOCITY
      PRINT 13
   13 FORMAT(/ 4X,2H Z,9X,2H A,9X,2H B,9X,2H C,9X,2H E,9X,2H R,9X,2H G,
     19X,2H M,9X,3H VC,9X,3H VI,7X,5H SUMF/)
      VC = 2.*ALPHA*EXP(-Y(7)*Y(8H)*Y(5)**2 + Y(2)
      WCO = VC
      VI = Y(2)/(1. + Y(1)*Y(5)**2)**2
      VIE = Y(4)
      PRINT 14, Y(8),(Y(I),I=1,7),VC,VI,SUMF
   14 FORMAT(11E11.3)
      PRINT 110, VIE,(F(I),I=1,7)
      DELZ = 1.0E-07
      ID = 1
   55 X(7) = 0.
```

```
      IF (NP.NE.0.AND.ND.EQ.999) NQ = NQ + 1
      IF (ID.GE.ND) GO TO 56
      IF (EXP(-Y(7)*Y(8)).LT.1.0E-03) ND = ID
      IF (ID.EQ.ND) PRINT 3,ID,Y(8),EX
    3 FORMAT (I3,2F11.3)
      IF (ID.EQ.ND) PRINT 6
    6 FORMAT(19HID AND TAPE-READ IN)
   56 IF (Y(8).LT.100.) GO TO 59
      PRINT 530, ID,Y(8)
  530 FORMAT(1H0,21HTOTAL NO. OF STEPS = I3,/////,11HMAX Y(7) = E12.4)
      GO TO 24
   59 IF (NP.NE.0.AND.NQ.LT.50) GO TO 60
      IF (ID.EQ.90) DELZ = 10.*DELZ
      IF (ID.EQ.180) DELZ = 10.*DELZ
      IF (ID.EQ.270) DELZ = 10.*DELZ
      IF (ID.EQ.360) DELZ = 10.*DELZ
      IF (ID.EQ.450) DELZ = 10.*DELZ
      IF (ID.EQ.540) DELZ = 10.*DELZ
   60 IF (ND.NE.999) +ELZ = 1.0
      IF (NQ.EQ.51) NP 3 0
      IF (NP.EQ.0) NQ = 0
      NS = 1
      DO 73 I = 1,8
      YY(I) = Y(I)
   73 CONTINUE
  403 DO 400 I = 1,7
      DO 401 J = 1,7
      A(I,J) = 0.
  401 CONTINUE
      B(I) = 0.
  400 CONTINUE
      SK1 = (SK*Y(5))**2
      CKA = (1. - (SK*Y(5))**2)/ALOG(SK*Y(5))
      DCKA = -2./ALOG(SK1) - 2.*((1. - SK1)/SK1)/(ALOG(SK1))**2
      EX = EXP(-Y(7)*Y(8))
      IF (ND.NE.999) EX = 0.
```

```
      FX = 1. + Y(1)*Y(5)**2
      GX = 1. + Y(3)*Y(5)**2
      IF (FX.LT.0.0) PRINT 16
   16 FORMAT(9HFX.LT.0.0)
      IF (FX.LT.0.0) GO TO 24
      A(1,2) = 4.*ALPHA*EX*Y(5)**2 + 2.*Y(2)
      A(1,5) = 16.*ALPHA**2*Y(5)**3*EX**2 + 8.*ALPHA*Y(2)*Y(5)*EX
      A(1,7) = -8.*ALPHA**2*Y(5)**4*Y(8)*EX**2 - 4.*ALPHA*Y(2)*Y(5)**2*Y
     1(8)*EX
      B(1) = EX*(8.*ALPHA**2*Y(7)*Y(5)**4*EX + 4.*ALPHA*Y(2)*Y(7)*Y(5)**
     12)*DELZ
      A(2,1) = -2.*Y(2)*Y(5)**2/FX**3
      A(2,2) = 1./FX**2
      A(2,4) = -1.
      A(2,5) = -4.*Y(1)*Y(2)*Y(5)/FX**3
      A(3,1) = Y(2)/FX**3 - 3.*Y(1)*Y(2)*Y(5)**2/FX**4
      A(3,2) = Y(1)/FX**3
      A(3,3) = -0.5*RMU*Y(4)
      A(3,4) = -0.5*RMU*Y(3)
      A(3,5) = -6.*Y(1)**2*Y(2)*Y(5)/FX**4 + 2.*RMU*GAMA/CK*(1. - SK1 +
     1 ALOG(SK1))/(Y(5)**3*(ALOG(SK1))**2)*Y(6)
      A(3,6) = -0.5*RMU*GAMA*(2.*SK**2 + CKA/Y(5)**2)/CK
      A(3,7) = -ALPHA*Y(8)*EX
      B(3) = ALPHA*Y(7)*EX*DELZ
      A(4,1) = -0.5*Y(2)*Y(5)**4/FX**2
      A(4,2) = 0.5*Y(5)**2/FX
      A(4,5) = 2.*ALPHA*Y(5)**3*EX + Y(2)*Y(5)/FX - Y(1)*Y(2)*Y(5)**3/FX
     1**2
      A(4,7) = -0.5*ALPHA*Y(5)**4*Y(8)*EX
      B(4) = 0.5*ALPHA*Y(7)*Y(5)**4*EX*DELZ
      A(5,3) = -0.5*Y(4)/Y(3)**2
      A(5,4) = 0.5/Y(3)
      A(5,5) = 2.*(GAMA*Y(6)/CK)*(Y(5)*(1. - SK1) - 1. - 0.5*Y(5)*CKA +
     1 0.5*Y(5)*(1. - SK1)*DCKA)
      A(5,6) = 2.*(GAMA/CK)*((1./SK - Y(5)) - 0.25*SK**2*(1./SK**4 - Y(5
     1)**4) + 0.5*Y(5)M*2*(1. - SK1) + (1. - SK1)*CKA/(4.*SK**2))
```

```
      A(6,1) = 2.*ALPHA*Y(2)*EX*(-Y(5)**6/FX**2 - Y(5)**4/(Y(1)*FX**2) -
     12.*Y(5)**2/(Y(1)**2*FX) + 2.*ALOG(FX)/Y(1)**3) - 1./6.*(Y(2)/Y(1))
     2**2*(1. - 1./FX**3) + 0.5*(Y(2)*YU5))**2/(Y(1)*FX**4)
      A(6,2) = 2.*ALPHA*EX*(Y(5)**4/FX - ALOG(FX)/Y(1)**2 + Y(5)**2/(Y(1
     1)*FX)) + 1./3.*(Y(2)/Y(1))*(1. - 1./FX**3)
      A(6,5) = 4.*ALPHA**2*Y(5)**5*EX**2 + 4.*ALPHA*Y(2)*EX*Y(5)**3/FX +
     1 Y(2)**2*Y(5)/FX**4
      A(6,7) = -4./3.*ALPHA**2*Y(5)**6*Y(8)*EX**2 - 2.*ALPHA*Y(2)*Y(8)*E
     1X*(Y(5)**4/FX - ALOG(FX)/Y(1)**2 + Y(5)**2/(Y(1)*FX))
      B(6) = (4./3.*ALPHA**2*Y(7)*Y(5)**6*EX**2 + 2.*ALPHA*Y(2)*Y(7)*EX*
     1(Y(5)**4/FX - ALOG(FX)/Y(1)**2 + Y(5)**2/(Y(1)*FX)))*DELZ
C     AN EXPONENTIAL INTEGRAL IS APPROXIMATED.
C     EE1 IS AN EXPONENTIAL INTEGRAL TIMES EXP(Y(3)*Y(5)**2)

      P = Y(3)*Y(5)**2
      IF (P.LT.1.) GO TO 11
      A1 = 8.5733287401
      A2 = 18.0590169730
      A3 = 8.6347608925
      A4 = 0.2677737343
      B1 = 9.5733223454
      B2 = 25.6329561486
      B3 = 21.0996530827
      B4 = 3.9584969228
      EE1 = (P**4 + A1*P**3 + A2*P**2 + A3*P + A4)/(P**4 + B1*P**3 + B2*
     1P**2 + B3*P + B4)/P
      GO TO 12
   11 A0 = -0.57721566
      A1 = 0.99999193
      A2 = -0.249 1055
      A3 = 0.05519968
      A4 = -0.00976004
      A5 = 0.00107857
      EE1 = EXP(P)*(-ALOG(P) + A0 + A1*P + A2*P**2 + A3*P**3 + A4*P**4
     1+ A5*P**5)
   12 A(7,3) = 2.*(GAMA/CK )*(2.*SK**2*Y(4)/Y(3)**3 + (SK1 - 1.)*Y(4)/Y(
```

```
     13)**2 + 0.5*CKA*(Y(4)/Y(3)**2)*(ALOG(SK1) + (1. - Y(3)*Y(5)**2)
     2 *EE1 + 1.))*Y(6) - 0.25*(Y(4)/Y(3))**2
      A(7,4) = 2.*(GAMA/CK )*(1./Y(3) - (SK/Y(3))**2*(1. + Y(3)*Y(5)**2)
     1 - 0.5*CKA/Y(3)*(ALOG(SK1) + EE1))*Y(6) + 1./2.*Y(4)/Y(3)
      T1 = -SK1**2 + 2.*SK1 - 1.
      T2 = 2. - SK1*(ALOG(SK1))**2 + 2.*SK1*ALOG(SK1) - 2.*SK1
      T3 = SK1**2/4. - SK1 + 3./4. - (0.5*SK1**2 - SK1)*ALOG(SK1)
      A(7,5) = 4.*(GAMA*Y(6)/CK)**2*(T1+ 0.5*CKA*T2*DCKA - (CKA*ALOG(SK1
     1))**2/4. - CKA*(SK1 - 1.)*ALOG(SK1) + T3*DCKA)*Y(5) - 2.*(GAMA*Y(6
     2)/CK)*(2.*SK1*Y(4)/(Y(3)*Y(5)) + SK1*Y(4)/(Y(3)*Y(5))*(ALOG(SK1) +
     3 EE1)*DCKA + Y(4)*Y(5)*CKA*EE1)
      GM1 = 2.*(GAMA*Y(6)/CK)**2*((1. - SK1)/SK**2 + (1. - SK1**3)/(3.*S
     1K**2) + 0.25*(CKA/SK)**2*(2. - SK1*(ALOG(SK1))**2 + 2.*SK1*ALOG(SK
     21) - 2.*SK1) - (1. - SK1**2)/SK**2 + (CKA/SK**2)*(0.25*SK1**2 - 0.
     35*SK1**2*ALOG(SK1) - 0.25) - (CKA/SK**2)*(SK1 - SK1*ALOG(SK1) - 1.
     4))
      GM2 = 2.*(GAMA*Y(6)/CK)*(Y(4)/Y(3) - (SK/Y(3))**2*Y(4)*(1. + Y(3)*
     1Y(5)**2) - 0.5*(CKA*Y(4)/Y(3))*(ALOG(SK1) + EE1))
      A(7,6) = 2.*GM1/Y(6) + GM2/Y(6)
      IF (ND.EQ.999) GO TO 402
      A(6,3) = A(6,3) + RRHO*A(7,3)
      A(6,4) = A(6,4) + RRHO*A(7,4)
      A(6,5) = A(6,5) + RRHO*A(7,5)
      A(6,6) = A(6,6) + RRHO*A(7,6)
      MA = 6
  402 IF (NS.EQ.2) GO TO 406
      IF (NS.EQ.3) GO TO 407
      IF (ID.NE.1) GO TO 700
      U1 = 32.*(ALPHA*EX + Y(1)*Y(2))/RE1
      V1 = 8./RE1*(ALPHA*EX*Y(5)**2 + Y(1)*Y(2)*Y(5)**2/(1.
     1 + Y(1)*Y(5)**2)**3)
      W1 = 4./RE2*(GAMA*Y(6)/CK*(2.*SK1 + CKA) + Y(3)*Y(4)*Y(5)**2)
      GO TO 701
  700 U1 = U4
      V1 = V4
      W1 = W4
```

```
701 B(1) = B(1) - U1*DELZ
    B(6) = B(6) - V1*DELZ
    B(7) = B(7) + W1*DELZ
    IF (ND.NE.999) B(6) = B(6) + RRHO*B(7)
    IF (ND.NE.999) GO TO 550
    CALL EQLIN(A,B,MA,X)
    GO TO 551
550 CALL LINIT(A,B,X,MA,1,DET,IEX,CNR,SINGUL,7,SCR)
    IF (SINGUL) PRINT 15
 15 FORMAT(13HA IS SINGULAR)
    IF (SINGUL) GO TO 24
551 DO 71 I = 1,7
    X0(I) = X(I)
 71 CONTINUE
    DO 74 I = 1,7
    Y(I) = YY(I) + X0(I)*0.5
 74 CONTINUE
    Y(8) = Y(8) + 0.5*DELZ
    NS = 2
    GO TO 403
406 U2 = 32.*(ALPHA*EX + Y(1)*Y(2))/RE1
    V2 = 8./RE1*(ALPHA*EX*Y(5)**2 + Y(1)*Y(2)*Y(5)**2/(1.
   1 + Y(1)*Y(5)**2)**3)
    W2 = 4./RE2*(GAMA*Y(6)/CK*(2.*SK1 + CKA) + Y(3)*Y(4)*Y(5)**2)
    B(1) = B(1) - U2*DELZ
    B(6) = B(6) - V2*DELZ
    B(7) = B(7) + W2*DELZ
    IF (ND.NE.999) B(6) = B(6) + RRHO*B(7)
    IF (ND.NE.999) GO TO 552
    CALL EQLIN(A,B,MA,X)
    GO TO 553
552 CALL LINIT(A,B,XTMA,1,DET,IEX,CNR,SINGUL,7,SCR)
    IF (SINGUL) PRINT 15
    IF (SINGUL) GO TO 24
553 DO 75 I = 1,7
    X1(I) = X(I)
```

```
 75 CONTINUE
    DO 76 I = 1,7
    Y(I) = YY(I) + 2.*X1(I) - X0(I)
 76 CONTINUE
    Y(8) = Y(8) + 0.5*DELZ
    NS = 3
    GO TO 403
407 U3 = 32.*(ALPHA*EX + Y(1)*Y(2))/RE1
    V3 = 8./RE1*(ALPHA*EX*Y(5)**2 + Y(1)*Y(2)*Y(5)**2/(1.
   1 + Y(1)*Y(5)**2)**3)
    W3 = 4./RE2*(GAMA*Y(6)/CK*(2.*SK1 + CKA) + Y(3)*Y(4)*Y(5)**2)
    B(1) = B(1) - U3*DELZ
    B(6) = B(6) - V3*DELZ
    B(7) = B(7) + W3*DELZ
    IF (ND.NE.999) B(6) = B(6) + RRHO*B(7)
    IF (ND.NE.999) GO TO 554
    CALL EQLIN(A,B,MA,X)
    GO TO 555
554 CALL LINIT(A,B,X,MA,1,DET,IEX,CNR,SINGUL,7,SCR)
    IF (SINGUL) PRINT 15
    IF (SINGUL) GO TO 24
555 DO 77 I = 1,7
    X2(I) = X(I)
 77 CONTINUE
    DO 78 I = 1,7
    Y1(I) = 1./6.*(X0(I) + 4.*X1(I) + X2(I))
 78 CONTINUE
    DO 81 I = 1,7
    Y(I) = YY(I) + Y1(I)
 81 CONTINUE
    Y(8) = YY(8) + DELZ
    EX = EXP(-Y(7)*Y(8))
    IF (ND.NE.999) EX = 0.
    U4 = 32.*(ALPHA*EX + Y(1)*Y(2))/RE1
    V4 = 8./RE1*(ALPHA*EX*Y(5)**2 + Y(1)*Y(2)*Y(5)**2/(1.
   1 + Y(1)*Y(5)**2)**3)
```

```
      W4 = 4./RE2*(GAMA*Y(6)/CK*(2.*SK1 + CKA) + Y(3)*Y(4)*Y(5)**2)

C     INTEGRATION BY TRAPEZOIDAL RULE

      SUM0 = SUM0 + DELZ*(U1 + U4)/2.
      SUM1 = SUM1 + DELZ*(V1 + V4)/2.
      SUM2 = SUM2 + DELZ*(W1 + W4)/2.

      CALL FUNC(Y,8,F,7,SUMF,SUM0,SUM1,SUM2)
      DX = 0.
      CX = EXP(-Y(3)*Y(5)**2)
      IF (CX.LT.1.0E-08) GO TO 84
      DX = Y(4)/CX
   84 VC = 2.*ALPHA*EX*Y(5)**2 + Y(2)
      IF (ID.LE.10) WC0 = VC
      IF (ID.EQ.10) FF3 = F(3)
      VI = Y(2)/(1. + Y(1)*Y(5)**2)**2
      VIE = Y(4)
      IF (ID.LT.449) GO TO 115
      PRINT 14, Y(8),(Y(I),I=1,7),VC,VI,SUMF
      PRINT 110, VIE,(F(I),I=1,7)
      PRINT 110, (Y1(I),I=1,7),DX
      IF (ND.NE.999) GO TO 111
      IF (ID.LT.20) GO TO 111
      IF (SUMF.LT.2.0E-08) GO TO 114
      NP = NP + 1
C     REDUCE THE SIZE OF DELZ WHEN APPROACHING A CRITICAL POINT.
      IF (NP.EQ.1) PRINT 113
  113 FORMAT (54HSKIP ID AND TAPE-READ UNTIL IT SWITCHES TO NONPARABOLA)
      IF (NP.EQ.50) STOP
      DO 112 I = 1,7
      Y(I) = Y(I) - Y1(I)
  112 CONTINUE
      Y(8) = Y(8) - DELZ
      SUM0 = SUM0 - DELZ*(U1 + U4)/2.
      SUM1 = SUM1 - DELZ*(V1 + V4)/2.
```

```
      SUM2 = SUM2 - DELZ*(W1 + W4)/2.
      DELZ = 0.5*DELZ
      GO TO 55
  114 IF (NP.NE.0.AND.NQ.LT.50) GO TO 55
      IF (NQ.EQ.50) PRINT 6
  115 ID = ID + 1
      GO TO 55
      END
```

```
      SUBROUTINE FUNC(Y,LS,F,LT,SUMF,SUMO,SUM1,SUM2)
      DIMENSION Y(LS),F(LT)
      COMMON     EX,RMU,DELZ,ALPHA,DEL1,DEL2,F1(7),F2(7),F3(7),F4(7),WCO
     1,ND,RRHO,GAMA,CK,SK,CKA,SK1,EE1,FF3,FF5,FF7
      IF (ND.NE.999) EX = 0.
      EX = 1. + Y(1)*Y(5)**2
      IF (FX.LT.0.0) GO TO 1
C     EX = EXP(-Y(7)*Y(8))
      SK1 = (SK*Y(5))**2
      CKA = (1. - (SK*Y(5))**2)/ALOG(SK*Y(5))

C     COMBINATION OF PARABOLA AND NONPARABOLA.
C     THE FOLLOWING EQUATIONS ARE,

C     1. EQUATION OF MOTION AT R = 0
      F(1) = (2.*ALPHA*EX*Y(5)**2)**2 + 4.*ALPHA*Y(2)*Y(5)**2*EX + Y(2)*
     1*2 - WCO**2 + SUMO

C     2. THE MATCHING OF VELOCITIES AT AN INTERFACE
      F(2) = Y(2)/FX**2 - Y(4)

C     3. THE MATCHING OF TANGENTIAL STRESSES AT AN INTERFACE
      F(3) = ALPHA*EX + Y(1)*Y(2)/FX**3 - 0.5*RMU*(GAMA/CK*(2.*SK**2 +
     1CKA/Y(5)**2)*Y(6) + Y(3)*Y(4)) - FF3

C     4. MASS BALANCE FOR A JET
      F(4) = 0.5*ALPHA*Y(5)**4*EX + 0.5*Y(2)*Y(5)**2/FX - 0.5

C     5. MASS BALANCE FOR A SRROUNDING FLUID.
      F(5) = 2.*(GAMA*Y(6)/CK)*((1./SK - Y(5)) - 0.25*SK**2*(1./SK**4 -
     1 Y(5)**4) + 0.5*Y(5)**2*(1. - SK1) + 0.25*(1. - SK1)*CKA/SK**2) +
     2 0.5*Y(4)/Y(3) - FF5

C     6. MOMENTUM BALANCE FOR A JET
      F(6) = 2./3.*ALPHA**2*Y(5)**6*EX**2 + 2.*ALPHA*Y(2)*EX*(Y(5)**4/FX
     1 - ALOG(FX)/Y(1)**2 + Y(5)**2/(Y(1)*FX)) + 1./6.*(Y(2)**2/Y(1))*(1
```

```
     2. - 1./FX**3) - 2./3. + SUM1

C     7. MOMENTUM BALANCE FOR A SURROUNDING FLUID
C     AN EXPONENTIAL INTEGRAL IS APPROXIMATED.
C     EE1 IS AN EXPONENTIAL INTEGRAL TIMES EXP(Y(3)*Y(5)**2)

      P = Y(3)*Y(5)**2
      IF (P.LT.1.) GO TO 11
      A1 = 8.5733287401
      A2 = 18.0590169730
      A3 = 8.6347608925
      A4 = 0.2677737343
      B1 = 9.5733223454
      B2 = 25.6329561486
      B3 = 21.0996530827
      B4 = 3.9584969228
      EE1 = (P**4 + A1*P**3 + A2*P**2 + A3*P + A4)/(P**4 + B1*P**3 + B2*
     1P**2 + B3*P + B4)/P
      GO TO 12
   11 A0 = -0.57721566
      A1 = 0.99999193
      A2 = -0.24991055
      A3 = 0.05519968
      A4 = -0.00976004
      A5 = 0.00107857
      EE1 = EXP(P)*(-ALOG(P) + A0 + A1*P + A2*P**2 + A3*P**3 + A4*P**4
     1+ A5*P**5)
   12 GM1 = 2.*(GAMA*Y(6)/CK)**2*((1. - SK1)/SK**2 + (1. - SK1**3)/(3.*S
     1K**2) + 0.25*(CKA/SK)**2*(2. - SK1*(ALOG(SK1))**2 + 2.*SK1*ALOG(SK
     21) - 2.*SK1) - (1. - SK1**2)/SK**2 + (CKA/SK**2)*(0.25*SK1**2 - 0.
     35*SK1**2*ALOG(SK1) - 0.25) - (CKA/SK**2)*(SK1 - SK1*ALOG(SK1) - 1.
     4))
      GM2 = 2.*(GAMA*Y(3)/CK)*(Y(4)/Y(3) - (SK/Y(3))**2*Y(4)*(1. + Y(3)*
     1Y(5)**2) - 0.5*(CKA*Y(4)/Y(3))*(ALOG(SK1) + EE1))
      F(7) = GM1 + GM2 + 0.25*Y(4)**2/Y(3) - SUM2 - FF7
```

```
      IF (ND.NE.999) F(6) = F(6) + RRHO*F(7)

      SUMF = F(1)**2 + F(2)**2 + F(4)**2 + F(5)**2 + F(6)**2
      IF (ND.NE.999) SUMF = SUMF - F(6)**2

      RETURN
    1 PRINT 2
    2 FORMAT(9HFX.LT.0.0)
      END
```

LEGAL NOTICE

This report was prepared as an account of Government sponsored work. Neither the United States, nor the Commission, nor any person acting on behalf of the Commission:

A. Makes any warranty or representation, expressed or implied, with respect to the accuracy, completeness, or usefulness of the information contained in this report, or that the use of any information, apparatus, method, or process disclosed in this report may not infringe privately owned rights; or

B. Assumes any liabilities with respect to the use of, or for damages resulting from the use of any information, apparatus, method, or process disclosed in this report.

As used in the above, "person acting on behalf of the Commission" includes any employee or contractor of the Commission, or employee of such contractor, to the extent that such employee or contractor of the Commission, or employee of such contractor prepares, disseminates, or provides access to, any information pursuant to his employment or contract with the Commission, or his employment with such contractor.

TECHNICAL INFORMATION DIVISION
LAWRENCE RADIATION LABORATORY
UNIVERSITY OF CALIFORNIA
BERKELEY, CALIFORNIA 94720